An Illustrative Look at Energy Flow through Hybrid Powertrains for Design and Analysis

Eli Hampton White

Thesis submitted to the faculty of the Virginia Polytechnic Institute and State University
in partial fulfillment of the requirements for the degree of

Master of Science
In
Mechanical Engineering

Chair: Douglas J. Nelson
Scott T. Huxtable
Robert L. West

May 07, 2014
Blacksburg, VA

Keywords: hybrid electric vehicle, plug-in hybrid electric vehicle, electric vehicle, environment, greenhouse gases, fuel economy, powertrain modeling, power split fraction

An Illustrative Look at Energy Flow through Hybrid Powertrains for Design and Analysis

Eli Hampton White

ABSTRACT

Throughout the past several years, a major push has been made for the automotive industry to provide vehicles with lower environmental impacts while maintaining safety, performance, and overall appeal. Various legislation has been put into place to establish guidelines for these improvements and serve as a challenge for automakers all over the world. In light of these changes, hybrid technologies have been growing immensely on the market today as customers are seeing the benefits with lower fuel consumption and higher efficiency vehicles. With the need for hybrids rising, it is vital for the engineers of this age to understand the importance of advanced vehicle technologies and learn how and why these vehicles can change the world as we know it. To help in the education process, this thesis seeks to define a powertrain model created and developed to help users understand the basics behind hybrid vehicles and the effects of these advanced technologies.

One of the main goals of this research is to maintain a simplified approach to model development. There are very complex vehicle simulation models in the market today, however these can be hard to manipulate and even more difficult to understand. The 1 Hz model described within this work aims to allow energy to be simply and understandable traced through a hybrid powertrain. Through the use of a "backwards" energy tracking method, demand for a drive cycle is found using a drive cycle and vehicle parameters. This demand is then used to determine what amount of energy would be required at each component within the powertrain all the way from the wheels to the fuel source, taking into account component losses and accessory loads on the vehicle. Various energy management strategies are developed and explained including controls for regenerative braking, Battery Electric Vehicles, and Thermostatic and Load-following Series Hybrid Electric Vehicles. These strategies can be easily compared and manipulated to understand the tradeoffs and limitations of each.

After validating this model, several studies are completed. First, an example of using this model to design a hybrid powertrain is conducted. This study moves from defining system requirements to component selection, and then finding the best powertrain to accomplish the given constraints. Next, a parameter known as Power Split Fraction is studied to provide insight on how it affects overall powertrain efficiency. Since the goal with advanced vehicle powertrains is to increase overall system efficiency and reduce overall energy consumption, it is important to understand how all of the factors involved affect the system as a whole. After completing these studies, this thesis moves on to discussing future work which will continue refining this model and making it more applicable for design. Overall, this work seeks to provide an educational tool and aid in the development of the automotive engineers of tomorrow.

Acknowledgements

I would like to first thank General Motors, the United States Department of Energy, and Argonne National Labs, for organizing and sponsoring EcoCAR 2 which has made my educational experience here at Virginia Tech unparalleled by any other program. I would also like to thank the Hybrid Electric Vehicle Team of Virginia Tech for all of the support throughout this thesis. Working with HEVT has been an incredible experience and has not only taught me the design process, but has challenged me to learn skills I will use throughout the rest of my engineering career. Next I would like to thank Dr. Nelson for being an exceptional faculty advisor, mentor, and friend. None of this would have been possible without his constant patience and unrivaled passion for this field of research. Finally, I would like to thank my friends and family. It is through their constant encouragement and support that I have been able to complete my studies and move forward with God's plans for my life.

Table of Contents

List of Multimedia Objects

List of Tables

List of Figures

List of Terms & Abbreviations

ANL	Argonne National Lab
AVTC	Advanced Vehicle Technology Competition
BEV	Battery Electric Vehicle
BMEP	Brake Mean Effective Pressure
BSFC	Brake Specific Fuel Consumption
CAD	Computer Aided Design
CAFE	Corporate Average Fuel Economy
CD	Charge Depleting
CS	Charge Sustaining
EPA	Environmental Protection Agency
ESS	Energy Storage System
ETE	Emissions Testing Event
EV	Electric Vehicle
Genset	Engine/Generator Combination in a Series HEV
GHG	Greenhouse Gas
HEV	Hybrid Electric Vehicle
HV	High Voltage
HwFET	Highway Fuel Economy Test
MBD	Model Based Design
P2	Position 2 Generator Motor (located between engine and transmission)
PEU	Petroleum Energy Usage
PHEV	Plug-In Hybrid Electric Vehicle
PSF	Power Split Fraction
PTTR	Parallel Through-The-Road
RTM	Rear Traction Motor
SHEV	Series Hybrid Electric Vehicle
SOC	State of Charge
UDDS	Urban Dynamometer Drive Schedule
US06	Aggressive, high speed drive cycle
VDP	Vehicle Development Process
WTW	Well-To-Wheels

1 Introduction

1.1 Background and Motivation for Advanced Vehicle Technologies

According to statistics from the U.S. Energy Information Administration, the public of the United States consumed approximately 135 billion gallons of liquid fuel through the use of motor vehicles in 2013 [1]. Furthermore, 27% of all Greenhouse Gas (GHG) emissions produced in the U.S. were due to the transportation industry causing about 1.54×10^9 metric tons of GHG emissions to be generated [2]. Considering how much is invested in transportation, a great opportunity is presented to reduce the amount of money spent each year on fuel as well as to reduce the effects this industry has on the environment.

One area undergoing vast improvements is that of passenger vehicles. Throughout the past few years, concerns have been raised about the amount of emissions passenger vehicles produce annually. Amongst the entire transportation industry, which includes on-road vehicles, as well as aircraft and ships, passenger vehicles and light duty trucks make up about 61% of the total GHG emissions produced [2]. In response to this contribution to total emissions, policy makers have instituted stricter guidelines for emissions as well as fuel economy to try and drive advancements in technology. Policies such as Corporate Average Fuel Economy (CAFE) and the Clean Air Act push the automotive industry to create vehicles with higher fuel economies and less emissions to ensure impacts of motor vehicles are lessoned. With this extensive push for new technology, hybrid vehicles have become an item of great interest for vehicle manufacturers and are quickly becoming the transportation of the future.

1.2 Introduction to Hybrid Vehicles

Hybrid vehicles are powered by two or more energy sources which can be anything from electricity, gasoline, or propane, all the way to hydrogen or mechanical potential stored in a fly wheel. This work will focus mainly on Hybrid Electric Vehicles (HEVs). This type of hybrid includes electricity as one of the multiple fuel sources on board in the form of a bi-directional, rechargeable source such as a battery. HEVs vary greatly in levels of electrification. Figure 1-1 shows the progression of vehicles starting with conventional vehicles in the upper left and moving down all the way to Battery Electric Vehicles (BEVs) which are totally electrified. As shown here, the first small step towards electrification for a conventional vehicle is introducing engine idle start/stop. This variation may include a small high voltage (HV) battery powering a small electric starter/alternator connected to the engine. When the vehicle comes to a stop, instead of wasting energy and fuel idling the engine where efficiency is low, the engine can be turned off. When the driver wishes to move on, the HV battery can then power the starter/alternator to restart the engine. As technology has progressed, this type of system can also be implemented with heavier duty 12V starters/alternators.

Aside from adding a simple, small auxiliary motor to allow for engine idle start/stop, HEVs also increase in complexity and electrification through adding larger motors and battery packs. Charge Sustaining (CS) HEVs use a larger motor to generate larger amounts of electricity to support the on board rechargeable battery and maintain it at a certain state of charge (SOC). CS HEVs also include a drive motor which can power the vehicle from the

HV system. With this more complex system, CS HEVs can have the ability to simply assist the engine for added efficiency or take over full propulsion of the vehicle under certain conditions like low driving speeds.

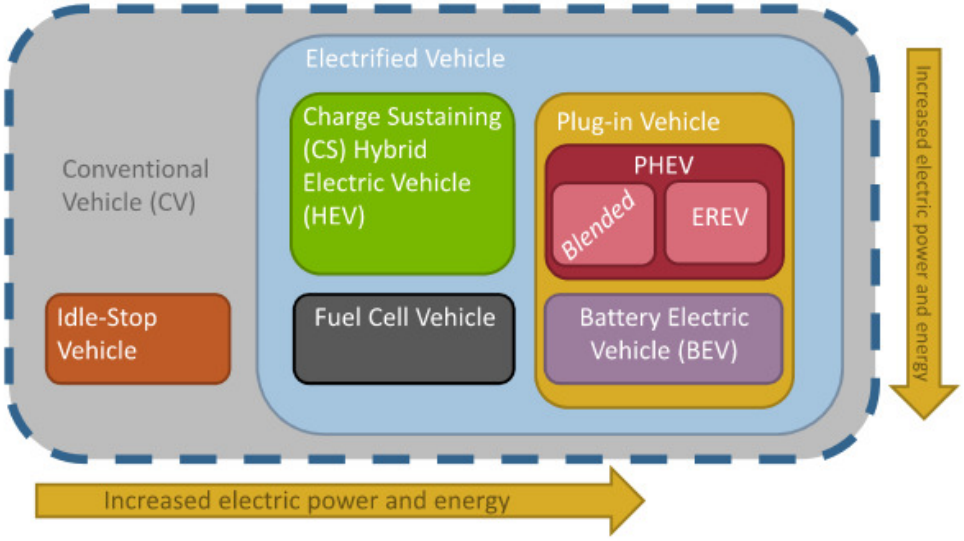

Figure 1-1: Vehicle powertrains with varying levels of electrification

Aside from simple Charge Sustaining HEVs, plug-in vehicles are the next level of electrification. These vehicles have many different powertrain configurations and operating strategies but usually all include a large battery pack, referred to as an Energy Storage System (ESS). This ESS allows the vehicle to have a Charge Depleting (CD) range. A CD range uses grid electricity stored within the ESS to power the vehicle completely until a lower SOC is reached. Throughout this operating window, the vehicle has near full performance as an Electric Vehicle (EV) without ever requiring another fuel to be used. Once the battery is depleted of usable energy, an Extended Range Electric Vehicle (EREV) which is one type of Plug-In Hybrid Electric Vehicle (PHEV) is able to continue operating with the use of a fuel converter. This "range extender" can be anything from a hydrogen fuel cell to a combustion engine, but has the overall function of allowing the vehicle to convert another energy source to fuel the vehicle. The benefit of an EREV is that the vehicle has a CD range, lowering overall emissions and petroleum energy use (PEU) while also not being limited by battery range considering the alternate fuel source can also be utilized.

The most electrified vehicle powertrain is very similar to an EREV but lacks the range extender. This BEV architecture, shown in Figure 1-1, only includes an ESS on board and thus is limited in range by the usable energy within this battery system. Overall, BEVs have much larger Energy Storage Systems to compensate for a range extender and include full vehicle performance. The benefits of this powertrain again are the CD range, but also cost to the driver since electricity cost almost a third of the price of gasoline [3]. With all these benefits, the downside of a BEV is the limited range and long charging time. Once the vehicle depletes the ESS to the lower SOC, it must be plugged in to charge. Traditionally a consumer could pull into a gas station and fill a vehicle's gas tank within a few minutes. BEVs however require anywhere from 2 – 10 hours of charging, depending on the size of the battery pack, level of charger, and capabilities of the vehicle. This creates

a slight disadvantage, but for consumers with a short daily commute and with increasing charging technology, BEVs are quickly outweighing short falls with advantages.

1.3 Introduction to Hybrid Powertrains

With the various levels of electrification in mind, this thesis will focus mainly on two different types of vehicle powertrains. First, the presented work explores the details of a BEV. This type of powertrain, which was discussed in the previous section, allows the operator to drive completely under the power of stored grid electricity. The high voltage ESS is electrically coupled to a motor/motor controller system which is in turn mechanically coupled through a single speed transmission to provide traction to the wheels. The HV system also provides energy to support the accessory loads within the vehicle. This powertrain has incredible benefits for efficiency, as electric motors operate with efficiencies around 85% - 95% where as conventional combustion engines operate more in the range of 20% - 39%. Additionally BEVs are much cheaper to refuel when compared to gasoline vehicles and are overall smoother to operate with the lack of a shifting transmission. An example of a BEV powertrain diagram is shown in Figure 1-2.

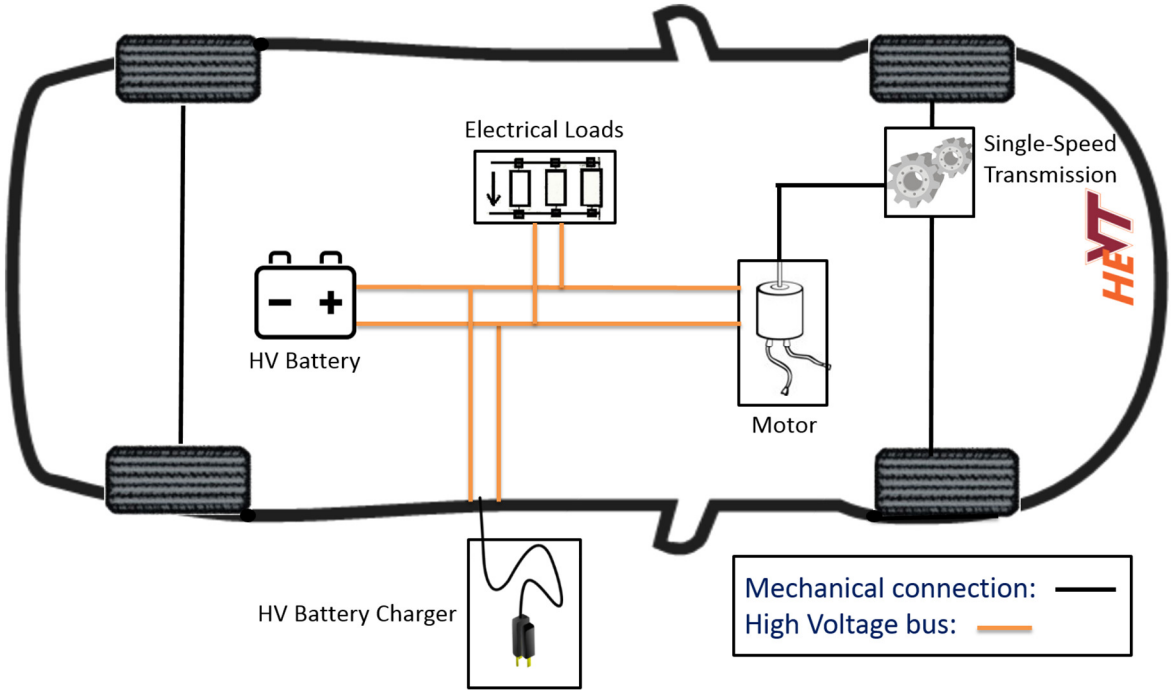

Figure 1-2: BEV powertrain diagram

The second powertrain this specific work will focus on is a Series HEV (SHEV). This genre of hybrid is a Charge Sustaining vehicle which can be either plug-in or have a smaller battery used for energy buffering. It does include an engine of some type, which is used as a range extender, but instead of directly providing traction, this engine is coupled to a generator which converts mechanical engine energy to electrical energy for the HV system. Traction is then provided through an electric drive motor much like in the BEV and excess energy is stored in the ESS until required for extra demand. The benefits of this powertrain are first, to offer a range extended hybrid thus increasing consumer acceptability. Secondly with efficiency in mind, a Series HEV can greatly increase in efficiency compared to a

conventional vehicle when it comes to city driving. Conventional cars are known to be less efficient at low speeds and in situations requiring constant stop and go demand. Series vehicle are able to be more efficient since the engine is not directly providing power to match the demand at the wheels. Instead, the "genset" or engine generator combination can be operated at a higher efficiency point and not be required to ramp up and down with demand at the wheels. This causes some excess energy to be generated, however this can simply be stored in the battery for use when the demand at the wheels is greater than the genset operating point. With this freedom, the vehicle can have an overall higher system efficiency while still meeting vehicle demand. Series control strategies which manipulate how energy flows through the vehicle and thus control efficiency will be discussed further in later sections. A basic powertrain layout for a SHEV can be seen in Figure 1-3.

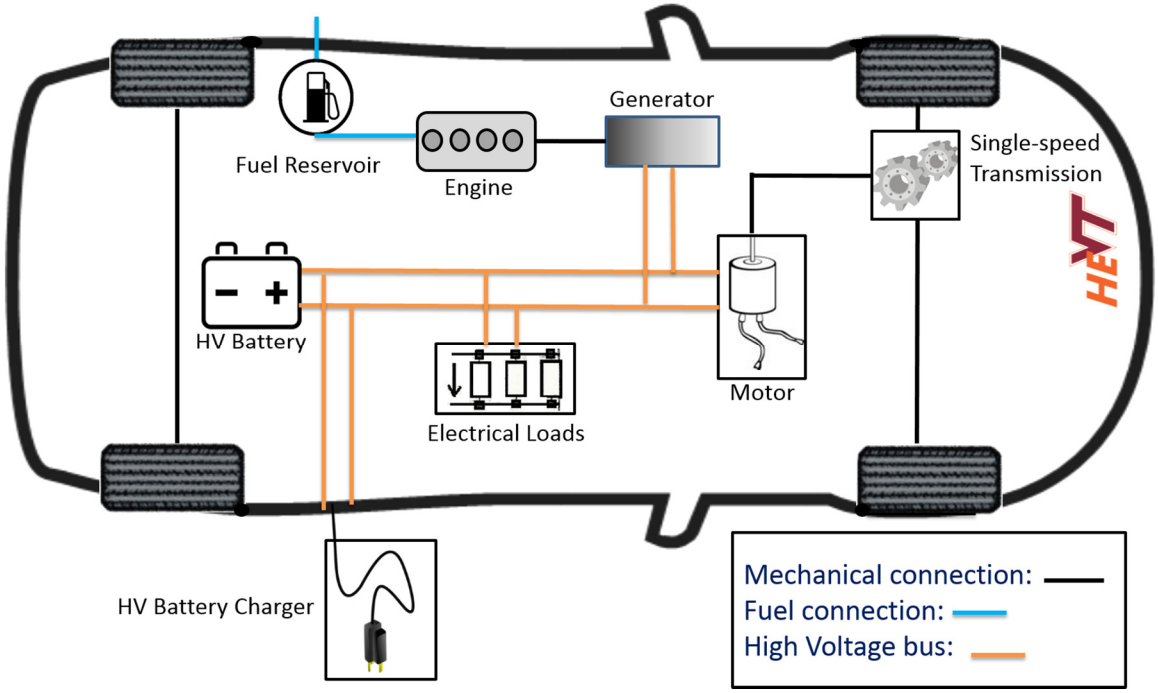

Figure 1-3: SHEV powertrain diagram

Although this work focuses on BEV and SHEV powertrains, one other common hybrid architecture is a Parallel Through-The-Road (PTTR). This powertrain is much like a SHEV in that it includes both a HV system in addition to a range extender. The largest difference is that instead of the fuel converter driving a generator to produce electricity, a multi-speed transmission is present as shown in Figure 1-4. This transmission allows engine torque to be directly coupled to the wheels and thus provide an alternative "parallel" path for power to reach the wheels. With this addition, both torque paths can aid one another in propelling the vehicle and freedom of component operation is achievable via the hybrid control strategy. One of the greatest benefits of a PTTR powertrain is that once the vehicle is up to highway speeds, the drivetrain is more efficient than a SHEV since it does not require the numerous energy conversions and thus does not incur as many conversion losses. Instead, these conversions can be bypassed and engine torque can go straight to the wheels with only the losses within the driveline present. Additionally, PTTRs increase performance when compared to SHEVs since the vehicle is not limited to the power capabilities of the drive motor but by the drive motor and engine combined. Overall, when

comparing hybrid powertrains, PTTRs are very beneficial but do require a much more complex control strategy to include gear shifting and torque security.

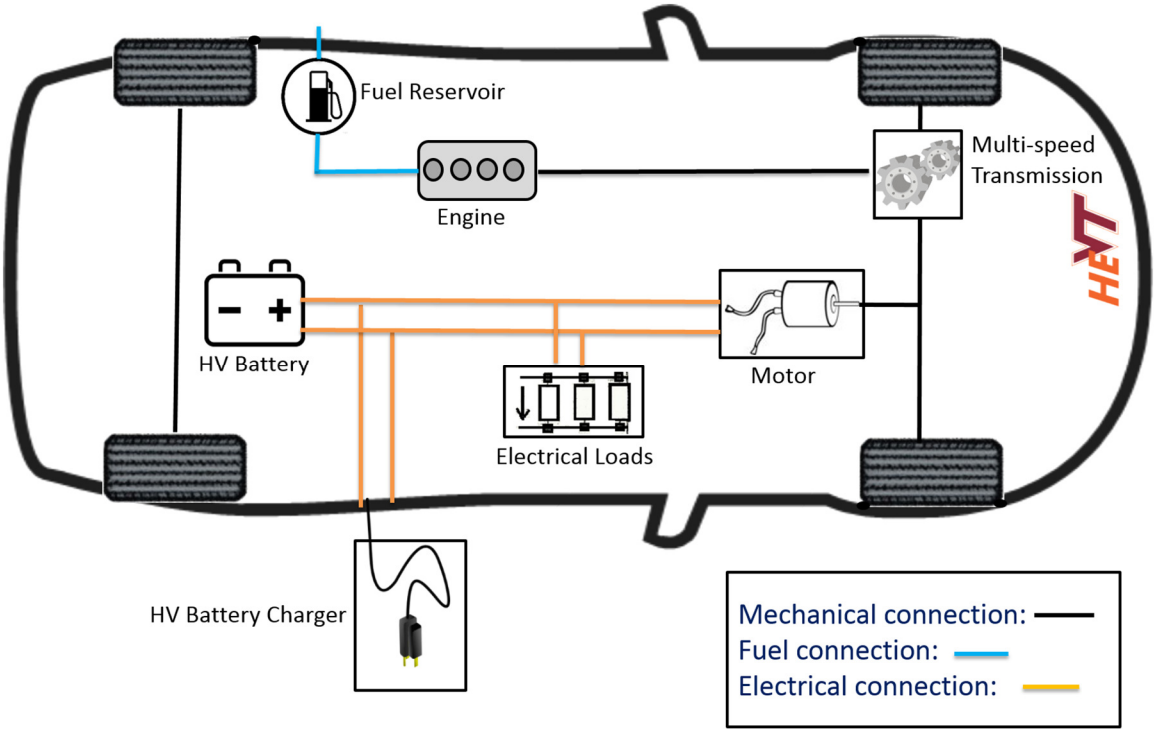

Figure 1-4: PTTR powertrain diagram

1.4 Participation in EcoCAR 2: Plugging into the Future

1.4.1 Overview

Motivation for this work comes in part from the author's work with the Hybrid Electric Vehicle Team of Virginia Tech (HEVT). HEVT is participating in the 2012 - 2014 *EcoCAR 2: Plugging In to the Future* Advanced Vehicle Technology Competition (AVTC) series organized by Argonne National Lab (ANL), and sponsored by General Motors Corporation (GM) and the U.S. Department of Energy (DOE). The goals of the competition are to reduce Well-To-Wheel (WTW) petroleum energy use (PEU), WTW greenhouse gas and criteria emissions while maintaining vehicle performance, consumer acceptability and safety. Following the EcoCAR 2 Vehicle Development Process (VDP), HEVT, along with 14 other schools across North America, are designing, building, and refining advanced technology vehicles over the course of the three year competition using a 2013 Chevrolet Malibu donated by GM as a base vehicle. Throughout this competition students are able to gain valuable experience with hybrid technologies and work towards becoming the next generation of automotive engineers.

1.4.2 HEVT Description

HEVT is divided into five main subteams: mechanical, electrical, controls, communications, and business. The three technical teams (mechanical, electrical, and controls) focus on the physical integration and software changes to the car. These groups consist mainly of senior mechanical and electrical engineering students along with various

underclassman engineering students. Each of these three subteams focuses on one of the major areas on the vehicle and have specific tasks to complete in order for the entire team to be successful. The business team handles the business strategy and finances of HEVT (including sponsorship). This subteam is also responsible for recruitment and knowledge transfer so that the team as a whole can continue being successful even with the transition of team members. The communications subteam handles the outreach portion of the project, including increasing the awareness of EcoCAR 2 as well as disseminating information for sustainable vehicle technologies throughout the community. The main objective of the competition as a whole is to train the next generation of automotive engineers and promote "green" technology throughout all aspects of the automotive industry. With a rise in demand for hybridized vehicles over the last few years, the need for automotive engineers trained in hybrid vehicle development has increased as well. EcoCAR 2 not only benefits the students' education but helps secure jobs for team members after graduation.

1.4.3 Vehicle Development Process

HEVT is following the EcoCAR 2 VDP to complete the redesign of the 2013 Chevrolet Malibu. This VDP closely mimics GM's Global Vehicle Development Process (GVDP) which is a detailed process that allows for truly decoupled development of subsystems and international work sharing [4].

1.4.3.1 Year 1

During the first year of the competition, HEVT was given the task of creating an overall design for a hybrid vehicle. This included not only a powertrain configuration, but also fuel and component selection along with initial modeling and controls. To begin the process, HEVT had to take into account several criteria and constraints when considering a powertrain architecture or a fuel. Some of these constraints are driven by the EcoCAR 2 competition rules [5], while others are driven by team goals unique to HEVT. The team must conform to all design and safety rules prescribed by the EcoCAR 2 rules. Per competition rules, the vehicle must have a total range of 200 miles and can have a maximum curb weight of 2078 kg. The stock vehicle has a Gross Vehicle Weight Rating (GVWR) of 2260 kg, so a maximum curb weight of 2078 kg accounts for two passengers at 91 kg each. There are also considerations for passenger space and cargo capacity. Stiff penalties are imposed for reducing the passenger capacity by removing seats or for reducing cargo capacity by raising the floor of the trunk. These penalties must be kept in mind when considering packaging possibilities for candidate architectures. In addition to rigid constraints, there are also various scored categories in the competition including: acceleration, braking, lateral handling, drive quality, as well as emissions and energy consumption. This means that performance and handling must be balanced against vehicle emissions and energy consumption. There are minimum thresholds and target values for several of these metrics set forth by competition rules; Table 1-1 summarizes these targets and minimums [5].

Table 1-1: EcoCAR 2 competition design targets and requirements

Specification	Competition Design Target	Competition Requirement
Acceleration 0–60 mph	9.5 sec	11.5 sec
Acceleration 50–70 mph	8.0 sec	10 sec
Braking 60–0 mph	143.4 ft (43.7 m)	180 ft (54.8 m)
Highway Gradeability @ 20 min	3.5% @ 60 mph	3.5% @ 60 mph
Cargo Capacity	16.3 ft^3	7 ft^3
Passenger Capacity	>=4	2
Test Mass	<2250 kg	<2250 kg
Starting Time	<2 sec	<15 sec
Ground Clearance	>127 mm	>127 mm
Vehicle Range	322 km [200 mi]	322 km [200 mi]

In addition to these EcoCAR 2 targets and requirements, HEVT has also established its own unique team goals. Reducing petroleum energy use is directly tied to fuel consumption and fuel consumption is often a trade-off with tailpipe emissions. Because of this, it is difficult to simultaneously reduce both tailpipe emissions and fuel consumption and, by extension, PEU. For various reasons, the team chooses to focus specifically on reducing the petroleum energy consumption of the vehicle. Consumer acceptability is represented in a significant portion of competition points, so the team purposefully includes consumer features in the vehicle design. One such consumer feature is a pure Electric Vehicle (EV) mode, where the vehicle has near full performance as an EV. The presence of a fully capable EV mode coupled with a significant EV range also greatly displaces WTW petroleum energy and marginally reduces WTW GHG and criteria emissions. Additionally, the team set the goal to retain the full passenger capacity of the vehicle. Table 1-2 summarizes the additional design goals set forth by the team.

Table 1-2: HEVT team goals

Goal	Description
Petroleum Energy Consumption	Reduce petroleum consumption by > 80 %
All-Electric Range	> 56 km (35 mi) range as a pure all-electric vehicle
Passenger Capacity	Retain stock 5 passenger capacity

These goals and requirements are used to guide the design process. Also taken into consideration are factors such as facility limitations, prior experience, component availability and budget limitations. HEVT does not have access to emissions testing facilities or a chassis dynamometer, so calibrating an engine or an emissions system is outside the capabilities of the team. The team also cannot undertake the task of integrating an architecture that requires expensive or exotic components without sponsorship and support of those components. Fortunately, EcoCAR 2 provides an array of sponsors that offer components and support to the program, especially including GM.

After establishing goals, HEVT then moved on to fuel selection and powertrain modeling. The team first considered available fuels on a WTW basis and then examined three distinct and unique architectures: a BEV, a Series EREV, and a Series-Parallel PHEV. Each architecture was modeled and the advantages and challenges were examined and considered. This analysis explored the various components involved with each powertrain and how well each performed in various drive cycles. The results of the analysis were then entered into a design matrix to evaluate the effectiveness of each architecture in the context of the EcoCAR 2 competition, and the best powertrain architecture was selected.

By the end of Year 1, HEVT's powertrain was chosen to be an E85 Series-Parallel PHEV and the majority of the subsystems for the powertrain were designed [6]. The primary electric drive system of this architecture consists of a 125 kW Rear Traction Motor (RTM) coupled to a single-speed transmission to deliver torque to the rear wheels. With an 18.8 kWh ESS donated by A123, the vehicle achieves a range of about 40 miles in EV mode. A GM-donated E85 fueled engine mated with a custom P2 (pre-transmission, post-engine position) generator motor from Kollmorgen and a GM donated 6-speed automatic transmission provides extended range capability. A complex control strategy delivers motor and engine torque to the wheels in the most efficient manner possible, while meeting driver demand in a safe and effective manner.

1.4.3.2 Year 2

After the completion of the design for the hybrid vehicle powertrain during Year 1, EcoCAR 2 teams then completed the build phase of the VDP in Year 2 [7]. This phase is all about physically implementing the designs from the previous year. During the summer between Years 1 and 2, HEVT received a 2013 Chevrolet Malibu from GM and was able to begin work on modifying the vehicle. Throughout Year 2, HEVT made several key modifications to the designs of Year 1. These changes came as a result of being able to analyze the physical vehicle and better understand the clearances and tolerances which are hard to fathom when working with 3D Computer Aided Design (CAD) models. In the face of this, physical integration was completed and a partial control strategy was implemented to allow the vehicle to operate in CD mode. The goal of Year 2 was to end with a 65% complete "mule" vehicle. This milestone within the EcoCAR 2 VDP represents having a partially complete vehicle with a focus on functionality instead of consumer acceptability.

1.4.3.3 Year 3

During the third and final year of the competition, EcoCAR 2 teams focus on achieving a 99%-buyoff level of vehicle readiness to complete the VDP process [4]. The vehicle utility and performance are further developed by using off-board math modeling tools and on-board testing and development. HEVT analyzed the mule vehicle created during Year 2 and trimmed down the design of the vehicle to be more efficient and effective for completing team goals. Some of the refinement items include light-weighting, optimizing performance both physically and from a controls standpoint, working on aesthetic appeal, as well as other more detailed tasks. The emphasis of Year 3 is consumer acceptability, showroom qualities, and the seamless operation of the vehicle powertrain and control subsystems [4].

1.4.4 Summary and Application

Overall, EcoCAR 2 encompasses almost every aspect of the vehicle design process. From initial design work such as fuel selection and powertrain modeling, all the way through physical implementation and construction, and finally finishing up with overall refinement and optimization, this competition does an incredible job of allowing students to learn and hone vital engineering skills. It is this design process that makes this thesis so applicable to educational experiences like EcoCAR 2 or any other AVTC, especially when initial powertrain selection is concerned. This thesis provides a simple tool for comparing several hybrid powertrains across various drive cycles. Another important aspect of this tool is to also provide easy manipulation for performing component sizing. Through utilizing this, students or professionals can better understand the effects of making components like engines, motors, and battery systems larger or smaller when it comes to overall vehicle performance. This modeling tool is not meant to replace more complex, in-depth computer models, it is simply meant to provide a first look at how a vehicle will react to drive schedules for initial design concepts which is perfect for design phases like Year 1 of EcoCAR 2. Further discussion concerning the applicability of this modeling tool is discussed in Section 1.6 below.

1.5 Application for EcoCAR 3

HEVT is excited about the opportunity to apply for participation in the next Advanced Vehicle Technology Competition. EcoCAR 3 is a new four year competition also sponsored by the Department of Energy and General Motors with the intention of promoting sustainable energy in the automotive sector. The goal of the competition is to guide students from universities in North America to create new and innovative technologies to reduce the environmental impact of modern day transportation. EcoCAR 3, like its predecessors, will give students hands-on experience in designing and implementing advanced technologies in a setting similar to that of current production vehicles. The primary goals of the competition are to improve upon a conventional internal combustion engine production vehicle by designing and constructing a powertrain that accomplishes the following:

- Reduce Energy Consumption
- Reduce Well-to-Wheel (WTW) GHG Emissions
- Reduce Criteria Tailpipe Emissions
- Maintain Consumer Acceptability in the area of Performance, Utility, and Safety
- Meet Energy and Environmental Goals, while considering Cost and Innovation

The application for this competition was very beneficial in the development of the modeling tool presented in this thesis. Much like Year 1 of the EcoCAR 2 VDP, the modeling problems explored in this proposal provided opportunities for model validation and comparisons to similar models [8].

1.6 Purpose, Goals, and Objectives

As mentioned in the previous section, the purpose of this work is to provide a simple, user-friendly vehicle model for understanding several types of hybrid powertrains and the component sizing involved with such designs. The tool discussed in the following thesis uses various inputs to track energy flow through an advanced vehicle powertrain. Although there are already various tools on the market today with much higher degrees of freedom, such as Autonomie [10], one of the main goals of this particular tool is to allow a user to gain accurate results while also allowing calculations to be easily viewed and tracked. This model uses a 1 Hz or second-by-second approach to increase simplicity while again, allowing users to easily understand the flow of calculations. The result of this is an accurate model which also provides much deeper understanding into the "how" and "why" behind the values produced as opposed to keeping calculations in a "black box" which cannot be viewed and simply produce results.

When it comes to actual performance, the 1 Hz model introduced in this thesis traces energy flow through an advanced vehicle powertrain from the wheels to the energy source. This "backwards" approach is a result of inputting a drive cycle which is desired to be analyzed. Once the velocity and grade (if applicable) vs. time are input, all forces are calculated and a required tractive effort at the wheels is determined. Power is then traced back through the entire powertrain until the energy source, being a HV battery or a fuel tank, is reached. Through this type of analysis, efficiencies and losses can be calculated for each component individually and overall energy consumption and powertrain efficiency can also be understood. WTW PEU and GHG emissions are also calculated based on values for each type of fuel being used.

The different powertrains that are analyzed within this model are a BEV and two different types of SHEVs containing separate control strategies which will be discussed in more detail in Sections 3.4.3 and 3.4.4 . For each of these different powertrains, the model also calculates results for the following drive cycles from the Environmental Protection Agency (EPA): Urban Dynamometer Drive Schedule (UDDS), 505 (first 505 seconds of a UDDS), Highway Fuel Economy Test (HwFET), US06, US06 City (city portion of a US06 cycle), and US06 Hwy (highway portion of a US06 cycle). From these cycles a combined Corporate Average Fuel Economy (CAFE) can also be calculated and analyzed since it is made up of 55% UDDS and 45% HwFET results. Additionally, 4-cycle weighted results can also be calculated, which are used by HEVT in EcoCAR 2 and are an approximation of the 5-cycle method used by EPA for fuel economy labeling. This cycle is calculated using 28.8% 505, 12.3% HwFET, 14.2% US06 City, and 44.7% US06 Hwy. This model also has the capabilities to allow a user to add additional drive cycles for analysis. An example of this application is for the EcoCAR 2 competition. This competition has its own variations of on-road drive schedules and thus needed to be input separately for analysis.

As mentioned previously, the model presented here does have many different input parameters which can be manipulated separately. This degree of freedom greatly increases the usefulness of this tool when it comes to completing design studies. Vehicle glider properties can be easily changed to represent vehicles of different sizes and shapes. Component parameters can also be manipulated with ease which is quite useful for sizing studies. This allows users to run separate cases for various component sizes and then compare results to better understand how the performance of the vehicle changes.

Additionally, values affecting regenerative (regen) braking are also tunable, so regen capabilities can be ramped up and down or turned off altogether.

The other main goal of this work is to also explore a parameter known as Power Split Fraction (PSF) [12]. This aspect of a hybrid vehicle, which will be discussed in more depth within Section 4.2, represents the balance of how much energy produced by the engine is used to directly propel the vehicle. This parameter is measured from 0 to 1, 0 being no energy is directly used and all of it is stored within the ESS and 1 being all energy comes directly from the engine for propulsion with no storage present. The study of PSF will support the design process in illustrating how powertrain efficiency is affected and where the balance is between engine performance and losses associated with transitioning energy in and out of the HV battery to achieve the highest overall system efficiency for a chosen vehicle.

In summary, the main purpose of this modeling tool is to support the design process and give an in-depth, "behind-the-scenes" look at energy flow throughout an advanced vehicle powertrain. While education is first and foremost, accuracy of results is obviously a priority, thus this model has been validated in several different ways. This validation process will be discussed in detail within Section 3.7 of this thesis. Overall, this model is a great resource for exploring the capabilities of various hybrid powertrains and understanding how sizing different components will affect the vehicle so that designers can confidently choose a powertrain for design study problems like those presented in the EcoCAR competitions. Table 1-3 summarizes the overall goals and objectives for this thesis.

Table 1-3: Thesis Goals and Objectives

(1) Provide a tool to help understand the in-depth functional details of several advanced vehicle powertrains and to aid in designing hybrid powertrains
(2) Demonstrate several energy management strategies used in hybrid vehicles today
(3) Provide insight on the effects of Power Split Fraction on overall powertrain efficiency

2 Literature Review

2.1 Sovran: On Understanding Automotive Fuel Economy and Its Limits

Sovran along with Blaser wrote this SAE paper in 2003 to help others better understand the physics behind calculating the fuel economy of vehicles in an "accurate, concise, and understandable form" [11]. This paper in particular focuses on the fuel economy of motor vehicles on UDDS and HwFET drive schedules, and in turn, targets CAFE results. The methods presented here give detailed explanations for what factors affect fuel economy and how manipulating these different factors can positively or negatively affect overall vehicle efficiency.

Sovran begins by defining the various parameters acting on a vehicle. This "tractive force" is a sum of the opposing forces acting on a vehicle that must be overcome in order for the vehicle to operate. Tractive force is made up of both road load and inertial forces. Road load forces are consistently acting on the vehicle when it is moving and are made up of both rolling resistance and aerodynamic drag. Rolling resistance in this case is only made up of a single term which is calculated using wheel radius, vehicle mass, and acceleration due to gravity. This calculation varies from the rolling resistance found in this thesis since an additional vehicle velocity dependent term also contributes. This will be explained further within the Model Definition section but should be noted here. Aerodynamic drag is consistent between this thesis and Sovran, and is proportional to vehicle velocity. The inertial forces included take into account the acceleration and deceleration of the vehicle.

Once tractive forces are defined, Sovran breaks the total down into 3 separate categories: propel ($F_{TR} > 0$), brake ($F_{TR} < 0$), and idle ($F_{TR} = 0$, $V = 0$). This decomposition allows fuel consumption to be calculated for each category and then summed together for overall drive cycle fuel consumption. Another important note is that for conventional vehicles, which are the focus of Sovran's paper, the brake and idle cases are relatively simple since friction brakes are used and idling only needs to overcome system losses. For HEVs, which are discussed briefly at the end of the paper, these two cases become much more complex with the addition of regenerative braking and loading a mechanically decoupled engine for added efficiency.

With the glider properties of the vehicle defined, the tractive energy required is then fully found through adding drive cycle specific information. This data is added into the fuel consumption calculations through the use of coefficients which are defined on a per drive cycle basis. This means that each particular drive cycle has different coefficients that represent what requirements the vehicle must meet to successfully run the schedule. Once these are developed, the energy required is understood and powertrain component efficiencies can be taken into account to find actual fuel consumption.

Overall, Sovran's work is quite useful for this thesis. The "backwards" energy flow concept from the wheels to the fuel source is utilized here. Additionally, most components analyzed include propel and brake cases. The largest different is that this thesis looks at power flow on a second-by-second basis and thus does not calculate fuel consumption in a lumped method through the use of Sovran coefficients. This thesis also focuses on hybrid

powertrains as opposed to mainly conventional vehicles, however concepts on increasing efficiency can be employed here as well.

2.2 Alley: On Understanding Energy Flow and Losses in Hybrid Powertrains

Alley's thesis, published in 2012, fills in several gaps left in the research completed by Sovran [12]. Like Sovran's method, Alley seeks to create a modeling tool for better understanding the energy flow through a vehicle powertrain. The main secondary goal is to make this tool applicable for comparing several different powertrains to determine which would best meet desired design goals. Much like the current work presented in this thesis, Alley's work creates a way to directly compare these various powertrains and predicts performance based on "slugs" of energy as opposed to a second-by-second approach. The main difference between the work of Alley and Sovran is that Alley develops his work for the analysis of hybrid vehicles as opposed to simply conventional vehicles. In fact, he includes work for not just EVs, but also Series and Parallel HEVs. Alley expands his work to explore many drive cycles instead of simply UDDS and HwFET schedules.

Alley begins by defining vehicle glider characteristics and deriving "Sovran" coefficients to characterize the chosen drive cycles. As mentioned, these coefficients are derived for not only UDDS and HwFET schedules, but also for the following cycles: a 505 and 867 (components of a UDDS), US06, US06 City and Hwy (components of a US06), SC03, and an LA92. After defining these values, the energy required to complete each drive cycle can be found and individual component efficiencies are found to aid in powertrain comparisons and overall understanding. It is important to note that this research has been successful and VTool was validated using real world test data collected during an AVTC.

One very important concept developed in Alley's thesis is Power Split Fraction which was discussed briefly in a previous section. This parameter is defined and briefly explored, however the current research presented in this thesis greatly picks up where Alley left off in gaining much more insight into PSF and the effects it has on hybrid powertrains. It is important to note that the definition of PSF presented previously was formulated from Alley's work.

Compared to Sovran's concepts, Alley's work proves to be even more valuable considering its focus on hybrid powertrains. This method coincides very closely with the goals of this thesis in the development of a tool to better understand the flow of energy throughout a vehicle powertrain and observe the effects of component sizing and vehicle glider properties on overall performance. Again, both of these tools seek to allow users to quickly and easily compare various hybrid powertrains on the basis of performance and energy consumption. Additionally, Alley presents some PSF analysis which is very valuable to this thesis as well, considering it is the starting point for the study included Section 4.2.

2.3 Ord: Advanced Powertrain Design Using Model Based Design

Ord's thesis greatly supports the work completed within this thesis [13]. Ord completed a Model Based Design (MBD) approach for powertrain sizing and selection using MatLAB Simulink. This method was developed mostly for education purposes to be used in AVTCs and was utilized in this case for a modeling problem presented within the application

HEVT submitted to be accepted into EcoCAR 3. This most recent addition to the AVTC series presented a problem much like that described for Year 1 of the EcoCAR 2 VDP in Section 1.4.3.1. Within his thesis, Ord describes his modeling process including his various energy management strategies, demonstrates results for each powertrain modeled, and shows some specific solutions to the EcoCAR 3 modeling problem to demonstrate the effectiveness of this MBD process. Overall, Ord has many similar objectives as this thesis simply with a different method.

After introducing his work, Ord begins with introducing the flow of energy through his model. Beginning with a driver model, this tool inputs a velocity profile (drive cycle) and generates an accelerator pedal position. This then flows forward through the powertrain from the engine or power generator, through the driveline to the wheels. The output is thus the tractive effort at the wheels to meet the driver demand. This is then compared to the input velocity to ensure no significant discrepancies between the two. In doing this, each component can be observed individually in addition to the system as a whole in terms of efficiencies and losses. This model-based technique is very beneficial because many iterations can be run quickly and consecutively and more complex control strategies can be tested. Within Ord's thesis, he looks at not only BEVs and SHEVs, but also conventional vehicle (both gas and diesel powered) in addition to various levels of Parallel vehicles. Through this broad scope, Ord is able to develop an intuitive walk through a powertrain selection process to meet specific goals and compare many different powertrains to see which performs in the most desired ways.

Ord's MBD approach is extremely useful to the work presented in this thesis. Firstly, it gives great insight into vehicle powertrains with energy management strategies that are more complex than those used in the 1 Hz model discussed here. PTTR vehicles must include shift strategies and other complexities which are simply outside the scope of this thesis. Secondly, Ord's thesis does provide a great way for model validation. As discussed in later sections, this MBD approach allows other models such as this 1 Hz model to be compared and validated based on inputting similar values and receiving similar results. This is even more useful since Ord's thesis bases energy flow in a forward looking direction whereas this thesis tracks energy from the wheels back through the powertrain. Through comparing both approaches, both models can help validate one another. This has been crucial for the development of the modeling tool explained within this thesis.

2.4 Wang: On Controls for a Series Hybrid Powertrain

This paper, published by Wang of the Ford Motor Company in 2011, discusses a Series configuration for an HEV [14]. Although the overall setup of this architecture is quite well known, Wang focuses on developing the controls architecture design and optimization with a "Model-in-the-Loop" approach for increased fuel efficiency. This is part of a larger scope of controls development known as Model Based Design which is discussed in Ord's thesis. Wang first discusses a SHEV control architecture before moving on to discussing the energy management and optimization strategies. The paper seeks to demonstrate the performance of the actual controls system and does so through showing simulation and real vehicle test data.

As mentioned, Wang first introduces a SHEV control architecture and the methodology through which Ford developed the vehicle controls for this study. Wang began with

creating a model to represent the vehicle which could be used to test the energy management strategy prior to full vehicle testing. After validation here, the optimized code could then be tested via software followed by hardware using a "Hardware-in-the-Loop" chassis. After validation here, the vehicle controls could then be used for in-vehicle testing. The process is used widely for controls development as it ensures safety with the systems since code must be validated through two separate systems before actually manipulating a vehicle. In fact, this is a very similar process to what is used in the EcoCAR 2 competition described earlier. Although this is a helpful method, the research presented in this thesis will not follow such as process since it is more for powertrain performance development and understanding when it comes to energy flow. As a result the energy management strategy section of this paper is of most interest, however, it is useful to understand the process behind developing real hybrid vehicle controls.

Before any controls could be tested, the energy management strategy had to be developed by Ford. Here, the system was analyzed and it was found that the entire SHEV system allowed for two degrees of freedom; the power split between the engine and battery to meet demand, as well as engine operation being independent of wheel speed since it is not mechanically coupled through a transmission. For this study, optimization curves for the efficiency of both the combined genset and the battery are used and after a battery power is chosen by the code, the power output of the genset is determined. Following this process, the engine can output this power while following an optimum engine operation line to maintain the most fuel efficient means for propelling the vehicle. This process is very useful the research within this thesis as the 1 Hz tool has several similarities. Although the simplified model does not include any instantaneous optimization strategies considering the nature of the research, the model does attempt to operate the engine and in turn the genset, at its most efficient point. An engine operating line is present to force to operate the engine at its most efficient point while still producing the desired amount of power output. Additionally, it is quite valuable to consider the degrees of freedom within the SHEV system as outlined in this paper. This information allows the model presented in this thesis to focus on similar variables and thus be representative of a real world energy management strategy.

As shown, the paper published by Wang is enlightening and supportive of the research presented within this thesis. Although Ford's research is much more in-depth and allows for optimization, it still supports the fundamental concepts discussed within this thesis. In fact, a key conclusion developed from vehicle testing shows that a Load-following versus a simple Thermostatic strategy is critical for powertrain sizing and maximizing overall system efficiency which is targeted here. This is mirrored in the current thesis, as maximizing overall system efficiency is the goal and both Load-following as well as Thermostatic strategies are tested.

2.5 Jalil: On an Energy Management Strategy for a SHEV

Jalil, Kheir, and Salman published a paper in 1997 comparing two control strategies for a Series HEV [15]. The overall goals of this publication are to demonstrate a method for improving the fuel economy of a SHEV through increasing component efficiencies without compromising vehicle performance. Jalil first introduces two main types of hybrid powertrains, Series and Parallel. After explaining the differences he moves on to focusing

on SHEVs and outlines a plan to compare different energy management strategies with the goal of observing changes in fuel economy.

The two energy management strategies introduced by Jalil include a Thermostat or "On/Off" strategy, as well as a rule-based "Power Split" strategy. It is important to note that this is not the same as Power Split Fraction which is explained further in this thesis. This Power Split is the control strategy defined by Jalil for SHEV operation and will be discussed shortly. Beginning with the simpler strategy, the defined Thermostat is controlled by two limits, SOC high and low. When the vehicle reaches SOC low, the genset is turned on and generates at an optimum engine efficiency until SOC high is reached. The vehicle then turns the genset off and charge depletes until again reaching SOC low.

The Power Split approach is similar in that is operates with a Thermostat as a base controls strategy, but then builds on this with several other rules. The Power Split uses PI controllers to send a power demand to the powertrain and determine if and how the genset and batteries need to operate. This strategy looks at SOC high and low initially, but then moves on to control operation through the use of power limits on the engine, as well as an acceleration command which alerts the controller when high power is required, defaulting the engine to maximum operation. The essence of this Power Split strategy is still Thermostat since it only ramps the engine up and down when the SOC high limit is reached, however it is similar to the Load-following energy management strategy discussed later in this thesis.

After completing this study, it was found that operating the engine and generator with more freedom then simply the on/off commands of a Thermostat control strategy does increase the fuel economy of a SHEV. When testing these two strategies on both UDDS and HwFET, it was determined that the Power Split strategy increased fuel economy by 11% in the city and 6% on the highway. It is important to note that for this study, the engine never turns "off" but actually idles without delivering power to the drivetrain. With this in mind, some unnecessary fuel consumption is a result but counterbalances the engine start penalties that would be incurred when cycling the engine. Regardless, this study demonstrates how increased complexity can benefit the vehicle's overall performance since more design conditions can be taken into account to maintain efficiency while not compromising performance.

Overall, this paper is very useful to this thesis. The work presented in this thesis also includes a Thermostat control strategy along with a Load-following strategy which closely resembles the Power Split strategy described here. It is useful to compare results to other studies to ensure trends are consistent in addition to realizing that several of the rules included in the energy management strategies are consistent as well. This paper does not use a 1 Hz model or a "backwards" energy flow approach. Additionally, it does not analyze energy flow on a component by component basis for increase understanding and impacts of component sizing. Despite these details, this paper is quite useful on a control strategy standpoint.

2.6 Rask: On Fuel Economy, Efficiency, and Regen Braking for Hybrid Vehicles

In 2013, Rask helped publish this paper which explores the capabilities of HEVs of various levels of electrification to improve fuel economy as a result of regenerative braking and reduced engine fueling during vehicle deceleration [16]. The main focus for this study is to evaluate how well equations used by Sovran for calculating fuel used in braking in addition to calculating regenerative braking model real vehicle data for the different vehicles under various conditions [11,17,18]. The drive cycles used for this study include the UDDS, HwFET, and US06, which includes the city and highway portions of aggressive driving. Data for this study was collected on a chassis dynamometer using various instrumentation throughout the vehicles.

Rask first discusses the fueling modes of vehicles during deceleration events. First describing conventional vehicles for comparison, Rask shows plots to show the rate at which fuel is being used for two separate conventional powertrains during decelerations. These illustrations show data for powered deceleration (not letting completely off of the accelerator pedal during decel) and a normal deceleration including "Decel. Fuel Cut-off (DFCO)". Shown here, less fuel is used during DFCO thus improving fuel economy. Rask also discusses how hybridizing systems allow for no fuel to be used during some deceleration events. This section is not utilized for this thesis, however this could be very useful information for future work when more complex energy management strategies could be implemented. As shown through the data displayed in this paper, reduced engine fueling does have advantages and should be explored.

The thesis presented here does greatly benefit from Rask's study of regenerative braking, especially when it comes to the limits placed on the vehicle for regen braking capabilities. As explained in the paper, HEVs have a "regenerative braking envelope" which limits how much regen brake energy is available for capture. These limits include low speed cutoff, maximum tractive force at the wheels, and finally maximum power at the drive motor or battery. Low speed cutoff is a limit, since friction brakes must be utilized at certain low speeds. This paper goes on to explain how regen "ramp-in" should be used to gradually decrease the amount of regen braking and increase friction braking when reaching low speeds to maintain drivability and stability. Tractive force at the wheels is limiting since many vehicles only complete regen on one axle. This becomes a torque limit on the motor completing the regen, since its negative torque capabilities are not infinite. This unbalance can also cause issues with vehicle handling and dynamics as one axle could lock causing road adhesion to diminish. For component and passenger safety, as well as vehicle handling, this must be prevented, thus a tractive limit. Finally, power limitations must be considered for both the drive motor and the battery. It doesn't matter how much brake energy is available for regen if the power level of the motor or battery prevents the vehicle from collecting it. This is a bottle neck in the system and must be taken into account.

As mentioned, this thesis uses the information concerning limits for regenerative braking presented within this paper. The "ramp-in" limit is simplified to a simple low speed cut-off for the regen braking. At this point, the model presented within this thesis simply allows friction brakes to take over completely at these low speed since not much energy is even available. Also, this model is quite simplified, so drivability is not considered since energy

flow is the main concern. The limits of maximum tractive force and component power abilities are fully integrated into this work and are presented in detail within Section 3.4.1. Overall, this paper has been quite integral to the development of a real world regenerative braking strategy for this thesis. It is very important to understand the various limits involved in regen braking in order to accurately apply the limits to generate valid results for HEVs.

2.7 Summary of Literature Review

This literature review explores various published works which contribute to HEV technology as a whole, and specifically aid in the development of the model discussed within this thesis. To start off, Sovran introduces a method for breaking down the resistant forces acting on a vehicle which must be overcome in order to meet an inputted drive cycle. His work also develops a "backwards" wheels-to-source look at energy flow. One of the limitations of Sovran's work is that it is focused mainly on conventional vehicles. This is where Alley's work picks up and expands on the previous work. Alley's thesis expands Sovran's theories from just conventional vehicles into the hybrid vehicle realm. Using similar techniques, Alley tracks lumps of energy through advanced vehicle powertrains and gives a method for learning and predicting energy flow through HEVs. His methods also allow for simple powertrain sizing studies and introduces the PSF concept. Both of these works are incredibly useful for this thesis. Not only are initial concepts gleaned from these works such as calculating tractive force from an inputted drive cycle, and tracing energy backwards through the powertrain, but this work is able to continue exploring topics such as PSF in greater detail to produce a better understanding of the parameter. Both Sovran and Alley provide a base and starting point for the work presented in this thesis to build on.

After examining the foundation of this research, several different methods for modeling HEV powertrains are explored. Ord presents a very similar method to the 1 Hz model developed within this thesis for tracking energy flow through vehicle powertrains and sizing components to meet certain performance goals. Ord uses Model Based Design to create forward looking models to demonstrate the performance of various powertrains including conventional vehicles, BEVs, SHEVs, and even PTTR hybrids. His approaches allow for easy comparison and even model validation through inputting similar values and achieving similar results. After Ord, Wang and Jalil both present great insight on control strategies for SHEVs. Although both use more complex modeling techniques, the energy management strategies support the research completed within this thesis and give an idea of what to expect through using both Thermostatic and Load-following control strategies. Additionally, Wang gives great background into the degrees-of-freedom within a SHEV and how manipulating certain parameters such as engine and battery operation can affect overall system efficiency. Jalil, in turn, provides an example of a simplified "rule-based" control strategy much like the one used in the model presented here. Many of the same limits are used for this work and similar results are produced.

Finally, specifically looking at regenerative braking, Rask's work gives in-depth discussion for limits to be considered in a regen braking strategy. There is a plethora energy available for capture and reuse, however, 100% of this energy cannot be retrieved due to factors such as tractive force and component power limits. In addition, regen braking is often counter-

productive at very low vehicle speeds since not much energy is available and there are losses within the system. For this reason, one other limit is low-speed cutoff. These limits have been incorporated into this thesis to produce a realistic regen strategy which would match a vehicle on the road today.

As demonstrated, this thesis is greatly supported by various research completed throughout the past few decades. Obviously research concerning HEVs is pertinent and important for the world today. This thesis seeks to continue the work begun by several of the authors reviewed in this literature review and provide an informative, useful tool for learning and application when it comes to powertrain selection and sizing. Further discussion on the details of this tool are provided in the sections below.

3 Model Definition and Explanation

The model described here has been compiled as a tool to better achieve the various goals included within Section 1.6, including understanding the overall energy flow through a hybrid powertrain. This section describes in detail each area of the model, from calculations to energy management strategies. This section should illustrate the "how" and "why" behind each aspect of the model and act as a "user's manual" for anyone wishing to manipulate the model.

3.1 Defining Nomenclature

Before explaining the various component models and energy flow throughout the tool presented here, it is important to understand the nomenclature used throughout this work. This nomenclature allows a user to better see what type of parameter is being analyzed and where in the system it is. Additionally, this "key" guides the direction of flow for energy, power, etc. Figure 3-1 displays the nomenclature key for this model. This terminology is based on the work completed by Alley [12].

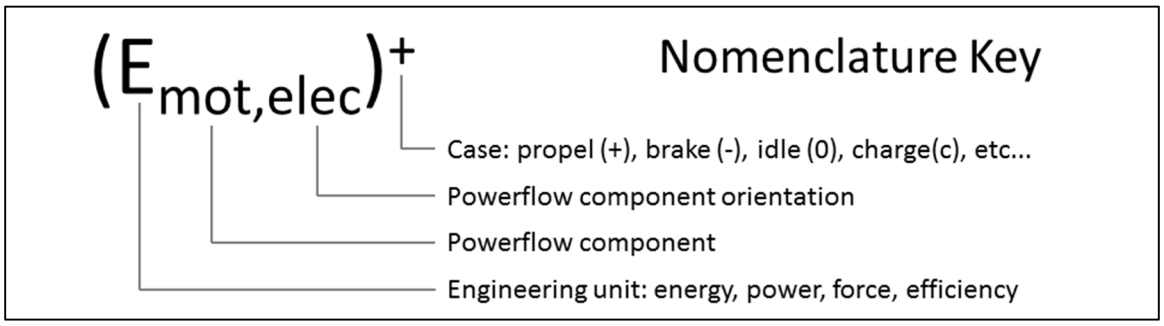

Figure 3-1: Nomenclature key for terms throughout the model

Shown here, the engineering unit is first displayed followed by which component within the model is being analyzed as a subscript. This could display "mot" to represent a "motor" or "eng" which stands for "engine". Each abbreviation is intuitive and within the model, each parameter is defined with a comment to increase ease of use. After defining the parameter and component, orientation and direction are important. This is specified using the next subscript which will say either "mech" or "elec" which stand for "mechanical" and "electrical" respectively. Many of the components within hybrid powertrains can allow energy to flow in both directions, as propel and regenerative braking are both typical cases. As a result it is easier to specify for example the electrical side of a drive motor as opposed to the mechanical side. This gives a constant orientation for both propel and regen cases. Finally, propel or regen must be specified which is done through the superscript outside the parentheses shown. For this model, only a + or – will be shown since these are the two cases tracked through the powertrain. It is important to note, that some variables do not contain a + or – meaning that these values are "net" values which include both propel and regen. This is true for internal battery power since this is completed on a net basis.

3.2 Drive Cycles Evaluated

This research focuses on several main drive cycles used by EPA for evaluating vehicles. The cycles presented contain both city and highway scenarios, as well as several extremely

aggressive traces. The presence of these various levels of intensity and driving situations greatly benefits the design process considering continuous and peak power ratings for powertrain components are put to the test. Additionally, these cycles closely model real world driving which ultimately, is what matters since any vehicle designed to be driven in a fleet must be able to handle how the public will actually drive them. The first drive schedule included within this 1 Hz model is a UDDS. This "urban" schedule, shown in Figure 3-2 demonstrates lower speed driving with numerous accelerations and decelerations. The first five hundred five seconds of the UDDS is known in industry as a 505 drive cycle. This is also modeled separately within this 1 Hz model to give a closer look at this driving situation and is shown in Figure 3-3.

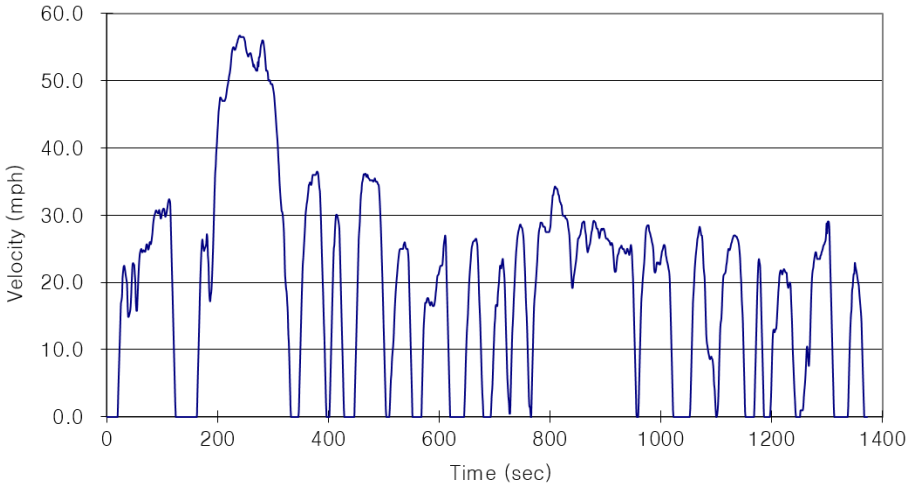

Figure 3-2: UDDS drive trace

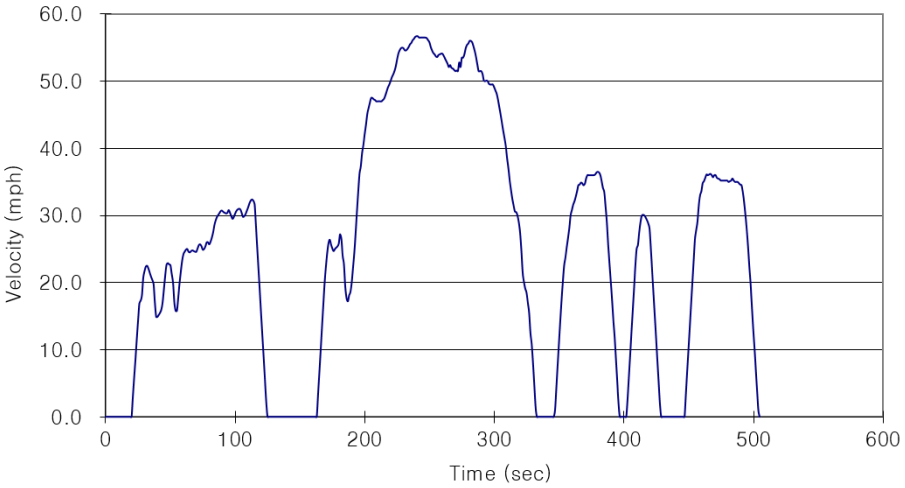

Figure 3-3: 505 drive trace

Aside from only city driving, highway situations are obviously also of interest when designing powertrains. This, as mentioned, helps evaluate a vehicle powertrain when it comes to continuous power where high demand is required over a long period of time. The Highway Fuel Economy Test provides this driving scenario and is shown in Figure 3-4. As displayed here, higher vehicle speeds are necessary at a more constant level.

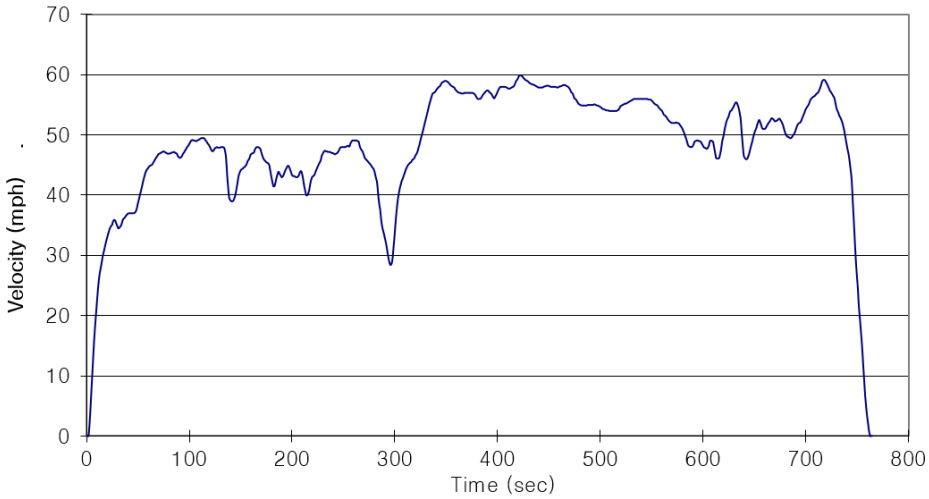

Figure 3-4: HwFET drive trace

To view how a vehicle will handle peak power capabilities and very aggressive driving, the US06 drive cycle is utilized. This schedule, shown in Figure 3-5, has a combination of constant high demand and extremely aggressive acceleration and deceleration events throughout the trace. It is very important to take this cycle into account when sizing components for a vehicle which will operate as an EV. This design must have a motor which can produce the amount of power required for this cycle, but also a battery which can supply the high power as well. These parameters are also vital to keep in mind for a SHEV, which is again why this cycle is important for this research. To better see what is happening in the city and highway portions of this US06 cycle, each of these is analyzed separately in addition to the full drive schedule. Figure 3-6 and Figure 3-7 show the individual drive traces used.

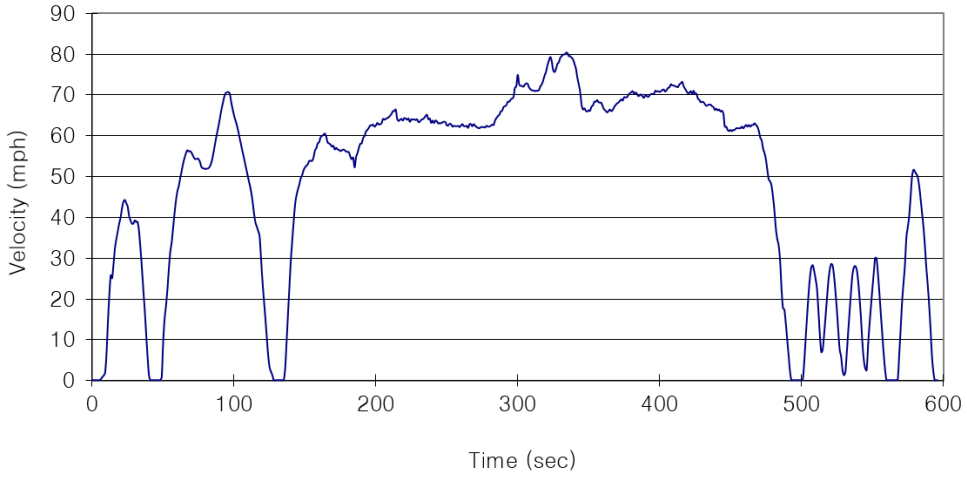

Figure 3-5: US06 drive trace

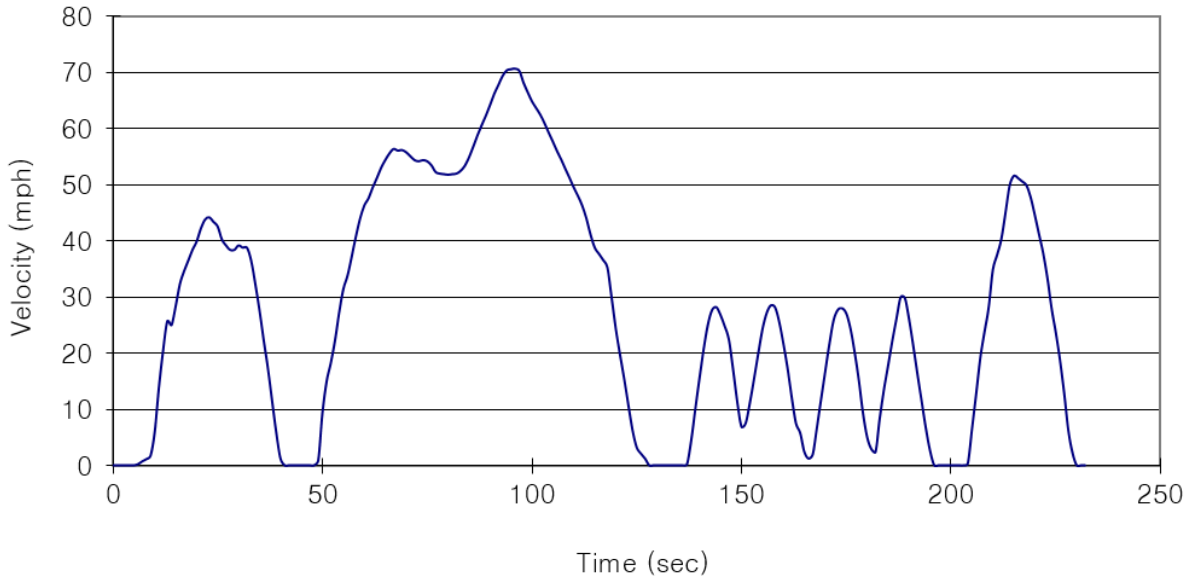

Figure 3-6: US06 City drive trace

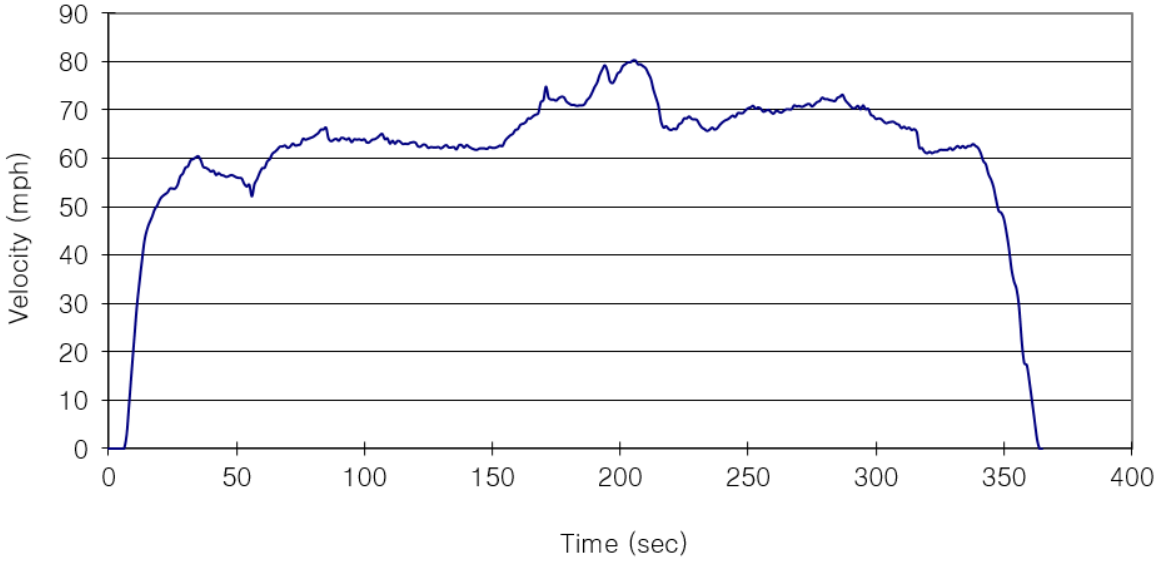

Figure 3-7: US06 Hwy drive trace

Table 3-1 displays a summary of the characteristics for the 6 different cycles defined above. Here, properties can be compared to better understand what different results gathered may mean, since some cycle are longer than others, and obviously some are more aggressive or mild than the rest.

Table 3-1: Drive cycle characteristics

Drive Cycle	Distance	Cycle Time	Idle Time	Powered Time	Max Speed	Average Speed	Max Accel	Min Accel
	[km]	[s]	[s]	[s]	[m/s]	[m/s]	[m/s^2]	[m/s^2]
UDDS	12.0	1372	244	753	25.4	10.6	1.48	-1.48
505	5.8	505	94	286	25.3	14.1	1.48	-1.48
HwFET	16.5	765	4	669	26.8	21.7	1.43	-1.48
US06	12.8	596	35	411	35.9	22.8	3.76	-3.08
US06 City	2.8	236	33	108	31.6	13.8	3.76	-3.00
US06 Hwy	10.0	360	2	303	35.9	27.9	3.08	-3.08

Aside from these defined drive cycles, this 1 Hz model also leaves room for a user defined drive cycle. The calculations are all set up, the user simply enters the velocity vs. time trace and drags the equations to cover the entire length of the drive cycle. This allows for flexibility amongst users and increases the design capabilities of this work since its scope is not limited to simply these common 6 drive schedules. Furthermore, results for this unique drive cycle are included directly on the user defined cycle sheet for convenience. The purpose of displaying these results here is to not disrupt the flow of results for the other schedules when the user defined option is not being used, as well as isolating these user defined results for simplified viewing.

Several cycle values are also calculated from the results of those presented above. One of these "combined" cycles is for Corporate Average Fuel Economy. This result, as mentioned in the introduction of this work, is made up of 55% UDDS and 45% HwFET results. Additionally, EcoCAR 2 "4-cycle weighted" values are also calculated. These results are made up of 28.8% 505, 12.3% HwFET, 14.2% US06 City, and 44.7% US06 Hwy. This combination of the main cycles explored above produces one simplified result allowing for easy comparison amongst various powertrains.

3.3 Component Models

To understand the energy flow throughout each powertrain presented here, it is important to define the various components used and how each behaves. This section will discuss the requirements and calculations behind each separate component.

3.3.1 Glider Model and Tractive Effort Requirements

A glider model is generated in order to find the force requirements at the wheels, followed by power and energy. A glider model is the equivalent of the characteristics of a vehicle, such as the aerodynamics and test mass of the vehicle, but does not include any of the powertrain components. The base equation for the glider model is seen in Equation 1:

$$F_{tr} = F_{rolling} + F_{grade} + F_{aero} + F_{inertia} \qquad \textbf{Equation 1}$$

Where F_{tr} is the tractive effort at the wheels, $F_{rolling}$ is the rolling resistance, F_{grade} is the force generated by a grade (uphill, downhill), F_{aero} is the aerodynamic drag, and $F_{inertia}$ is the inertial force of the vehicle. Each of these forces makes up a component of the tractive force required to propel the vehicle. Figure 3-8 illustrates the force balance for a moving vehicle. The tractive force must overcome the sum of each opposing force in order to propel the vehicle into motion.

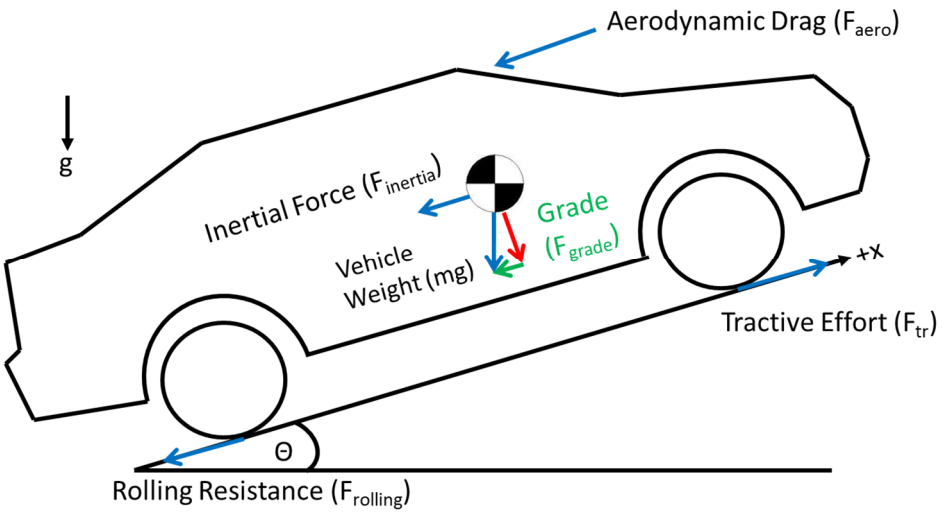

Figure 3-8: Tractive force balance for vehicle in motion

The rolling resistance force $F_{rolling}$ describes the resistance encountered at the wheel of a vehicle generated by the contact patch on the tire and also the velocity proportional friction produced in areas like the wheel bearings. The calculation for the rolling resistance is simple and includes a two coefficients of rolling resistance. Generally for use within this thesis, the velocity proportional component is set to zero, however it can be applicable and thus is considered.

$$F_{rolling} = F_{rr} + F_{rr1} = C_{rr0}mg + C_{rr1}mgV \qquad \textbf{Equation 2}$$

Equation 2 describes the rolling resistance, where C_{rr0} and C_{rr1} are the coefficients of rolling resistance (C_{rr1} being the velocity proportional component), m is the vehicle mass, g is the gravitational constant, and V is the vehicle velocity. The coefficients of rolling resistance are generated based on specific tire tread, pressure, and numerous other factors. These constants remain static in this modeling.

The grade force is calculated using Equation 3:

$$F_g = F_{grade} = mgsin\theta \approx mg * grade \qquad \textbf{Equation 3}$$

Where θ is road angle. Since θ is such a small angle for this application, the value of $sin\theta$ can be approximated as simply grade of the road expressed as a percentage. Grade force accounts for the resistance or in a downhill case, the assistance that gravity produces on the vehicle. For many drive cycles, grade is not included with the drive trace, however it is an option as an input for this model.

Aerodynamic drag is calculated by Equation 4:

$$F_{aero} = \frac{1}{2}\rho C_d A_f V^2 \qquad \textbf{Equation 4}$$

Where ρ is air density, C_d is the coefficient of drag, A_f is the frontal area of the vehicle, and V is the current velocity of the vehicle. Once again, the vehicle is parameterized by picking specific values for C_d and A_f, allowing results to be generated based on any input vehicle. This force is heavily dependent on velocity, as it contains a V^2 term.

The final force, and the most significant force is the inertial force of the vehicle, described in Equation 5:

$$F_i = F_{inertia} = m_i a = m_i \frac{dV}{dt} \quad \textbf{Equation 5}$$

Where m_i is the inertial mass of the vehicle, and a is the longitudinal acceleration of the vehicle which is calculated as the change in velocity over change in time. Since this model is second-by-second, this calculation is completed for each time step and thus is quite simple; finding the difference of the current and previous velocity divided by the difference of the time step. The inertial mass takes into account the rotating inertia of the components of wheels, tires, and brakes of the vehicle, and therefore is slightly larger than the actual mass of the vehicle (~4%). Equation 6 shows how m_i is calculated:

$$m_i = \left(1 + \frac{4I_w}{mr_w^2}\right) m \approx 1.04m \quad \textbf{Equation 6}$$

Where I_w is the rotational inertia of the wheels and r_w is the radius of the wheels.

As mentioned, the tractive force described here must overcome the sum of the opposing forces in order to propel the vehicle into motion. Once this force is found, the instantaneous power requirements at the wheels for each time step of a drive cycle are calculated and in turn, the power is integrated over time to provide the total energy required at the wheels to complete the designated drive cycle. Equation 7 and Equation 8 show the calculations for each of these parameters. For these equations, P is power, F is force, V_{avg} is average vehicle speed, V_n is the vehicle speed at the current time step, V_{n-1} is the vehicle speed at the previous time step, amd E is energy. Note that since this is a 1 Hz model, energy is easily found by summing each power over the entire drive cycle, thus throughout this discussion power will be tracked with the knowledge that energy is easily found and tracked as well.

$$P = F * V_{avg}, where\ V_{avg} = \frac{V_n + V_{n-1}}{2} \quad \textbf{Equation 7}$$

$$E = \int P dt \quad \textbf{Equation 8}$$

Once the net tractive power is calculated, it can be broken down into positive and negative components to better understand propel and brake scenarios, shown in Equation 9. The propel case is quite simple and straight forward. When $F_{tr} > 0$, the vehicle must be generating power to move. Braking involves both friction and regen braking when $F_{tr} < 0$. As a result, certain tests must be completed to determine if regen braking is applicable and if so, how much should be applied. The details of this strategy are included in Section 3.4.1 of the Energy Management Strategies. The main calculation to be made is shown in Equation 10, where after the regen power available is determined, the power lost to friction braking can be found. This friction power is treated as a loss in the system since it cannot be recovered. It is important to note that these propel and brake scenarios do not occur at the same time but are evaluated at each time step, thus when propelling, $(P_{tr})^+$ has a value and $(P_{tr})^-$ is zero at that time step and vice versa when braking.

$$P_{tr,net} = (P_{tr})^+ + (P_{tr})^- \quad \textbf{Equation 9}$$

$$(P_{tr,friction})^- = (P_{tr})^- + (P_{tr,regen})^- \quad \textbf{Equation 10}$$

At this point in the model, the power and energy at the wheels is completely determined. For both propel and regen cases, the power demand to be produced by the powertrain and the power available to charge the battery are determined. The power can now be traced back up the driveline and into the powertrain for further analysis of components.

3.3.2 Power loss and Torque-Speed Modeling

Being a reliable and simple method to generate useful results, power loss models are generated for each powertrain component. Each power loss model can be derived from Equation 11:

$$P_{in} = P_{out} + P_{loss} \qquad \textbf{Equation 11}$$

Where P_{in} is the power going into the component, P_{out} is the power leaving the component, and P_{loss} is the power lost during component operation. Different applications of this equation based on components will be discussed later. Most of the components in the simplified powertrain structures can be modeled using this equation. Figure 3-9 shows a generic example of the power balance through a powertrain component to understand how loss affects the power flow.

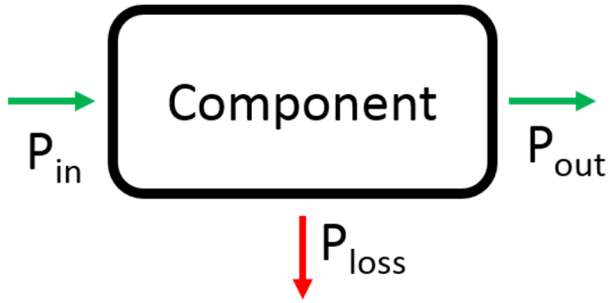

Figure 3-9: Power loss diagram

Although power loss illustrates the overall balance used to understand the flow through each component, torque-speed characteristics are actually used to calculate this power. This technique allows for the details of components to be observed and understood which helps achieves one of the overall goals of better understanding power flow. For this research specifically, torque-speed characteristics are observed mechanically for the drive axle, motor, engine, and generator, as well as electrically for the battery in the form of current and voltage. These characteristics will be discussed in the individual model sections below.

3.3.3 Driveline Model

Since this is a backwards flowing model, the energy through the driveline is analyzed next. The driveline described here illustrates a single-speed transmission coupling the electric drive motor to the driven axle of the vehicle. This transmission includes a simple gear ratio input, and for most results studied in this model has a ratio of 7.13:1. Another parameter input along with the driveline is an N/V value which is a parameter to quickly convert vehicle speed to motor speed. This value has to do with the characteristics of the driveline along with the wheel radius, hence it is included within this model. Equation 12 shows the

calculation for N/V to convert from meters per second (m/s) to revolutions per minute (rpm).

$$N/V(rpm/[m/s]) = \frac{GearRatio}{r_w*(\pi/30)} \quad \textbf{Equation 12}$$

Prior to calculating values through the driveline, torques and speeds are determined at the drive axle. These values are derived from the vehicle speed, along with the tractive force calculated at the wheels. Using these values, torque is found using Equation 13 while speed is found using Equation 14. Equation 15 shows the special equation used to calculate the torque at the axle for the regen case. This is a special case since regen power is already calculated via a very specific strategy discussed in Section 3.4.1, and therefore must use this power to find torque.

$$T_{axle} = F_{tr} * r_w \quad \textbf{Equation 13}$$

$$S_{axle} = V_{avg} * \frac{30}{\pi * r_w} \quad \textbf{Equation 14}$$

$$(T_{axle,regen})^- = \frac{(P_{tr,regen})^-}{V_{avg}} * r_w \quad \textbf{Equation 15}$$

Now that torques and speeds are defined, the loss through the driveline can be found. The torque loss through the driveline is scaled directly from the drive motor parameters. For this specific motor model, described below in Section 3.3.4, torque loss is defined as 1.2% of the maximum allowable torque of the motor. Once this is established and motor power is determined, a power balance can be completed across the driveline and the power loss can be found, as shown in Equation 16. Note this is only for the propel case. The regen case is calculated in the same way, only it has parameters with the correct corresponding nomenclature.

$$(P_{DL,loss})^+ = (P_{mot,mech})^+ - (P_{tr})^+ \quad \textbf{Equation 16}$$

3.3.4 Motor Model

After calculating torque and speed values through the driveline, the motor can be analyzed. Before power can be found, motor mechanical torque and speed are found. Torque is found using the axle torque calculated in the driveline model section along with the gear ratio of the single-speed transmission and torque loss generated in the driveline (also described in Section 3.3.3). Equation 17 shows the calculation for mechanical motor torque.

$$(T_{mot,mech})^+ = \frac{(T_{axle})^+}{GearRatio} - (T_{mot,loss})^+ \quad \textbf{Equation 17}$$

Motor speed is calculated using the N/V parameter described in the previous section. This allows for a simple calculation and one easily scaled with changing gear ratios. The equation used for finding motor speed from vehicle speed is shown in Equation 18.

$$S_{mot}(rpm) = V_{avg}(m/s) * N/V(rpm/[m/s]) \quad \textbf{Equation 18}$$

Since power flow is a focus of this model, power input of the motor is found next. This power is calculated using Equation 19. This result is combined with a calculated power

loss to then find the electrical power required to achieve this mechanical power through the motor.

$$(P_{mot,mech})^+ = (T_{mot,mech})^+ * S_{mot} * \frac{\pi}{30} \qquad \textbf{Equation 19}$$

The torque-speed motor equation for calculating power loss in the motor is defined by Equation 20:

$$P_{loss} = (\frac{T_{max}*\omega_{max}}{T_{ref}*\omega_{ref}})(k_c T_{ref}^2 \left(\frac{T}{T_{max}}\right)^2 + k_i \omega_{ref} \left(\frac{\omega}{\omega_{max}}\right) + k_w \omega_{ref}^3 \left(\frac{\omega}{\omega_{max}}\right)^3 + C) \qquad \textbf{Equation 20}$$

Where k_c, k_i, k_w ,and C are constants specific to an electric motor. T_{ref} and ω_{ref} are also constants associated with a specific motor. The motor loss equation is set up to help easily scale the power of an electric motor for sizing purposes. T_{max} and ω_{max} can be scaled up or down in order to vary the maximum power of the motor. This is ideal for powertrain component sizing, and the purpose of the study. Finally, T represents the dynamic motor torque and ω represents motor speed. For this study, a UQM 125 Powerphase electric motor is used as a base model. This permanent magnet AC motor has a wide range of operation and a high power rating which meets all of the performance needs in this model. Table 3-2 shows the values for the various constants used in Equation 20 for this model.

Table 3-2: Input parameters for UQM 125

Parameter	Value	Units
kc	0.12	[W/(Nm)^2]
ki	0.01	[W/(rad/s)]
kw	1.20E-05	[W/(rad/s)^3]
C	600	[W]
T_{ref}	300	[Nm]
T_{max}	300	[Nm]
ω_{ref}	838	[rad/s]
ω_{max}	838	[rad/s]

The efficiency and power loss maps are also provided by Ord in his thesis, as he also used similar models for his calculations [13]. Figure 3-10 shows the efficiency map for the UQM 125. As shown here, high efficiency (red area) is achieved when the motor is operating outside of low speed, low torque situations. Since the motor is usually operating outside of this area of low efficiency (blue area), it is expected to have higher efficiencies for the electric system. This contributes to the idea behind offsetting conventional powertrain components with extremely low efficiencies with advanced vehicle powertrains. It is important to note that only the region for positive torque is shown here. Within the low speed, low torque region, the loss within the motor is greater than the loss being brought into the motor through regen. This causes the battery to also discharge to overcome more losses, thus disrupting the efficiency calculations for the motor since two inputs are coming in to simply contribute to losses. This can be controlled with regen operating strategies to cutoff this region of operation, thus only positive torque is shown. Additionally, the motor would operate normally outside of this range, thus the negative torque map would appear as a mirror image of the positive torque map outside of the low speed, low torque area.

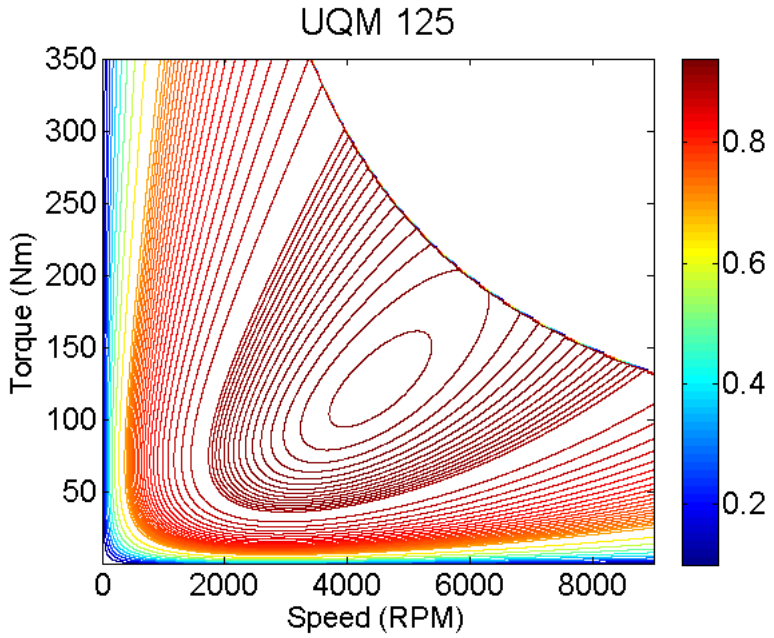

Figure 3-10: Efficiency map for a UQM 125

The power loss for the motor is also mapped out in a similar manner. Figure 3-11 displays the loss produced in the motor using Equation 20. As shown here, in very low speed, low torque scenarios, the loss is low (blue area) whereas in high speed, high torque situations, the losses are higher (red area). It is also evident that the negative torque loss region is a mirror image of the positive torque loss map showing the symmetry of electric motor operation.

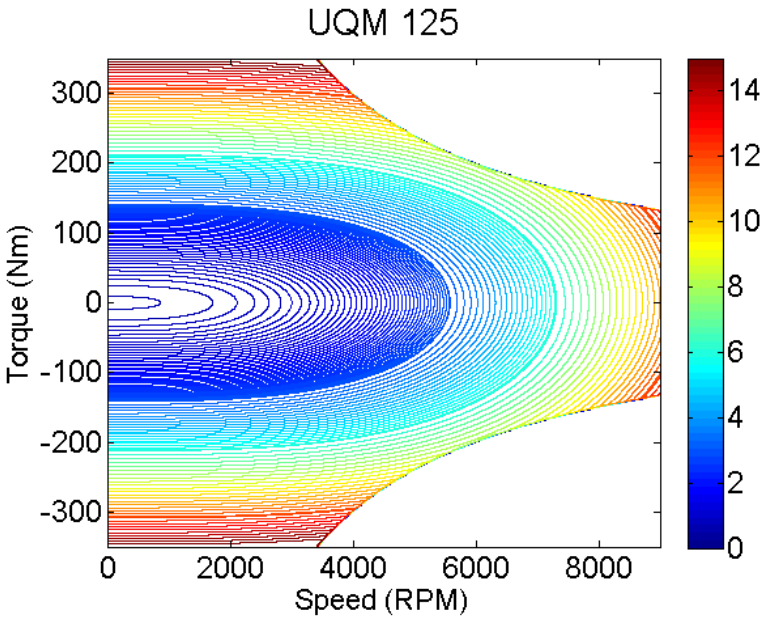

Figure 3-11: Power loss for a UQM 125

The last necessary step in the motor model is finding the electrical energy of the motor. This is completed through the simple power balance found in Equation 21a. Here, P_{loss} is added to the $P_{mot,mech}$ to find the electrical power.

$$(P_{mot,elec})^{+} = (P_{mot,mech})^{+} + (P_{mot,loss})^{+} \qquad \textbf{Equation 21a}$$

$$(P_{mot,elec})^{-} = (P_{mot,mech})^{-} + (P_{mot,loss})^{-} \qquad \textbf{Equation 21b}$$

As with some of the other models, this motor model is used for both propel and regen cases. The equations used for calculating values in the regen case are similar to those shown for the propel case, only having the different conventions, as demonstrated in Equation 21b. To clarify for this regen situation, power is flowing into the mechanical side of the motor to the electrical side instead of from the electrical to mechanical sides as in the propel case. Due to these similar calculations, the equations are demonstrated in the actual model but are not shown here for the other components.

3.3.5 Accessory Load Model

Accessory load is a small detail but very important to overall energy consumption and power loss within a vehicle powertrain. This parameter is an input for the model presented in this thesis and is generally defaulted to a value of 600 W. This value represents the various constant loads on a vehicle, including vehicle control modules, radio, climate control switches, lights, etc. Since this load is constant anytime the vehicle is on, it is taken into account throughout an entire drive cycle and must be overcome in both propel and regen cases. For simplicity, accessory load is accounted for at the terminals of the HV battery. This would be representative of an actual vehicle since this is part of the HV bus normally connected to a DC/DC converter responsible for charging the 12V system within the vehicle. The accessory load parameter can be ramped up or down to reflect situations like high beams being on, or the air conditioning compressor being active.

3.3.6 Battery Model

For this electrified powertrain model, a simple internal resistance model for a battery is generated to calculate energy losses and state of charge. A schematic for the battery modeled is shown in Figure 3-12.

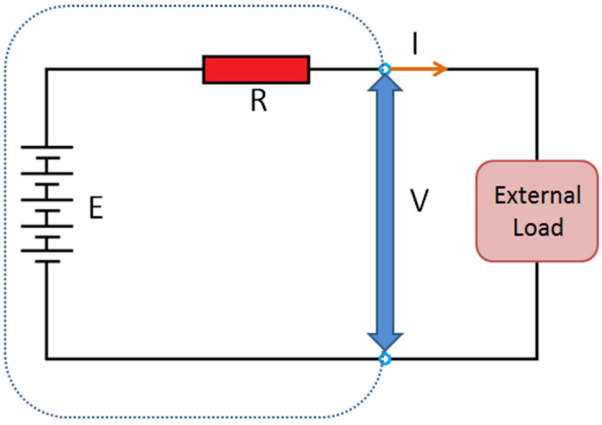

Figure 3-12: Battery model schematic

In Figure 3-12, *R* represents the internal resistance of the battery modeled, *V* is the battery voltage at the terminals, *I* is the battery current, and *E* is the energy source (at potential V_{oc} or "open circuit voltage") of the battery. In order to find the change in state of charge of the battery based on a power demand, the output current of the battery is needed.

Initially, Equation 22 and Equation 23 represent the ideal power of the battery, and the means of calculating power loss of the battery. This ideal power is equivalent to the internal battery power neglecting the internal resistance which is always present.

$$P_{batt,int} = I_{batt}V_{oc} \quad \textbf{Equation 22}$$

$$P_{batt,loss} = I_{batt}^2 R_{int} \quad \textbf{Equation 23}$$

When $P_{batt,loss}$ is plotted, as in Figure 3-13 for a 7.1 kWh battery, the trend for how it relates to I_{batt} is quite easy to see. As shown in the figure, the loss follows a quadratic trendline with a minimum when current draw is equal to zero. As more current is drawn from the battery or put into the battery, more loss is proportionally produced according to Equation 23.

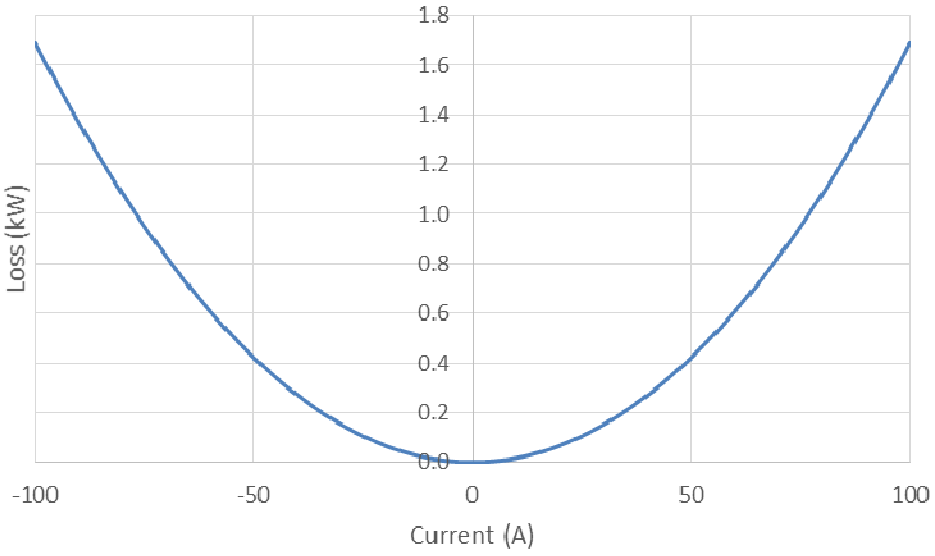

Figure 3-13: Battery loss vs. battery current

With these equations, it is easy to establish the actual power output of the battery at the terminals through the power balance shown in Equation 24. After substituting values from Equation 22 and Equation 23, an equation with one unknown is produced as displayed in Equation 25.

$$P_{batt,net} = P_{batt,int} - P_{batt,loss} \quad \textbf{Equation 24}$$

$$P_{batt,net} = I_{batt}V_{oc} - I_{batt}^2 R_{int} \quad \textbf{Equation 25}$$

Equation 25 can now be rearranged to give an equation to solve for the current flowing out of the battery. Considering the quadratic nature of the equation, Equation 26 is formulated via the Quadratic Equation and used to solve for I_{batt}.

$$I_{batt} = V_{oc} - \sqrt{\frac{V_{oc}^2 - 4R_{int}P_{batt,net}}{2R_{int}}} \quad \textbf{Equation 26}$$

It is important to note that due to the backwards flow of this model, $P_{batt,net}$ is an unknown here but is calculated by adding the demand at the battery terminals. This demand is

produced from the drive motor. After the calculations completed within the motor model, the demand at the DC side of the motor/inverter system. This demand is then combined with the constant accessory load to give the net demand at the battery terminals. This net value includes both positive and negative power at the battery terminals, which translates to both propel and regen cases. Positive demand at the battery terminals demonstrates power discharging from the battery to propel the vehicle. Negative demand here represents the regen case and thus power entering the battery to charge the ESS. With $P_{batt,net}$ known, I_{batt} can be found via Equation 26, followed by $P_{batt,loss}$ from Equation 23 and V_{batt} from Equation 27 shown below. This parameter tracks the fluctuations in voltage throughout operation of the vehicle.

$$V_{batt} = V_{oc} - I_{batt}R_{int} \qquad \textbf{Equation 27}$$

Figure 3-14 demonstrates the trend associated with how changing current values affect the voltage of the battery. As shown here for a 7.1 kWh battery, when no current is being drawn from the ESS, the voltage remains at its open circuit voltage, which in this case is 350 V. When current is being drawn due to load, voltage follows a linear trend, increasing or decreasing depending on charging or discharging. The relationship described in the figure shows that V_{oc} is the y-intercept of the trendline, while R_{int} (which is .168 Ω for this case) represents the slope. The internal resistance of the battery cab be a function of SOC and temperature. However, the results given here are for a constant R_{int} at an average SOC and operating temperature.

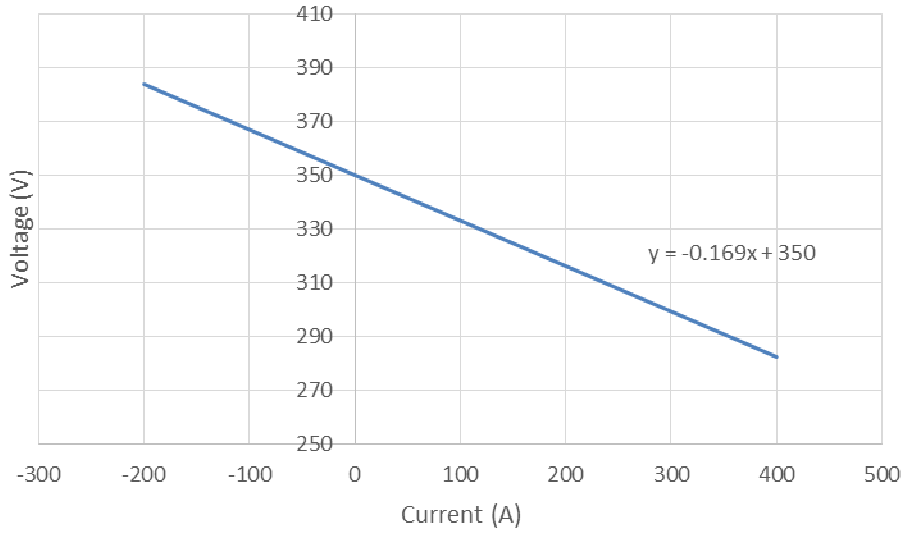

Figure 3-14: Battery voltage vs. battery current

With the current and loss of the battery calculated, the internal power and energy can be found through rearranging Equation 24 and then integrating the power over the time of the drive cycle. This energy can then be subtracted from or added to an initial condition of energy capacity based on the battery size, to calculate and track the SOC, as shown in Equation 28.

$$SOC_{new} = SOC_{old} - \left(\frac{E_{batt,int}}{E_{batt,cap}}\right) \qquad \textbf{Equation 28}$$

Where $E_{batt,cap}$ is the total energy capacity of the battery pack set as an input. Note that the change in energy can be both positive and negative for the generated model in order to account for charging the battery with regenerative braking. It should also be noted that energy discharge for propelling is positive current, while charging is indicated as negative current.

Aside from calculating values based on power flow through the powertrain, several values must be set prior to running any simulations for the battery model to operate accurately. These parameters control what size battery is included in the vehicle as well as several characteristics such as open circuit voltage and total change in SOC permitted. Table 3-3 shows an example of the parameters used as inputs for the battery model. These inputs are for a PHEV with a Charge Depleting mode hence the battery is reasonably large. With these values for $SOC_{initial}$ and ΔSOC, the vehicle would deplete the battery until it reaches the lower SOC of 20%. These parameters are also important for calculating overall EV range for the vehicle since useable capacity is necessary for this calculation. It is important to note that R_{int} is actually a calculated value from several of the other inputs within the table, as shown in Equation 29. Another input of importance is the efficiency of the on-board HV battery charger, $\eta_{charger}$. This parameter allows the DC energy within the ESS to be traced back to the AC grid energy necessary to recharge the ESS after driving. The AC value is quite useful in energy consumption calculations.

Table 3-3: HV battery characteristics

Parameter	Value	Units
V_{oc}	350	[V]
R_{int}	0.064	[ohm]
E_{cap}	18800	[Wh]
m_{batt}	330	[kg]
$SOC_{initial}$	98.5	[%]
Δ SOC	78.5	[%]
$\eta_{charger}$	87	[%]

$$R_{int} = .012/\frac{E_{batt,cap}}{1000} \qquad \textbf{Equation 29}$$

3.3.7 Engine Model

The engine is modeled using two different methods, one for each of the SHEV operating strategies. For both of these energy management strategies a torque-speed based model is used since the output power of the engine is known. This is because in order to meet the driver demand, a specified amount of power needs to be commanded. Within this overall vehicle model, this is the only instance of forward based power flow. Since engine operation is based on an engine speed and torque, values for these parameters must be determined prior to continuing to trace power through the vehicle.

3.3.7.1 Thermostatic Engine Model

The engine model for the Thermostatic SHEV is quite simplified. Since engine operation is quite restricted within the "bang-bang" strategy described in Section 3.4.3, one speed

and one torque value are specified by the user to produce an engine power. Usually, this operating point would correspond to the maximum efficiency point of the chosen engine, but the freedom of manipulation is left up to the user. Once a speed and torque are chosen, Equation 30 is used to calculate the mechanical engine power to be outputted to the generator.

$$P_{eng,mech} = T_{eng} * S_{eng} * \frac{\pi}{30} \qquad \textbf{Equation 30}$$

Aside from using engine torque to simply calculate engine power, fuel energy can eventually be calculated to produce values for fuel consumption based on the fuel type selected. Prior to this, an engine efficiency is found using Equation 31.

$$\eta_{eng} = \frac{\eta_{therm}}{1+\frac{fmep_0 V_d}{4\pi T_{eng}}} \qquad \textbf{Equation 31}$$

Where η_{therm} is the thermodynamic efficiency of the specified engine, which is assumed a constant. $fmep_0$ is the friction mean effective pressure (kPa) at zero power, V_d is the volumetric displacement (L) of the engine and T_{eng} is the output torque (Nm) of the engine, which was previously selected. In this model, engine efficiency is only a function of torque and not speed. Values for engine parameters greatly depend on what type of fuel is being used, and thus what type of engine is present. Table 3-4 shows values for several different types of engines used in this model. Note that BMEP stands for brake mean effective pressure and is a value used to scale engine efficiency with V_d. Also note that although the compression ignited direct injection (CIDI) diesel engine is not used at this moment within this 1 Hz model, it is displayed for comparison.

Table 3-4: Engine efficiency parameters

Engine Type	η_{therm}	fmep0	Max η_{eng}	BMEP at Max η_{eng}
Units	%	kPa	%	kPa
Base SI	40.0	145	35.0	1000
Improved SI	44.0	140	38.6	960
CIDI TC	45.5	200	40.6	1650

Figure 3-15 illustrates an example of how engine efficiency is affected by increasing torque. The example shown here is for a 1.5L E85 engine which has the characteristics shown in the table above labeled "Improved SI". As shown, efficiency is directly proportional to torque in that with increasing torque, efficiency also increases. This efficiency does have a maximum however so that if power continues increasing up to the limits defined in the engine model, the torque and therefore the efficiency is limited to 38.6%.

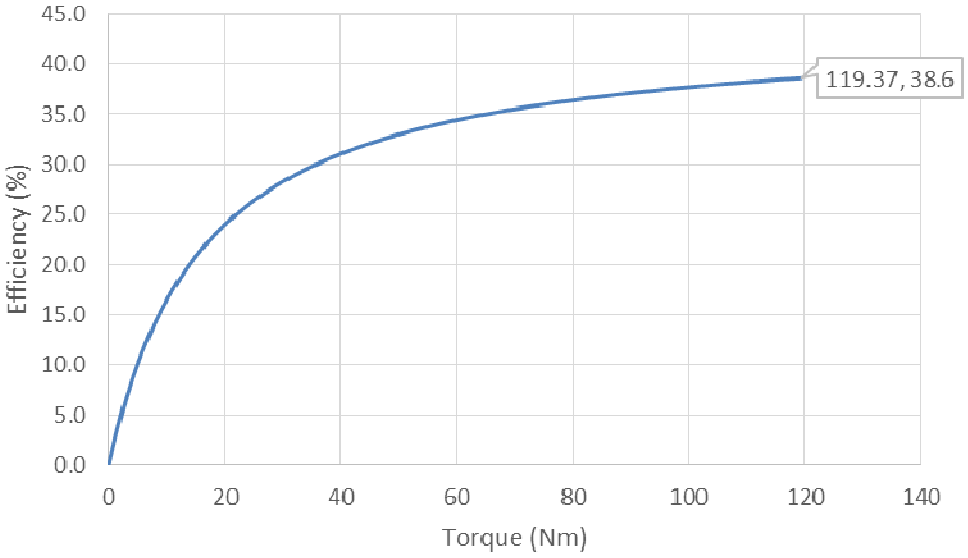

Figure 3-15: Engine efficiency vs. engine torque

Now that an engine efficiency is found, the power can be traced back to the fuel input power and in turn, fuel energy. The engine power loss is calculated using Equation 32. Here, the engine output power and efficiency are used to find the power loss. Next, a standard power balance seen in Equation 33 is completed to produce the power needed in fuel at each time step to complete the drive schedule. This power is integrated to find total fuel energy and in turn, gallons of fuel used to complete a drive cycle. This calculation is of utmost importance as it allows for fuel consumptions for various vehicles to be compared and thus achieve one of the overall goals of this vehicle model.

$$P_{eng,loss} = \frac{P_{eng,mech}}{\eta_{eng}} - P_{eng,mech} \qquad \textbf{Equation 32}$$

$$P_{eng,fuel} = P_{eng,mech} + P_{eng,loss} \qquad \textbf{Equation 33}$$

3.3.7.2 Load-following Engine Model

The engine model required for the Load-following SHEV is slightly more complex compared to the Thermostatic engine model. This is due to a wider range of operating points as opposed to the one single operating point. The main difference between actual calculations that occur within these two models is related to finding engine torque and speed. Instead of simply commanding these two values, each is calculated based on the power demand on the engine. Equation 34 shows the method for determining $P_{eng,mech}$. It is important to note that the power demand is defined by these parameters since the engine is not affected by regenerative braking, thus only the propel case for the battery terminals is applicable. The losses of the generator motor are included here since this additional loss is removed from the power flow after the engine. Because of this, to get the appropriate power level at the battery terminals, this loss must be included within the demand. Due to the limits of the 1 Hz model, the $P_{gen,loss}$ parameter is from the previous time step since a circular reference loop is created when using the loss from the current time step. Over the entire cycle, this equation allows the vehicle to be Charge Sustaining which is desirable.

$$P_{eng,mech} = (P_{batt,T})^{+} + P_{gen,loss} \qquad \textbf{Equation 34}$$

Once this parameter is found, the speed and torque of the engine can now be calculated. This again is much more complex for this situation. As mentioned, instead of simply one operating point for the engine, a line of best operation is followed for the selected engine. Figure 3-16 shows this operating line for a 2.4 L E85 engine. The orange line represents wide open throttle (WOT) which is the maximum power line for the engine. This is not, however, the most efficient way to operate the engine. To mitigate this, the "absolute operation" line in the figure shows the range for efficiently operating the engine across various power levels and approximates the minimum brake specific fuel consumption (BSFC) line. This line is calculated based on engine torque and speed from scaling performance with volumetric displacement and brake mean effective pressure. The "user defined limits" shown on the figure represent the ability of the user to restrict operation of the engine. These limits are for the minimum and maximum allowable operating powers at which the engine can operate. These limits will be discussed further in Section 3.4.4.

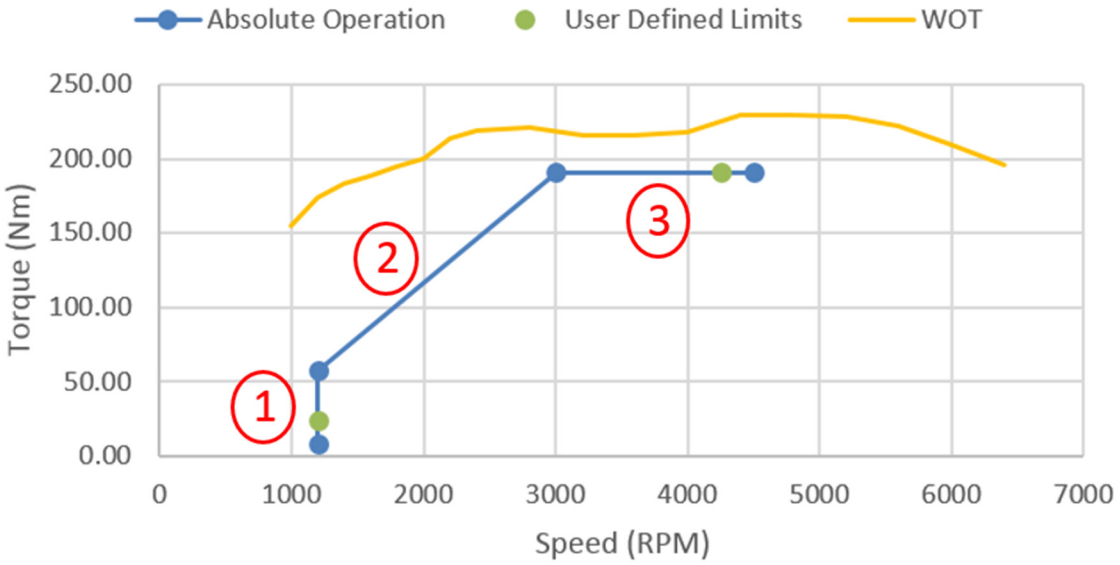

Figure 3-16: 2.4 L engine operating line

With an operating line established, engine speed can be easily found for a given $P_{eng,mech}$. Each of the corners of the absolute operation line found in Figure 3-16 show changes in operation. The presence of these corners show the three distinct regions labeled in red within the figure. When calculating engine speed, the region where $P_{eng,mech}$ falls on the operating line is determined, thus specifying the corresponding speed. Looking at region 1, the speed is constant, thus if the engine is operating within this area, the speed is given by the scalable parameter $S_{eng,low}$. Region 2 offers a slightly more complex calculation process as the relationship is not constant, but linear. Using the scalable values used to create the operating line, the engine speed is derived through solving a quadratic equation. Finally, Region 3 has a constant torque, thus speed is calculated using Equation 35 where $T_{eng,opt}$ is the constant torque throughout region 3.

$$S_{eng} = \frac{P_{eng,mech}}{T_{eng,opt}} * \frac{30}{\pi}$$ **Equation 35**

The final parameter to be solved for prior to resuming normal operation described in the previous section is engine torque. This is very simply calculated using Equation 36 considering S_{eng} and $P_{eng,mech}$ are both known values at this point. With this torque calculated, efficiency can be found and eventually total fuel energy consumed.

$$T_{eng} = \frac{P_{eng,mech}}{S_{eng}} * \frac{30}{\pi}$$ **Equation 36**

3.3.8 Generator Model

The generator model is created using similar torque-speed methods as the motor model. This is an accurate representation considering both are similar types of electric motors. The main difference between the generator and the motor is that where the motor receives its electrical power from the battery to then be delivered to the wheels mechanically, the generator accepts mechanical power from the engine and converts this to electrical power to charge the ESS or power the drive motor. Due to this fact, speed and torque are very simple calculations for the generator and are based off of engine speed and torque along with a ratio to allow for mechanically geared applications such as having a pulley or chain drive coupling the two components. Equation 37 and Equation 38 show the methods for calculating generator speed and torque. The values found here are then used in Equation 20 with appropriate input parameters to match the motor type and size to find the power loss. Finally, a power balance is completed using Equation 39 to find the total output power for the generator. Note that the sign convention for the generator is always positive since power is only flowing in one direction; from the engine to the generator.

$$S_{gen} = S_{eng} * SpeedRatio_{gen}$$ **Equation 37**

$$T_{gen} = \frac{T_{eng}}{SpeedRatio_{gen}}$$ **Equation 38**

$$P_{gen,elec} = P_{eng,mech} + P_{gen,loss}$$ **Equation 39**

The generator used for the majority of this study is represented by a custom built, in-line permanent magnet AC motor used by HEVT in the EcoCAR 2 competition. This generator is made to fit precisely into HEVT's vehicle and is referred to as the "P2" motor/generator which is derived from its post-engine, pre-transmission position. The P2 generator has the characteristics described in Table 3-5.

Table 3-5: Input parameters for P2 generator

Parameter	Value	Units
kc	0.288	$[W/(Nm)^2]$
ki	0.003	[W/(rad/s)]
kw	7.63E-06	$[W/(rad/s)^3]$
C	300	[W]
T_{ref}	125	[Nm]
T_{max}	125	[Nm]
ω_{ref}	680	[rad/s]
ω_{max}	680	[rad/s]

Once the output power for the generator is found, this power is combined with the power at the terminals of the battery. Through doing this, the generator power meets the demand of the vehicle when it is on and is combined with the battery output power to buffer changes. This allows the battery to either be charged, through more power being generated than is necessary to meet demand, or supplement extra power in addition to that produced by the generator during moments of very high demand. Equation 40 shows how the electric generator power is subtracted from the net power at the battery terminals. This value is subtracted since any excess will charge the ESS and thus maintains the nomenclature defined previously.

$$P_{batt,net} = P_{batt,T} - P_{gen,elec} \qquad \textbf{Equation 40}$$

Where $P_{batt,T}$ is the net power demand at the battery terminals. This $P_{batt,net}$ is then input into the battery model for SOC calculations.

3.4 Energy Management Strategies

With each of the models for the various powertrain components defined, it is also vital to understand the energy management strategies behind manipulating and coordinating these different components to perform in a way that makes since. Each of the sections below illustrates a different section of hybrid vehicle controls and shows how decisions are made based on various limits and conditions. It is important to note that within the model itself, all of these decisions are made via coded "IF" statements but are displayed graphically for ease of deciphering.

3.4.1 Regenerative Braking

Regenerative braking is the first area where energy flow really needs to be managed outside of simply calculating the energy going to the next component in the powertrain. This is a parameter that can be turned on and off but is quite useful for recapturing energy available at the wheels during a braking event. Over all, regen braking increases the EV range of a PHEV and aids in decreasing overall energy consumption since energy normally being lost to friction braking is reused. Prior to discussing the process for decision making as it applies to regen braking, it is important to define the various parameters and limits involved in the process. Table 3-6 shows the inputs required for controlling regen.

Table 3-6: Regenerative braking characteristics

Parameter	Value	Units
ζ	0.6	[---]
V_{min}	2.24	[m/s]
$-P_{tr,lim}$	-50	[kW]
$-T_{w,lim}$	-1100	[Nm]
$-F_{tr,lim}$	-3.40	[kN]

Where, ζ represents the regen brake fraction, V_{min} is the minimum cutoff vehicle speed for regen, $-P_{tr,lim}$ is the negative power limit of the drive motor, $-T_{w,lim}$ is the minimum allowable negative wheel torque, and $-F_{tr,lim}$ is the negative tractive force limit of the vehicle for regen braking. To begin, ζ is used to determine how much regen should be completed during a braking event and in turn, how much braking should be done using friction brakes. This is an input chosen by the user and can range from 0 to 1, where 0 is all friction brakes and 1 is 100% regen.

V_{min} is also selected by the user and causes regen braking to cutoff below this minimum vehicle speed. This limit is set in place to maintain efficiency within the system. At extremely low vehicle speeds, regen braking is not always beneficial since the energy collected at the wheel is not enough to overcome the losses to reach the battery, thus causing the battery to discharge energy to overcome those losses. To prevent the battery from releasing energy to simply overcome losses, this minimum vehicle speed is set, below which friction brakes take over 100% of braking.

As mentioned, $-P_{tr,lim}$ is the negative power limit of the drive motor. This is set by the user, however, it is affected by the size of the drive motor selected for the vehicle powertrain. For this research, a value of -50 kW is chosen to coordinate with the 125 kW motor. Where operation is concerned, any time the vehicle is attempting to regen a higher power than this limit, the regen power available will be defaulted to this value and thus not allow unrealistic values to be produced which would be representative of capabilities not available to the vehicle.

The final constraint placed on the regenerative braking strategy is caused by the tractive force limit discussed in the Rask paper within the literature review for this thesis [16]. This parameter, again, is a maximum regenerative braking force for the specific traction system and prevents dangerous stability and handling situations on the vehicle. As a result this value causes regen to cut out should the negative tractive force experienced by the vehicle exceed $-F_{tr,lim}$. This limit is not a direct input from the user, but is calculated based on $-T_{w,lim}$, which in turn is a parameter calculated based on several vehicle parameters. The drive motor used for this research includes a negative continuous torque limit of -150 Nm. This value is traced through the driveline to the axle after multiplying by the gear ratio and removing losses incurred. From this point, $-F_{tr,lim}$ is calculated for the vehicle based on Equation 41. Note that this parameter must be scaled with motor size and driveline characteristics and is approximated for use in this research.

$$-F_{tr,lim} = \frac{-T_{w,lim}}{r_w} \qquad \textbf{Equation 41}$$

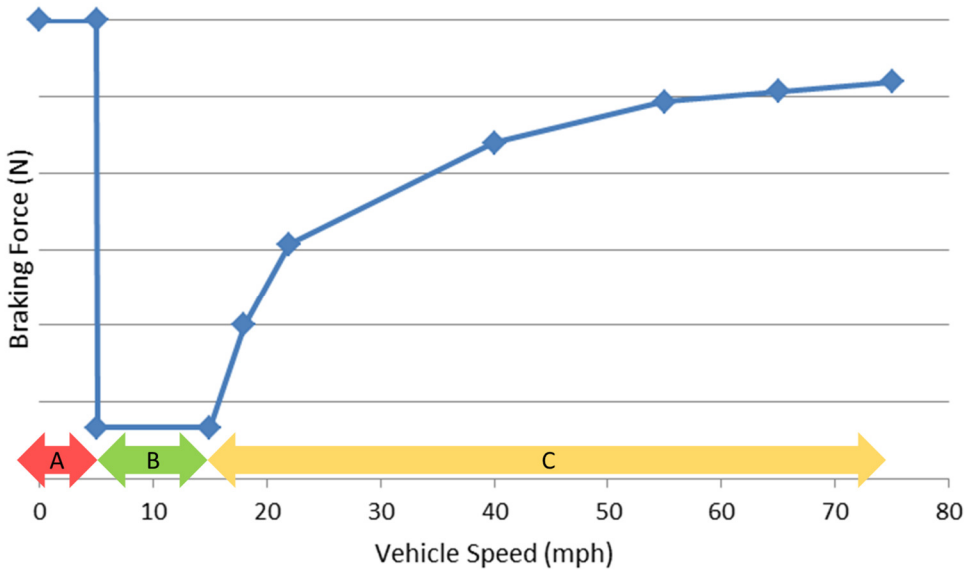

Figure 3-17: Example regenerative braking envelope

With all of these limits in mind, Figure 3-17 demonstrates the operating window for regenerative braking. For every situation, the vehicle applies the regen fraction to the total negative tractive power. Once this desired power is calculated, the limits are then applied to it to see if the desired regen power is possible or if it needs to be limited in any way. Region A in the figure shows the V_{min} cutoff. At 5 mph, the vehicle cuts off regen and friction brakes take over 100% of the braking power. It is important to note that for physical implementation, ramping into regen is important for drivability, however for this simplified model, drivability is not a concern, thus a simple cutoff is used. Region B then shows the $-F_{tr,lim}$. Here, instead of a point in the figure where traditionally power would be the only other limit, a flat cutoff is shown representing this constraint. Finally, Region C shows the maximum power limit due to the drive motor. As long as the desired regen power is within this envelope, the desired power will be the actual regen power produced. If one of the limits are incurred however, the actual regen power defaults to the limits described above. Through following this strategy, regenerative brake energy is able to be utilized accurately by the modeled vehicle. In fact, Figure 3-18 shows the correlation between regenerative braking and energy consumption. This example is completed for a US06 drive schedule and demonstrates how with regenerative braking, energy consumption from the ESS is reduced by about 2.5 MJ.

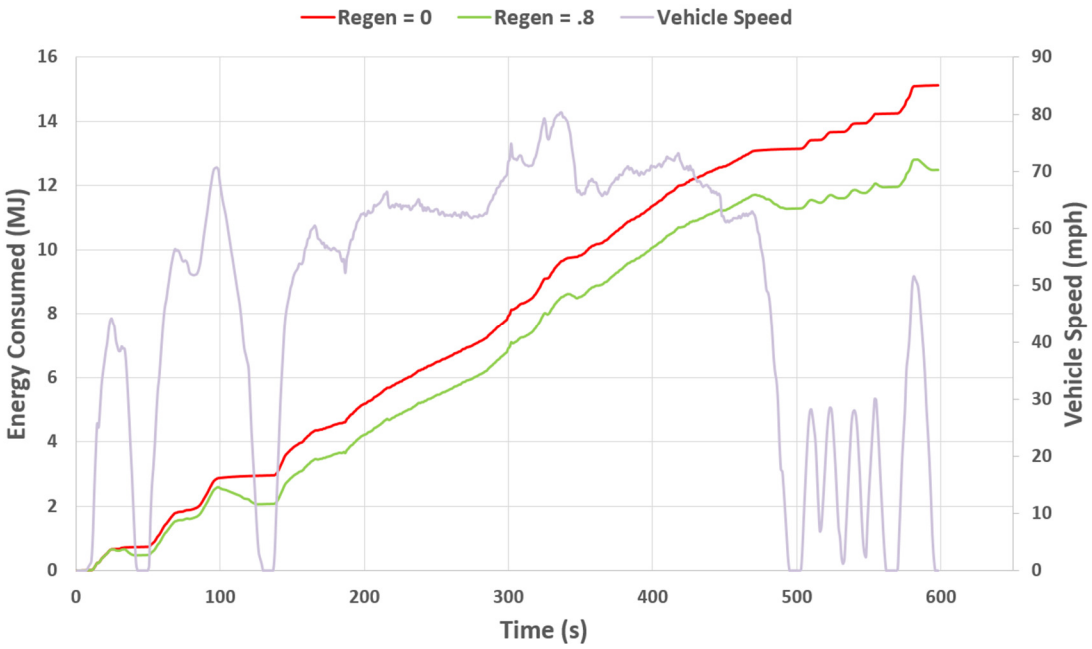

Figure 3-18: Energy consumption with respect to regen brake fraction

Finally, although regen brake fraction is an input for this model, it is important to also calculate the actual fraction at the end of each simulation. This is to see what portion of braking is done through regen with the various limits included. This is found simply through using Equation 42 below:

$$\zeta = \frac{(P_{tr,regen})^-}{(P_{tr})^-} \qquad \textbf{Equation 42}$$

As shown here, the power due to regen braking is divided by total negative tractive power to see what portion of the braking is done through regen. This value can then be compared to the input value for regen brake fraction to ensure that the vehicle is behaving properly and as expected. This regen brake fraction value is an overall, integrated, drive cycle average energy ratio. Although regen braking can be a very complex control strategy, this model allows for regen to be introduced with several limits in a simple and understandable way, which achieves the educational goal here. It is also quite easy to manipulate which is again very beneficial for freedom of design.

3.4.2 BEV Controls

For a Battery Electric Vehicle, the control strategy is very straight forward. Considering there is solely one fuel source and one torque source, energy must flow from the battery to the motor and then travel through the single-speed transmission to reach the wheels. There are losses through each component, as mentioned previously, thus this must be accounted for during calculations. The only complex piece of BEV controls is managing regenerative braking. This area was discussed in the previous section which shows how energy is recovered from the tractive energy at the wheels. Once the energy is gathered, it flows backwards through the driveline, motor, and back into the battery to charge the ESS. With such a simplified strategy, this model tracks SOC within the ESS to calculate energy consumption. It is important to note that this model does not cap the battery at a lower

limit, since none of the drive cycles would fully deplete the battery. If a user defines a longer drive cycle which may deplete the full charge of the ESS, user discretion is advised to track where the useable lower limit of the battery is, which should then be taken into account for full energy consumption results. The total useable capacity is taken into account by the Δ SOC on the inputs page. This value aids in the total range calculation (shown in Equation 43), which is present in the results tab of this model.

$$EV\ Range(km) = \frac{E_{batt,cap} * \Delta SOC}{E_{batt,int}} \qquad \textbf{Equation 43}$$

Where $E_{batt,cap}$ is in Wh, Δ SOC is a fraction, and $E_{batt,int}$ is in DC Wh/km.

3.4.3 SHEV Thermostatic Controls

In a Series hybrid, energy management is more complex than a simple BEV. This is because controlling multiple torque sources means modulating the output of an engine and generator along with having the battery as a fuel source. With two fuel sources, a control strategy must decide how and when to use the genset and/or the battery to supply power to the drive motor. The goal of the strategy is to minimize fuel consumption of the vehicle, while maintaining the battery within SOC limits. In this 1 Hz model, a Thermostatic, also known as a "bang-bang", control strategy is implemented. Figure 3-19 shows an example of the thermostatic control strategy. An upper and lower battery SOC limit is implemented and if the upper limit of the SOC is reached, the genset is switched off. If the lower SOC limit is reached, then the genset is commanded to turn on. These limits are determined by the user within this model and are often referred to as an "SOC window". A target SOC is input, which will be the middle of the SOC window. Then the SOC High and SOC Low, as these parameters are called within this model, are set to be + or – the SOC window from the target SOC. Table 3-7 shows an example of these inputs used for a Charge Sustaining SHEV. An important note is that for this strategy, the engine operates only at its most efficient point. Since the only command given to the engine is on or off, the operating point remains constant when on, as described in Section 3.3.7.1.

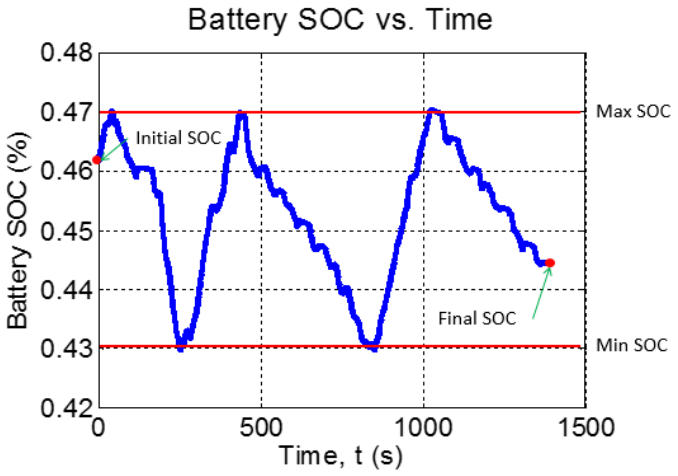

Figure 3-19: Example of Thermostatic control strategy

Table 3-7: Sample CS SOC inputs

Parameter	Value	Units
CS SOC Target	45	[%]
CS SOC Window	±2	[%]

Figure 3-20 shows the actual decision making process for implementing this Thermostatic strategy. First, the SOC from the previous time step is observed and undergoes two tests. It is determined if this previous SOC is above SOC High or if it is below SOC Low. If it is exceeding SOC High and the previous engine status is on, then the engine status must go to off. This is to prevent too much power from being generated, thus causing battery SOC to go outside the SOC window. Comparably, if the previous SOC is below SOC Low and the previous engine status is off, not enough power will be produced to stay within the SOC window, thus the engine status is changed to on. If the SOC is not meeting any of these conditions, the vehicle is obviously operating within the allowable SOC window, thus the engine status remains whatever it was during the previous time step, either off or on. This strategy, although quite simple, is able to maintain charge within the ESS and operate as a Charge Sustaining vehicle while preventing rapid engine on/off situations. It is also important to note that this strategy does still incorporate regenerative braking, however since the controls are based on SOC, as regen charges the battery, the engine operating strategy still looks at the resulting SOC changes and is thus unaffected.

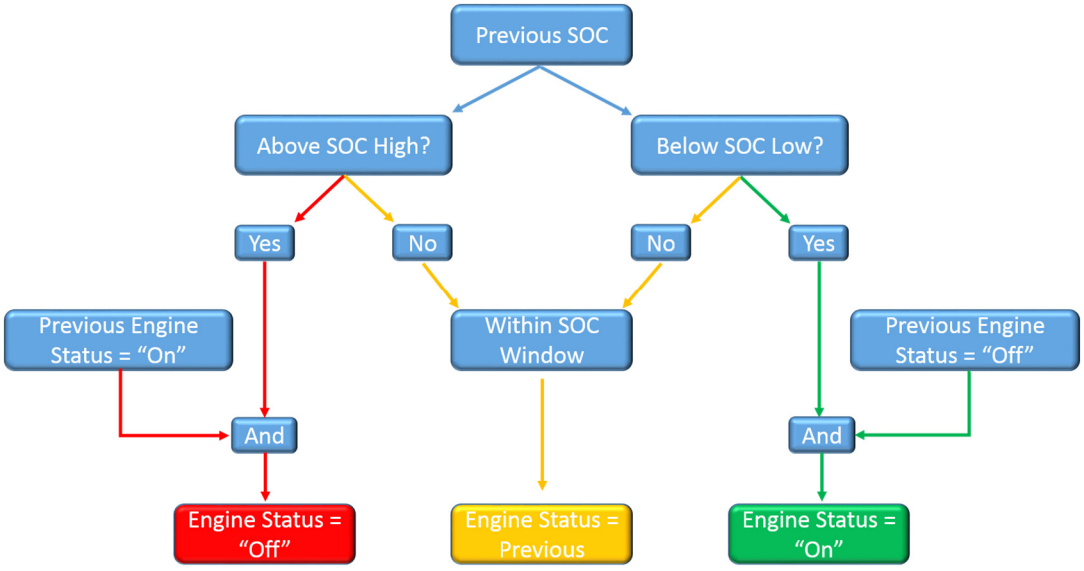

Figure 3-20: Thermostatic control strategy

In order to generate meaningful consumption values for Charge Sustaining PHEVs, results should be charge balanced. This means that the initial SOC and final SOC need to be near equal, which in turn means that the energy consumption from the ESS is less than 1% of the energy consumption of the fuel tank. This is ensure that the energy consumption numbers accurately reflect the performance of the powertrain. In order to maintain a charge-balance, initial SOC values are iterated over repeating drive cycles until the initial and final SOC are close. For this model, this is completed through the use of a programmable macro within Microsoft Excel. The macros used will be discussed in more detail within Section 3.5.2. It is important to note that when charge balanced results are

desired, strict attention must be paid to sizing components. For example, when selecting an engine, the size and power operating point specified for the engine must be enough to meet the power demands of the drive cycles or the vehicle will continue Charge Depleting and thus be unable to charge balance.

3.4.4 SHEV Load-following Controls

The energy management strategy for a Load-following SHEV is quite a bit more complex than that of a Thermostatic SHEV. This strategy does build on the SOC-bound Thermostatic, however, Load-following must also consider engine operating limits. When using this strategy, the engine is on whenever possible. The main idea is for the genset to output the appropriate amount of power to meet the demand at the battery terminals, thus removing the need to charge and discharge the battery unless absolutely necessary. To understand how this is accomplished, Figure 3-21 displays the decision making process in a step-by-step manner. It is important to note that prior to even looking at the SOC window, this SHEV is forced to Charge Deplete until reaching SOC Low for the first time. At this point, the strategy shown takes over with the SOC comparison test. As seen in the Thermostatic strategy, if SOC High is reached, the engine turns off to prevent too much power from being generated. Comparably, if SOC falls below SOC Low, the engine is turned on and operates at $P_{eng,opt}$ which is the optimum operating point of the engine. This is so the battery will gain charge in an efficient way. After the control strategy ensures that the vehicle is operating within the SOC window, power limits are now tested. As explained in Section 3.3.7.2, this model creates an operating line (Figure 3-16) of best efficiency for the engine at a chosen power level. Additionally, the user can introduce power limits for the engine both for minimum and maximum operation. With these in mind, the demand for the genset is compared against these limits to decide where it can operate. As seen in the figure, if P_{demand} is less than the minimum allowable engine operating power, $P_{eng,min}$, the engine is forced off. In addition, if P_{demand} is greater than the maximum allowable engine power, $P_{eng,max}$, the engine is turned on at $P_{eng,max}$ and additional power needs can come from the battery. This is an event where some battery discharge is required to meet an unusually high demand, however, as soon as this high demand situation is over, the vehicle resumes normal operation to again minimize ESS charge and discharge. Finally, if P_{demand} does not exceed either of these conditions, the engine is allowed to operate at the specified power level and does so to meet the demand of the vehicle.

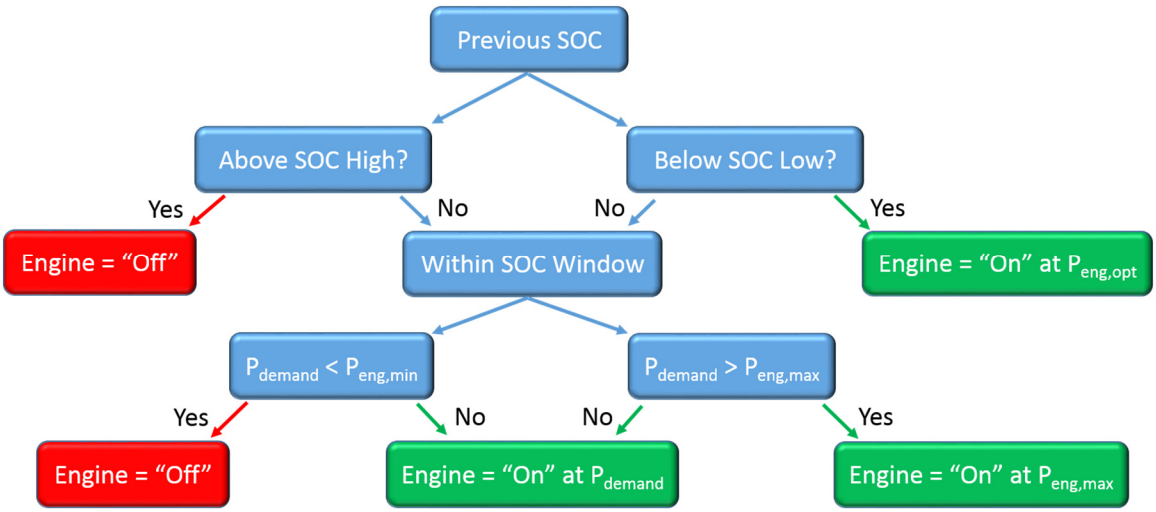

Figure 3-21: Load-following control strategy

To further refine this energy management strategy, a timer is input into the model. Since this model is not a physical vehicle, certain unrealistic situations can occur if not prevented by limits. One of these situations which could occur is very rapid engine on/off. When not limited, the model would decide when the engine should be off and may in the next second decide the engine should be on. This may occur several times in rapid succession causing numerous engine starts. This is not quite realistic since, although many engine starts could occur, though this is not recommended, a physical engine would not be able to simply turn on and operate at, for example, maximum power in one second and then turn back off. It would take some time to ramp up to this power level and slow back down after being commanded off. As a result, this model implements an engine timer to prevent this pulse-width modulating behavior. The engine remains in an on or off state for at least 30 seconds at a time. After this time, the control strategy decides if the engine should continue in the state it is in, or change states. This is an example of improving the integrity of a computer model to make it more realistic. Aside from this, the results for this Load-following strategy are also found via charge-balancing to ensure valid results.

An example of this operating strategy is seen in Figure 3-22 below. As shown here for a Charge Sustaining SHEV with a 3.1 kWh battery, as the vehicle follows the velocity trace, the engine provides power to propel the vehicle. The drive cycle shown here is a 505 schedule, which is the first 505 seconds of a UDDS. The green line here shows the engine on/off status, and the engine can only produce power when the "on" command is given. It can also be noted that the minimum engine operating power for this vehicle is set to 5 kW. This is to keep the engine out of extremely inefficient regions. Aside from the engine on flag, this figure also demonstrates the 30 second engine timer. The engine is forced to maintain whatever state it is in for 30 seconds before it is allowed to change states. This again prevents rapid starts and stops for this already inefficient component. When the engine is off, the vehicle enters a CD state where the EV system takes over propulsion. This can be seen in the figure when the SOC begins decreasing when the engine is off. When the SOC reaches a point where it is falling below the lower SOC limit, the engine is forced to operate at its optimum operating point. An example of this is shown around second 300 in the figure where the engine output is at a constant 37.5 kW. This is to bring the SOC back to an acceptable level prior to resuming normal operation.

Figure 3-22: $P_{eng,mech}$ and SOC vs. time for 3.1 kWh battery

3.5 Inputs and Outputs

Within the 1 Hz model described within this thesis, there are numerous inputs and outputs present to both describe the components present within a vehicle powertrain and display the results of running this vehicle through various drive schedules.

3.5.1 Inputs

Although the inputs of the model have been described separately throughout the component models above, it is important to note how these inputs are manipulated and what values should or should not be changed by the user. On the inputs tab of the model, seven component inputs are shown, including regenerative braking characteristics. These input tables provide a single area within the model where the vehicle can be manipulated, increasing ease of use and understanding from the user. The main detail vital to the operation of this model when it comes to the inputs page is paying close attention to the variables that are highlighted versus those that are not. These highlighted cells represent parameters that can be changed by the user. The cells which are not highlighted are variables which should not be changed since the values are, for the most part, calculated from the highlighted cells. Table 3-8 shows an example of this through displaying the "Vehicle Glider Characteristics" information. As shown here, most cells are highlighted since many of these inputs are vehicle specific. In spite of this, both the "C_dA" cell and the "m_i" cell are not highlighted since these are calculated from other cells within the table. Through following this strategy, users can define vehicle powertrains while maintaining the integrity of the model.

Table 3-8: Example parameter input table

Vehicle Glider Characteristics		
Parameter	**Value**	**Units**
C_{rr0}	0.0102	[---]
C_{rr1}	0	[1/(m/s)]
C_d	0.313	[---]
A	2.3	[m^2]
C_dA	0.720	[m^2]
ρ_{air}	1.2	[kg/m^3]
m	2260	[kg]
m_i factor	1.04	[---]
m_i	2350.4	[kg]
g	9.81	[m/s^2]
r_w	0.324	[m]
P_{acc}	600	[W]

One other area of the inputs page which is slightly different from most of the tables present is the fuel data. This data is selected by one simple drop-down box to choose the fuel being used. The values for GHG_{WTW}, PEU_{WTW}, the lower heating value of the fuel (LHV_{fuel}), and the density of the fuel (ρ_{fuel}) are all referenced from the "Fuel Properties and WTW" tab. This fuel data is generated by ANL's Gasses, Regulated Emissions and Energy Use in Transportation (GREET) model and gives details values for emissions and PEU impacts of various fuels [19,20]. One other important note concerning the inputs of this model is that comments are included on many cells throughout the entire model. This is to provide insight on nomenclature, variables, and decision making processes.

3.5.2 Outputs

After understanding how values are input into this model, it is also very important to understand where and how data is output. First and for most, most detailed data is displayed on each drive cycle sheet. Here, second-by-second power flow is generated and displayed for the vehicle being studied. Also included within each sheet is total energy for each component where power is tracked, as well as power minimum, maximum, and average for each component. This allows a user to find any detailed data of interest and explore what is happening on a component by component basis.

Since there is such a large amount of detailed data present within this model, it is also important to view data easily when common information is desired for different drive schedules. Much of this useful data is displayed in easy to read summary tables within the results tab of the model. Here, drive cycle data is gathered from each separate sheet and compared to one another within tables. This tab follows the same flow path as in each cycle sheet, beginning with a table to display power and energy requirements at the wheels. These values are simply referenced from the individual drive cycle sheets but sometimes include unit conversions to values used commonly in industry, such as Wh/mi or Wh/km. Knowing these tractive requirements at the wheels aids in the overall design process, since these are the forces and power demands which must be met in order to propel the vehicle through the various drive cycles.

After understanding the requirements at the wheels, the next summary tables displayed are for the energy consumption of the Battery Electric Vehicle model. Here, net tractive energy is again displayed for clarity, but then various other values such as battery internal energy consumption and actual regen brake fraction, which was discussed in Section 3.4.1. Aside from these values, AC grid energy consumption is found since this is truly the energy source for a BEV. This is done simply through using the charger efficiency defined by the user on the inputs tab and using Equation 44.

$$ACE_{grid} = \frac{DC\ E_{batt,int}}{\eta_{charger}} \qquad \textbf{Equation 44}$$

With this value now known, GREET WTW values for GHG emissions and PEU are both calculated via Equation 45 and Equation 46. Additionally, overall EV range is calculated as discussed in Section 3.4.2.

$$GHG\ WTW = AC\ E_{grid} * GHG_{fuel,WTW} \qquad \textbf{Equation 45}$$

$$PEU\ WTW = AC\ E_{grid} * PEU_{fuel,WTW} \qquad \textbf{Equation 46}$$

The final parameters calculated from values obtained during drive cycle analysis are two efficiencies. Propel based powertrain efficiency is first displayed and is a result of the total energy required at the wheels for propelling the vehicle divided by the total net DC energy consumption. This value demonstrates the efficiency of the entire powertrain neglecting effects of braking and so is the efficiency of a single "slug" of energy to exit the ESS, go meet the accessory load, travel through the motor and driveline, and finally reach the wheels. Although regen braking is still occurring in the vehicle, the propel efficiency only includes the energy used for the propel case as a reference. This efficiency value is almost always larger than the other efficiency calculated which is the net based efficiency. This second type is calculated including all braking cases and thus is usually much smaller since friction braking appears as a loss in the calculations. Equation 47 and Equation 48 show the calculations involved with finding these two parameters.

$$\eta_{PT,propel} = \frac{(E_{tr})^{+}}{E_{batt,int}} \qquad \textbf{Equation 47}$$

$$\eta_{PT,net} = \frac{(E_{tr})^{net}}{E_{batt,int}} \qquad \textbf{Equation 48}$$

After values for the BEV case are displayed, Thermostatic SHEV results are shown followed by Load-following SHEV results. The parameters shown in these tables are calculated in very similar ways as for the BEV. The only difference is that instead of using electric energy, liquid fuel is the energy source. Thus for all calculations, fuel energy consumption and fuel characteristics are utilized. It is important to note that even though some electric energy is used, the amount is negligible since the results are charge balanced. One calculation that is completely different for fuel versus electricity is vehicle range. Here, instead of a battery with an energy capacity, a fuel tank is used with a certain volumetric capacity ($V_{fuel,cap}$). This fuel then has a density (ρ_{fuel}) and a lower heating value (LHV_{fuel}) which must be taken into account to find the total range of the vehicle, along with the CS fuel energy consumption (E_{fuel}). Equation 49 demonstrates how CS range is calculated based on these parameters. It is important to note that a "power split fraction"

parameter is also included for Load-following cases, however, it will be defined in Section 4.2.

$$CS\ Range(km) = \frac{V_{fuel,cap} * \rho_{fuel} * LHV_{fuel}}{E_{fuel}} \qquad \textbf{Equation 49}$$

As mentioned, charge balancing is vital for finding CS results in this model. This process is completed through ensuring that the total electric energy consumption is valued at less than 1% of the total fuel consumption used to finish a drive cycle. Due to the control strategies turning the genset on and off, this is sometimes not completed in one iteration of a certain drive cycle. As a result, multiple drive cycle iterations are essentially strung together making, for instance, one large UDDS by adding another UDDS to the end of the first one and so forth until the test condition is true. While this sometimes can take many iterations depending on component sizes, this model has included programmable macros within Microsoft Excel to automate the process. Each macro runs a drive cycle and tests to see if it is charge balanced. If it is, the results are simply displayed and post processing can continue. If not, the ending SOC becomes the initial SOC and the drive cycle simulation is run again. The macro then iterates this process until the total drive cycle is charge balanced. It is important to note that throughout this process, parameters like total fuel consumption, total electric energy consumption, and total cycle distance are all recorded continuously to output final consumption values. Buttons for charge balancing are located in the results tab and make the process quite user friendly as opposed to trying to analyze this by hand. Important Note: Any added rows or columns will disrupt cell references within all macros, so if a user does make a change like this, macros will need to be adjusted. Each macro does include comments to guide manipulation to make this process easier and more understandable.

Finally, the results tab includes a summary table for drive cycle average component efficiencies across all cases for all drive cycles. This includes BEV and SHEV control strategies, as well as propel and regen cases. This again maintains the goal of increasing understanding of energy flow through the powertrain and viewing where areas of greatest loss occurs within the system. Overall, the outputs within this model give a complete scope as to what is happening within the modeled vehicle powertrain and allow a user to understand every aspect of power and energy flow, as well as final consumption values for every drive cycle and control strategy.

3.6 Assumptions and Limitations

Throughout the model development process, certain assumptions must be made and limitations acknowledged based on the simplified nature of this 1 Hz model. With a more complex model, more degrees of freedom can be introduced and strategies can be used to optimize the operation of the vehicle [14]. When restricting operation to simplified, rule-based decision making, these degrees of freedom are reduced necessitating assumptions to be made to still allow for accurate modeling. Within this model, there are several key assumptions and limitations not described in the component models that must be outlined to allow for understanding when it comes to operation and performance.

One key assumption relates to the drive motor within the model. Typically for a 3-phase motor, power would need to flow to a motor controller (also known as a motor inverter)

before being directed to the motor itself. This inverter converts the DC power to an AC signal to manipulate the motor to the desired operating point. This inverter is just like any other component within the model in that it includes and input and output power, in addition to loss. For simplicity, this inverter has been lumped in with the drive motor for loss purposes. This is acceptable since any time the motor is operating, the inverter has to be operating, thus both losses would be present. For these reasons, the inverter and motor are treated as one system for this model.

Additionally, there are several key assumptions/limitations of this 1 Hz model when it comes to Series operation. Firstly, although it correctly turns the genset on and off depending on demand and SOC limits, one of the limitations within this model is the lack of a fuel penalty when turning the engine on. Typically, extra fuel is used during an engine start than continuously operating. In addition, emissions are greatly affected with more engine starts. Both of these characteristics are not included within this model for simplicities sake. The overall energy flow is the goal, which is achieved and for further data on these situations, a more complex model would be necessary. This 1 Hz model is also limited in the fact that the engine does not need time to ramp up to the power demand, it is simply instantly on and operating at the desired point. This again, is not quite representative of a physical system, but is an approximation to maintain model simplicity.

Finally, one other large limitation of this model is the failure of the vehicle to meet certain extremely high power demands. This occurs especially during the Thermostatic SHEV case and is a result of the battery not being able to supply enough power when the engine is off. For the drive cycles modeled, the only area where this is a problem is during the US06 cycle when using a very small battery within the SHEV powertrain. To mitigate this limitation, the SOC window can be restricted to keep the engine on more often, thus allowing the engine power to aid the battery. This is not necessarily an ideal solution, however after exploring the effects of restricting the SOC window for situations like this, variation in results are not an issue, thus the assumption is acceptable. To better handle this situation, users should consider power demand of a drive cycle when sizing an HV battery for the hybrid powertrain being modeled. If the drive motor will be the only source of torque, and the vehicle will depend solely on the ESS as a power source during some moments of operation, the battery should be sized to meet the demand.

3.7 Model Validation

When creating modeling tools, it is very important to ensure the results gathered are accurate, especially when so many assumptions have been made. Considering how many details must be considered during the model development process, it is quite easy for small mistakes to be made which can either go unnoticed or be very difficult to track down. To mitigate these potential issues, model validation processes are used. Below, three different techniques are discussed for how this model is validated to ensure useful results are generated.

3.7.1 Energy Balance through Powertrain

One quick and easy way to validate if the energy flow through the model is accurate is through completing an energy balance through the powertrain of the vehicle. Since there are numerous components integrated into the vehicle model, each one having an input,

output, and a loss, many equations are present to keep track of all the energy, as described in the component models. This energy balance procedure involves looking at how much energy flows from the fuel source to the wheels through each component, and takes into account all the losses within the system. Once this balance is completed, the energy at the wheels to meet tractive effort combined with the total losses should equal the amount of energy at the fuel source.

Figure 3-23 shows an example of an energy balance for a BEV completed in this 1 Hz model for a UDDS case. As seen here, out of the total 171 DC Wh/km net internal energy exiting the battery, 76 Wh/km supplies the net road load demand at the wheels (some discrepancy due to rounding values). The remaining 95 Wh/km is consumed as various component losses. The charger losses are not part of the vehicle model, and are calculated as a simple post-processing operation using the overall charging efficiency (87%) to find the total ac grid energy required to restore the battery internal energy to the initial SOC.

While each bar represents the energy output from each component, the arrows demonstrate the losses from the previous energy output that are associated with that aspect. This validates that the energy flow for the model is accurate and no energy is lost in calculation or is mysteriously created. Note that "Motor Elec." represents the energy on the electrical side of the motor while "Motor Mech." represents the energy on the mechanical side. This nomenclature is used to clarify locations since energy sometimes flows in both directions (propel and regen) through the vehicle powertrain.

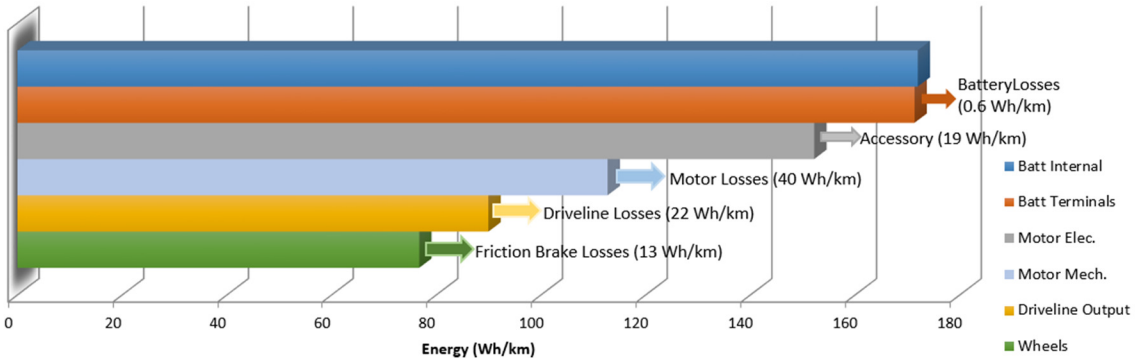

Figure 3-23: BEV energy balance for UDDS

Considering this model also includes Series powertrains, an energy balance was also completed to confirm that all of the energy used from the fuel tank is utilized to meet driver demand at the wheels, or is consumed by losses. As shown for the UDDS case in Figure 3-24, of the total 486.8 Wh/km fuel energy consumption, 67.5 Wh/km supplies the net road load demand at the wheels. As expected, the lower net road load demand is due to a lower vehicle mass compared to the BEV modeled above. The remaining 418.3 Wh/km is consumed in total losses throughout the powertrain. It is important to note that the small net energy stored in the battery is displayed as a loss in the chart for simplicity since this is a Charge Sustaining model. Again, while each bar represents the energy output from each vehicle component, the arrows demonstrate the losses from the previous energy output that are associated with that aspect. This validates that the energy flow for the model is accurate and that no energy has been lost or created in model and calculation.

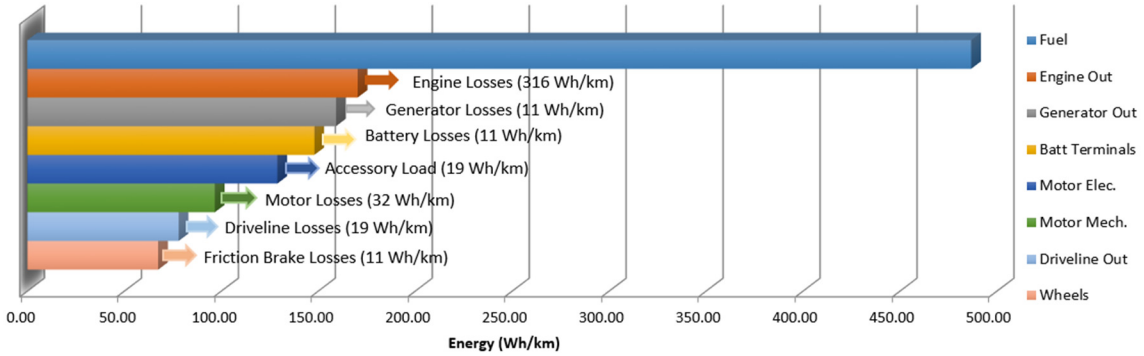

Figure 3-24: SHEV energy balance for UDDS

3.7.2 Comparison with Model Based Design

Another method used to validate this 1 Hz model is comparison with Model Based Design. As mentioned earlier within this thesis, the Hybrid Electric Vehicle Team of Virginia Tech has applied to participate in the next AVTC series called EcoCAR 3 [8]. During this application process, a design problem was completed to develop a hybrid powertrain to achieve certain specified goals. Through this proposal, HEVT used several different modeling tools to develop results and design powertrains to meet the desired goals. Through this process, this model, along with several MBD tools were validated against one another to ensure similar results were being found.

With this in mind, the 1 Hz SHEV model presented in this thesis was compared to a MBD tool created using MatLAB Simulink. This MBD approach is more complex, but as a result, helps validate the assumptions made within this 1 Hz model and the results gathered. Table 3-9 and Table 3-10 show several results found for two separate vehicles by both the 1 Hz model and Simulink model (Note: Simulink results are shaded and italicized for clarity). Case 1 represents a base Series vehicle with a 100 kW and a relatively small HV battery, while Case 2 is a heavier vehicle with a downsized 84 kW engine and a larger, heavier HV battery pack. As seen here, both models output very similar results for net tractive energy required at the wheels, CS fuel consumption, and powertrain efficiency. Although there are slight variations, these can be attributed to the Simulink model using "forward looking" approach for determining vehicle demand [8]. This approach includes a driver model with an accelerator pedal position which controls vehicle speed, thus this MBD tool produces slightly different results compared to the 1 Hz input drive cycle. Since two separate approaches are taken to find these results, it can be confidently said that the results shown here and generated by the models are dependable and useful.

Table 3-9: Simulink vs. 1 Hz CS energy consumption results Case 1

Test mass: 1633 kg Engine Size: 100 kW	**Units**	**UDDS**	**HwFET**	**Combined**	**US06**
Net Tractive Energy	Wh/km	67.5	105	84.2	136.3
Net Tractive Energy	*Wh/km*	*66.3*	*103*	*82.8*	*136*
CS Fuel Energy Consumption	Wh/km	487	526	505	739
CS Fuel Energy Consumption	*Wh/km*	*485*	*521*	*501*	*752*
CS Road load $\eta_{powertrain}$	%	13.9	19.9	16.6	18.4
CS Road load $\eta_{powertrain}$	*%*	*13.7*	*19.8*	*16.5*	*18.1*

Table 3-10: Simulink vs. 1 Hz CS energy consumption results Case 2

Test mass: 1692 kg Engine Size: 84 kW	Units	UDDS	HwFET	Combined	US06
Net Tractive Energy	Wh/km	68.9	106	85.7	138
Net Tractive Energy	*Wh/km*	*67.2*	*104*	*83.9*	*137*
CS Fuel Energy Consumption	Wh/km	471	486	478	648
CS Fuel Energy Consumption	*Wh/km*	*465*	*489*	*476*	*635*
CS Road load $\eta_{powertrain}$	%	14.6	21.8	17.9	21.3
CS Road load $\eta_{powertrain}$	*%*	*14.4*	*21.3*	*17.6*	*21.6*

3.7.3 EcoCAR 2 Vehicle Data EV Data from Emissions Testing Event

The final and most valuable way in which this model has been validated is through comparison to physical vehicle test data. Through participation in the current AVTC, EcoCAR 2, HEVT was able to take its competition vehicle to an Emissions Testing Event (ETE) held at the Transportation Research Center in East Liberty, Ohio. Here, the team was able to simulate various drive schedules on a chassis dynamometer under very specified conditions. Although the vehicle was only operating as an EV, this data is still extremely valuable when it comes to model validation since the vehicle was in a closed and very regulated environment much like the conditions for a vehicle that is modeled. After collecting this real-time data, simulated model results were able to be compared.

One area compared is the operation of the HV battery. Figure 3-25 shows a drive cycle completed at ETE which closely models a city/highway situation and was developed for use in the EcoCAR 2 competition. During this drive schedule, the vehicle depleted the ESS from 58.5% SOC to 31%. The actual velocity profile was then input into the 1 Hz model and its results can also be seen in the figure. As displayed, the model was slightly more conservative in depleting the battery, only going down to 32.7%. This trend is further supported in Figure 3-26, which shows the change in energy at the battery terminals in DC kWh. Again, the modeled data demonstrates a value slightly different from the actual data, 5.2 kWh vs. 5.6 kWh. Although this data demonstrates minor variations in the actual vs. modeled data, results are very close and thus shows that the vehicle is being modeled accurately and energy is flowing in a way that reflects the physical powertrain.

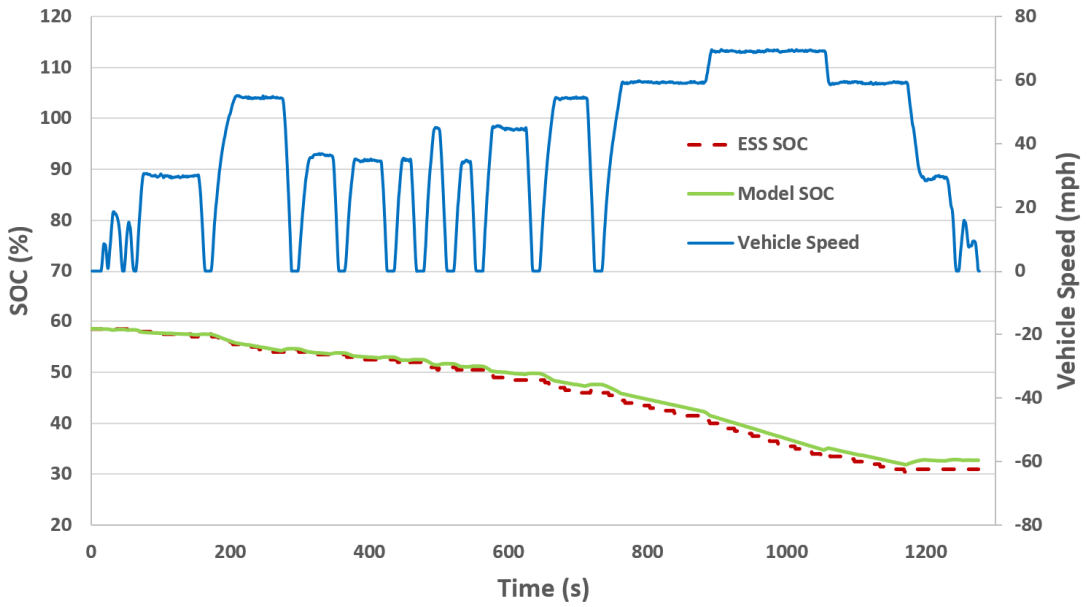

Figure 3-25: Battery SOC validation data

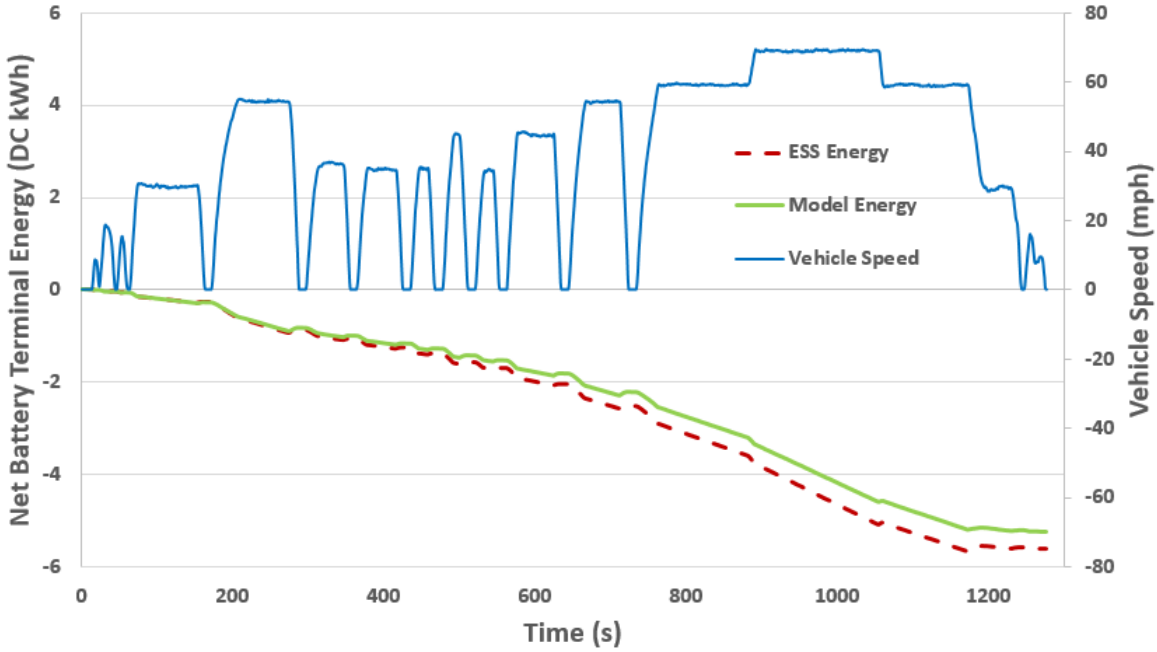

Figure 3-26: Battery energy validation data

Another component of interest is the Rear Traction Motor of the vehicle. Again, it is vital to see if the model accurately represents what is happening with the drive motor when it comes to delivering torque to the wheels. Figure 3-27 shows another drive trace completed by the vehicle at ETE and the corresponding motor torque throughout the cycle. Just as before, the model torque almost exactly matches the physical motor torque once again verifying that the 1 Hz model is acting in a way that reflects a physical vehicle. With this in mind, data can now be confidently collected with this model and used to better

understand what will occur in a hybrid powertrain when it comes to performance and energy consumption.

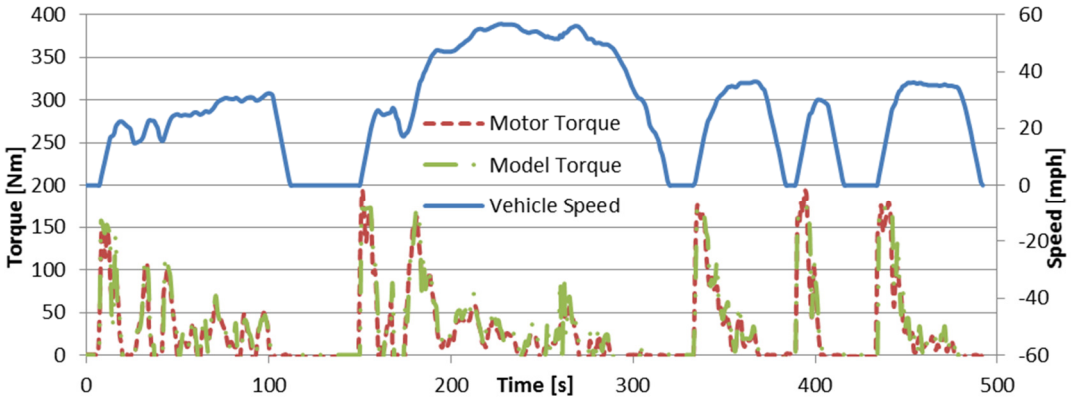

Figure 3-27: RTM torque validation data

4 Model Application

After completely defining the 1 Hz model, this thesis will now explore several applications of this powertrain model. A powertrain sizing study will first be shown to better explain how this model can be useful in component, as well as powertrain architecture selection. Once this is examined, power split fraction will then be better defined and studied as to how it relates to overall powertrain efficiency and the balance between engine and battery losses. It is important to note that these are two example applications and this model should not simply be limited to these two types of studies.

4.1 Powertrain Sizing Study

4.1.1 Sizing Study Goals

This sizing study is completed as an example from the proposal for HEVT to participate in EcoCAR 3. This competition has specific minimum modeling design targets. These targets are summarized in Table 4-1. Although these targets may not be the final targets for the actual competition, they do serve as acceptable guidelines for powertrain modeling. The goal of the study is to not only meet the requirements listed in Table 4-1, but to exceed them using scalable modeling methods that will provide a solid basis to design a future advanced technology vehicle.

Table 4-1: EcoCAR 3 vehicle design & modeling requirements

Performance/Utility Category	Vehicle Modeling Design Targets
Energy Consumption (unadjusted energy use on combined Federal Test Procedure [FTP] city and highway cycles)	Less than 370 Wh/km (600 Wh/mi) combined city and highway (55%/45% respectively)
GHG emissions (WTW combined city and highway cycles)	Less than 120 g of carbon dioxide equivalent (CO_2 eq)/km (200 g CO_2 eq/mi)
Interior size/number of passengers	Minimum 4 passengers
Luggage Capacity	More than 230 L (8 ft^3)
Range	> 320 km (200 mi) combined city and highway
Top Speed	> 135 kph (85 mph)
Acceleration time of 0 to 97 kph (0 to 60 mph)	< 11 seconds
Highway gradeability (at gross vehicle weight rating [GVWR])	> 3.5% grade @ 97 kph (60 mph) for 20 minutes

4.1.2 Energy and Power Requirements

The first step for this study is to use the glider model to find the energy needed at the wheels to propel the vehicle through a given drive cycle. This is the energy required to power a specified vehicle without including any powertrain losses. Table 4-2 includes the vehicle characteristics that are used to define the vehicle glider being modeled in this example. It is important to note that this is the "base" conventional vehicle and the studies included below assume changes being made to this vehicle.

Table 4-2: Vehicle glider properties

Parameter	Value
Test Mass, m	1500 kg
Gross Vehicle Weight Rating (GVWR)	2000 kg
Drag Coefficient*Frontal Area ($C_d A_f$)	0.75 m^2
Coefficient of rolling resistance (C_{rr})	0.009
Rotating Inertia factor applied to test mass	1.04

Using the vehicle characteristics described, the energy requirements at the wheels are found using the equations described in Section 3.3.1. Along with energy at the wheels, other useful information is gathered such as peak tractive power, average tractive power, propelling energy and braking energy. The results for energy and power requirements at the wheels are listed in Table 4-3.

Table 4-3: Drive cycle (1 Hz) results at the wheels

Test Mass: 1500 kg	Units	UDDS	HwFET	Combined	US06
Positive propulsion energy	Wh/km	119.6	113.2	116.7	187.2
Negative (braking) energy	Wh/km	-55.4	-11.7	-35.8	-54.2
Net (road load) energy	Wh/km	64.2	101.5	81.0	133.0
Average positive propulsion power	kW	6.79	9.92	8.20	20.9
Peak power output	kW	33.1	27.4	30.5	84.5
Peak tractive force	kN	2.49	2.38	2.44	5.99
Percent idle time	%	17.8	0.52	10.0	5.87

The results presented in this table can be very useful in evaluating potential energy losses and savings in a vehicle. The positive propulsion energy is the minimum amount of energy required to propel a vehicle regardless of powertrain losses. Negative braking energy is representative of the energy lost during braking events of the corresponding drive cycle. Capturing some of this lost energy will increase overall vehicle efficiency. Also, peak and average power and force values help to size powertrain components.

To meet the performance requirements and further aid in component sizing, acceleration tests are also run using the glider model. The competition requires a minimum 0-60 mph acceleration time of 11 seconds. To establish a base for performance requirements in terms of power and energy, the average power for an acceleration run as well as a constant 60 mph on a grade are calculated. In addition to the minimum acceleration time of 11 seconds, the average power required for an 8 second 0-60 mph acceleration is also calculated as it represents a more realistic acceleration time for a vehicle with similar properties. In order to calculate the average power required for both the minimum and target acceleration time, a discretized velocity model is used. The equation for the velocity trace used is:

$$V = V_m \left(\frac{t}{t_m}\right)^z \qquad \textbf{Equation 50}$$

where V_m is the target velocity (60 mph), t_m is the target time in seconds. The exponent, z, is set equal to 0.6 to approximate the acceleration characteristics for most light duty vehicles. Time t is the input, and for this calculation a time step of 0.1 seconds is used. This model is unbounded in speed which leads to increasing power at the wheels. Actual vehicles are limited by peak power, and this prescribed velocity model provides an appropriate speed trace up to around the 400 m (¼ mile) mark.

All results can be found below in Table 4-4. The average power (over the whole 0-60 mph acceleration event) is provided for both acceleration times, as well for grades of 3.5% and 6% at 60 mph, and average power for cruising at 85 mph on a flat road. These performance results are what is required to propel the given vehicle glider at the wheels, and have no powertrain associated with them. The acceleration power represents a short-term or peak power requirement, while grade and cruise powers represent typical continuous power requirements (often limited by thermal considerations).

Table 4-4: Average power requirements at the wheels

Requirement	Power
Acceleration time of 11 seconds at test mass of 1500 kg	56 kW
Acceleration time of 8 seconds at test mass of 1500 kg	75 kW
Climb 3.5% grade at 60 mph at GVWR (2000 kg)	32 kW
Climb 6% grade at 60 mph at GVWR	45 kW
Cruise on 0% grade at 85 mph at GVWR	31 kW

An additional grade case is performed since a 6% grade at 60 mph more closely models industry standards for production vehicles. Cruising at 85 mph with no grade is close to the average power required for climbing a 3.5% grade at 60 mph. This result is due to the fact that the component of force that is caused by the grade is nearly equal to the additional aerodynamic force acting on the vehicle at the higher speed. With all of these requirements defined and understood, powertrain components can be accurately selected to overcome these demands and operate the vehicle throughout the drive cycles.

4.1.3 BEV Design

A pure Battery Electric Vehicle powertrain configuration is modeled to evaluate the potential of a BEV to meet the competition energy consumption and GHG goals. Figure 4-1 is a diagram of the BEV model configuration.

The torque-speed characteristics of an electric motor allow a single-speed transmission to suffice as a transmission in a BEV. This is modeled as a simple driveline with no shift strategy in both torque-speed and power loss models and only involves a constant torque loss based on 1.2% of maximum motor torque for the torque-speed loss model. The DC/DC converter is modeled as a pure loss to meet the accessory load of the vehicle. This model also includes regenerative braking. Table 4-5 provides a summary of the BEV powertrain and sizing to meet performance and range goals. The motor torque and gearing also allow for launch on a grade of greater than 30%.

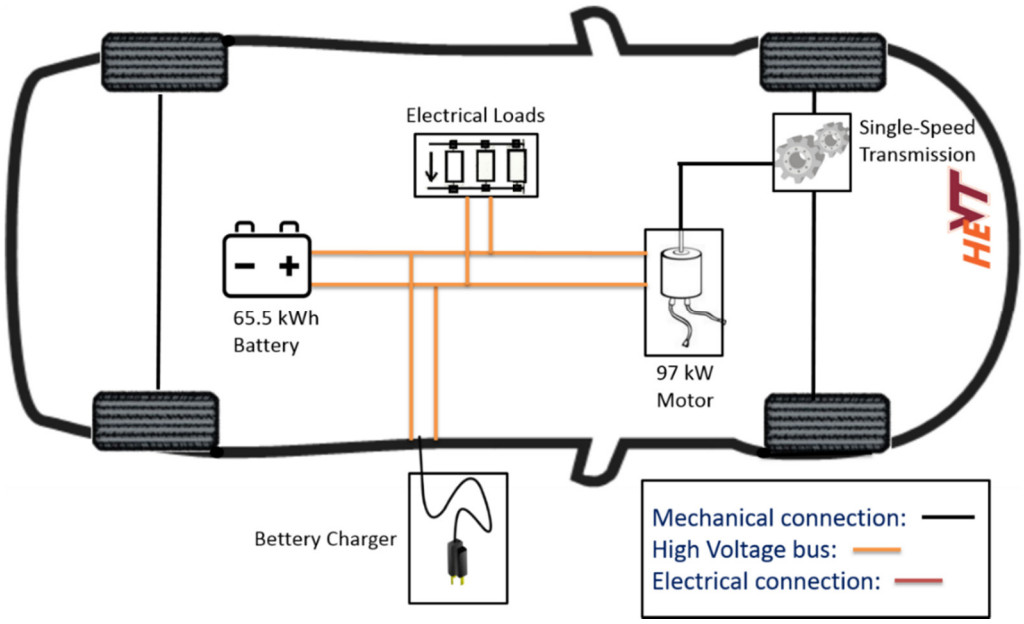

Figure 4-1: Battery Electric Vehicle model configuration

When sizing the drive motor and battery, the acceleration target and range both come into play. The 97 kW motor is chosen since it is able to meet the necessary peak power at the wheels to achieve the acceleration target and continuous power for highway gradeability. Range is the key characteristic when sizing the battery since enough energy must be present to complete the 320 km (200 mi) minimum range. This energy in turn sizes the battery power; the battery must be able to source enough power for the motor to meet the acceleration goal, but due to the energy sizing requirements, the available power is well above the required motor power. To ensure all criteria are met, a battery model is used to relate battery size and mass to the power and energy available from the battery. Using data for specific energy (Wh/kg) and specific power (W/kg) for both power and energy batteries, the characteristics of lithium ion batteries as a function of mass are generated [21]. Through analysis of these results, the energy battery mass in Table 4-5 is chosen for use in this BEV. Note that this same battery model is also used to size the battery systems discussed later sections.

Table 4-5: BEV powertrain sizing to meet range requirements

Test Mass	2000 kg (GVWR)
Top Speed	135 kph (85 mph)
0-60 mph Acceleration	11.0 s
Highway Gradeability @ 60 mph @ Test Mass	> 5%
Powertrain Configuration	Front Wheel Drive BEV
Powertrain Sizing:	
Motor Peak Power	97 kW @ 3000 rpm
Motor Peak Torque	310 Nm
Single Speed Transmission Gearing	7.05:1 (N/V = 94 rpm/mph)
Battery Energy Capacity	65.5 kWh
Battery Peak Power	218 kW
Battery Mass/ESS Mass	540/625 kg
Battery Usable Energy (95% - 10% SOC)	55.7 kWh
Regenerative Brake Fraction	85%
Accessory Load	600 W
Grid AC Charging System Efficiency	87%

Table 4-6 documents the battery model scaling parameters used throughout the modeling process [21]. The main trade-off in battery development is between power and energy: batteries can be either high-power or high-energy, but not both. Often manufacturers will classify batteries using these categories. Depending on the battery requirements for a powertrain, an energy battery or power battery may be chosen, or something in between. For example, if the purpose of the battery is to meet the power demand of a traction motor, a power battery may be chosen. On the other hand, if the battery is to be designed for a specific Charge Depleting range, an energy battery may be more suitable to the situation. A 350 V nominal battery voltage is assumed and allows the internal resistance to be scaled inversely to Amp-hour or energy capacity. Thus a battery with twice the energy capacity has about half of the internal resistance. Further details of the battery model are included in Section 3.3.6.

Table 4-6: Battery model scaling parameters

Battery Classification	Energy Battery	Power Battery
Specific Energy	120 Wh/kg	75 Wh/kg
Specific Power	400 W/kg	1200 W/kg
Internal Resistance	1.2 Ω-kWh	

To estimate the test mass for the BEV, the net increase for changing the powertrain from conventional to battery electric is approximated as the mass of the ESS. This is due to the engine and multispeed transmission being removed, and the comparable motor and single speed transmission being added. Thus the conventional vehicle test mass (1500 kg, including two people) has the mass of the ESS added to it, but the BEV is still limited to GVWR. Note that using this component mass approximation, the battery/ESS sized to meet range (625 kg) would require an additional vehicle light-weighting of 125 kg to maintain a vehicle mass under GVWR of 2000 kg with only 2 people on board. Thus to achieve the goal of 4 passengers would require even more light-weighting (180 kg, or a

total of 305 kg) which is not very practical for the vehicle. Table 4-7 shows the results of running the specified BEV for energy consumption values.

Table 4-7: Drive cycle energy consumption results for BEV

Test mass: 2000 kg Motor Size: 97 kW	Units	UDDS	HwFET	Combined	US06
Net Tractive Energy	Wh/km	76.5	113.7	93.2	145.3
Internal Battery Energy	DC Wh/km	171.3	176.26	173.5	241.4
AC Grid Energy	AC Wh/km	196.9	202.6	199.4	277.4
WTW GHG	g CO_2 eq/km	127.6	131.3	129.2	179.8
Range	km	325.1	315.9	320.9	230.7
Road load DC $\eta_{powertrain}$	%	44.6	64.5	53.6	60.2

The BEV has a high (road load) powertrain efficiency because it does not have the energy conversion losses of an IC engine. This lowers the vehicle energy use below a conventional vehicle and also allows the goal of 370 Wh/km to be met and even exceeded by 170 AC Wh/km for the combined case. However, the WTW GHG is still comparable to a conventional vehicle because grid electricity has a high rate of GHG emissions per unit of energy. The low energy consumption combined with the high GHG of grid electricity does come close to the competition WTW GHG goal. As stated previously, the emissions goal for the modeling problem is 120 g/km for WTW GHG, and the minimum range requirement is 320 km (200 mi) for the competition.

This BEV design is able to meet the minimum combined range, but only with very significant mass reduction in other vehicle systems, and limited two-person mass capacity. At a test mass of 2000 kg with two people, and 435 kg of battery/500 kg ESS (so no extra light-weighting), the combined range is 160 miles. A BEV with room for 4 people at GVWR, but tested with two people at 1820 kg using 280 kg battery/320 kg ESS has a combined range of only 107 miles. This range is more typical of conventional vehicles converted to a BEV. The Tesla S is a dedicated, high-range (greater than 200 mi) dedicated BEV design using light-weight materials, and is also very expensive.

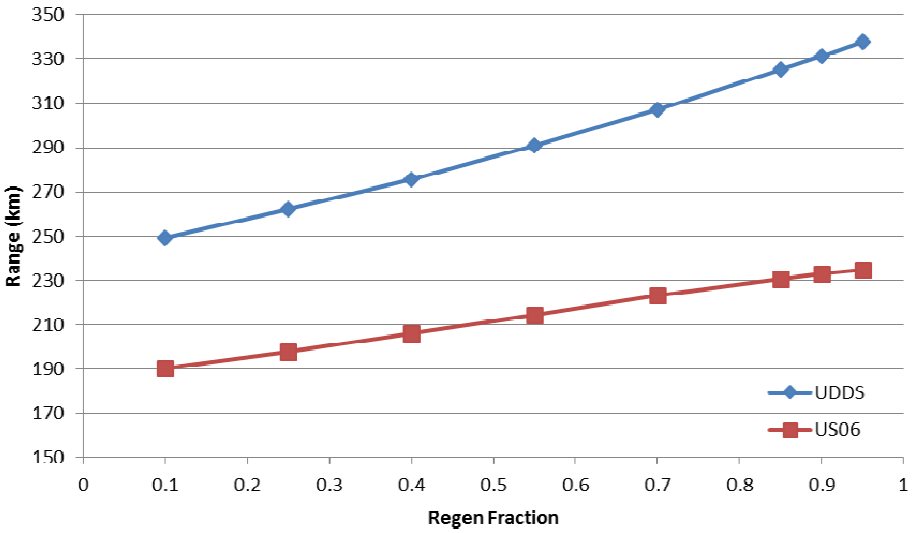

Figure 4-2: Regenerative brake fraction vs. range for BEV

In addition to battery capacity sizing, regenerative braking does play a large role in the ability of the BEV to meet the range requirement. Figure 4-2 shows how increasing the regen brake energy capture fraction also increases range. Since a higher regen fraction allows for more braking energy to be captured and stored in the battery (including losses along the way), it makes sense for range to be directly related to this fraction. The figure shows correlations for both the UDDS and US06 drive cycles. The UDDS has a higher range over all considering the US06 is much more aggressive and thus requires higher energy use. In both cases however, regen is able to increase range thus solidifying the effectiveness of a well-planned regen braking control strategy.

4.1.4 SHEV Design

The Series hybrid is the first configuration modeled in this sizing study that has multiple torque sources included. The powertrain configuration can be seen in Figure 4-3.

The Series model is driven by the traction motor coupled with a single-speed transmission, similar to the BEV. An engine-generator also has a fuel energy conversion path to the high voltage bus. This allows the genset to maintain energy in the battery while also supplying the traction motor that drives the vehicle. Regenerative braking is also possible in this configuration, using the traction motor to demand negative power and restore energy into the battery. More detail on the control strategy and model setup of the Series vehicle can be found in the component modeling sections above.

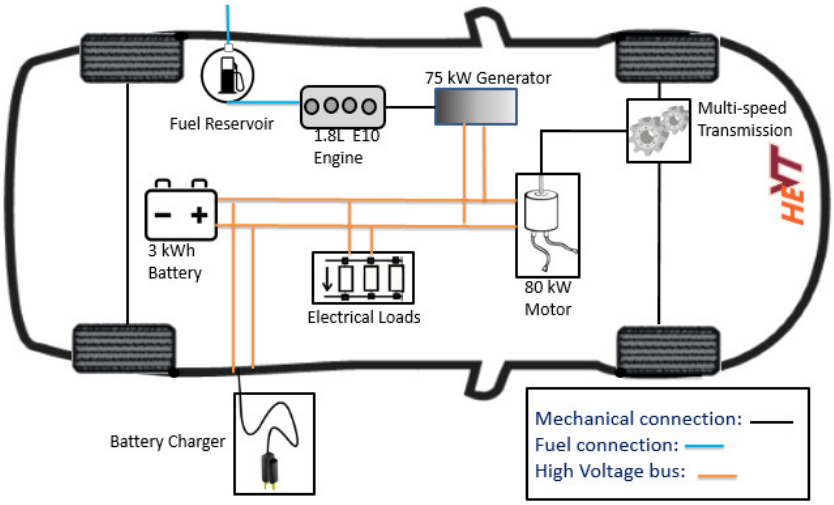

Figure 4-3: Series hybrid powertrain configuration

4.1.4.1 Series Hybrid Base Case

The base Series hybrid case for this modeling problem requires that specified powertrain component sizes are used. This base case establishes a baseline for improving the powertrain by resizing the components as well as modifying the control strategy. The initial case for the Series hybrid is shown in Table 4-8.

Table 4-8: Base Series hybrid vehicle powertrain sizing

Test Mass	1633 kg
Top Speed	135 kph (85 mph)
0-60 mph Acceleration	11.0 s
Highway Gradeability @ 60 mph @ Test Mass	> 5%
Powertrain Configuration	Series HEV, E10 Fuel
Powertrain Sizing:	
Engine Peak Power	100 kW
Engine Peak Efficiency	35%
Generator Power (Peak/Continuous)	75/41 kW
Motor Peak Power	80 kW @ 3000 rpm
Motor Peak Torque	255 Nm
Single Speed Transmission Gearing	7.05:1 (N/V = 94 rpm/mph)
Battery Energy Capacity	3.1 kWh
Battery Peak Power	50 kW
Battery Mass/ESS Mass	42/50 kg
Battery Usable Energy (80% - 40% SOC)	1.2 kWh
Regenerative Brake Fraction	85 %
Accessory Load	600 W

To calculate the estimated SHEV test mass, a conventional test mass of 1500 kg (including a 100 kW engine) has 63 kg added for the generator system, a net gain of 20 kg for the traction motor and single-speed transmission in place of a 6 speed transmission, and 50 kg added for the ESS. This yields a total test mass of 1633 kg. The charge balanced results of running the preliminary model are shown in Table 4-9.

Table 4-9: Base Series HEV drive cycle (1 Hz) energy consumption results

Test mass: 1633 kg Engine Size: 100 kW	**Units**	**UDDS**	**HwFET**	**Combined**	**US06**
Net Tractive Energy	Wh/km	67.5	105	84.2	136.3
Fuel Energy Consumption	Wh/km	487	526	505	739
Net Battery Energy	DC Wh/km	3.49	-1.16	1.40	-1.69
WTW GHG	g CO_2 eq/km	157	169	162	238
Range	km	664	614	641	437
Road load $\eta_{powertrain}$	%	13.9	19.9	16.6	18.4

Table 4-9 shows that the base Series hybrid powertrain is able to meet some of the design requirements such as range, acceleration, top speed, etc. The base case does not, however, meet the energy use or GHG WTW goals, and therefore does not serve as a viable option as a powertrain selection. In order to verify accurate modeling the values were measured for a charge balanced system as shown by the net battery energy being less than 1% of the fuel energy consumption.

Since this powertrain does not meet energy consumption and GHG goals, further investigation for the Series hybrid is done by resizing components to try to meet the design targets. Note that it is difficult to improve drastically because running with the base sizing yields an engine-generator efficiency of about 32%. Additional battery energy to allow

use of grid electricity in a Charge Depleting mode can significantly reduce total energy consumption, but only slightly reduces GHG emissions.

4.1.4.2 Series Hybrid Improved Case

After failing to reach all design targets with the Series base case, components are resized to achieve as many design targets as possible with a Series hybrid. Table 4-10 displays the variations between the base and improved case. The main changes are a downsized E85 engine with a higher efficiency, a larger drive motor (scaling used in motor model), and larger battery sized to meet the motor peak power demand for CD operation. With these new components, the mass increases but the acceleration time decreases with the increased motor and battery sizes. Highway gradeability is considered in this design as the 41 kW continuous power rating for the generator is ample power to exceed the required 32 kW at the wheels to maintain 60 mph for 20 min on a 3.5% grade. The mass estimation is consistent with the description for the base case. The only difference is the increased mass of the battery (and therefore ESS) since the masses for the smaller engine and larger motor approximately offset.

Table 4-10: Improved Series hybrid vehicle powertrain sizing

Test Mass	1633 kg	1692 kg
Top Speed	135 kph (85 mph)	
0-60 mph Acceleration	11.0 s	8.9 s
Highway Gradeability @ 60 mph @ Test Mass	> 5%	
Powertrain Configuration	Base Series HEV, E10 Fuel	Series PHEV, E85 Fuel
Powertrain Sizing:		
Engine Peak Power	100 kW	84 kW
Engine Peak Efficiency	35%	38.5%
Generator Power (Peak/Continuous)	75/41 kW	
Motor Peak Power	80 kW @ 3000 rpm	100 kW @ 3000 rpm
Motor Peak Torque	255 Nm	320 Nm
Single Speed Transmission Gearing	7.05:1 (N/V = 94 rpm/mph)	
Battery Energy Capacity	3.1 kWh	7.1 kWh
Battery Peak Power	50 kW	114 kW
Battery Mass/ESS Mass	42/50 kg	95/109 kg
Battery Usable Energy	1.2 kWh	5.7 kWh
Regenerative Brake Fraction	85 %	
Accessory Load	600 W	

The engine chosen for this improved case is sized to first meet the power demand for running the generator at peak power and accounting for the losses between the two components. In addition, however, it is also sized to match the region of high efficiency of the engine at part load with the region of high efficiency of the generator with a pulley ratio set to 1.5. This pulley ratio assumes that the engine and generator are not "in-line" but are coupled with a belt, chain, or some other torque coupling. Through choosing this 1.5 L (84 kW) engine, operation can stay about on the minimum brake specific fuel consumption line and still meet the generator continuous power rating of about 41 kW.

Additionally, the peak power can be met thus allowing all conditions to be met with a higher efficiency over the 100 kW base case engine.

4.1.4.2.1 Charge Sustaining Operation

With the much larger battery included in this improved case, the Series hybrid is able to have both Charge Depleting and Charge Sustaining operation modes. Table 4-11 displays the values for the charge balanced Charge Sustaining case. As shown here, values for fuel consumption and WTW GHG emissions decrease significantly, while efficiency increases when compared to the base case. This is mostly a function of the downsized E85 engine. Firstly, the smaller size also has a higher maximum efficiency at which it can be operated. Additionally, the fuel has been changed to E85 which has benefits when it comes to WTW GHG emissions. It is important to note that the range is decreased, however, this is a function of the lower energy density of E85 fuel. The vehicle still has an overall more efficient powertrain but has less overall energy stored in the 10 gallon fuel tank. Unfortunately, even though this vehicle meets the range, top speed, acceleration, gradability, and luggage capacity targets, the energy consumption and WTW GHG values are not quite low enough. The WTW GHG value is on the brink of passing the design target, so possible light-weighting of the vehicle could push that value below the target. The energy consumption value, however, is improved by the Charge Depleting mode discussed in the next section.

Table 4-11: Improved SHEV drive cycle CS energy consumption results

Test mass: 1692 kg Engine Size: 84 kW	**Units**	**UDDS**	**HwFET**	**Combined**	**US06**
Net Tractive Energy	Wh/km	68.9	106	85.7	138
CS Fuel Energy Consumption	Wh/km	471	486	478	648
CS Net Battery Energy	DC Wh/km	-2.46	-2.35	-2.41	4.77
CS WTW GHG	g CO_2 eq/km	123	127	125	169
CS Range	km	503	488	496	366
CS Road load $\eta_{powertrain}$	%	14.6	21.8	17.9	21.3

4.1.4.2.2 Charge Depleting Operation

As mentioned above, an added benefit of this improved case is the addition of a Charge Depleting mode. The battery is now large enough to have both a large energy capacity and a large enough power to allow for full battery electric operation. This addition in battery capacity does come at the price of added mass. It is very important to consider the tradeoffs of a large battery before implementing one into the vehicle. The larger the battery, the higher the mass of the vehicle, which in turn, increases the resistance the powertrain must overcome to move the vehicle. In spite of this, added battery mass does allow for an offset in liquid fuel use which involves a much less efficient (much higher losses) energy conversion process, and the use of a much more efficient energy path to the wheels. The larger battery also provides a decrease in internal resistance, thus battery losses are also reduced making that energy path even more efficient than for a smaller battery. Overall, the added benefits outweigh the negative aspects for adding a larger battery to this improved case. Table 4-12 shows the values for the Charge Depleting mode of the SHEV. As shown, a very low energy consumption allows for added range.

Table 4-12: Improved SHEV drive cycle CD energy consumption results

Test mass: 1692 kg Engine Size: 84 kW	Units	UDDS	HwFET	Combined	US06
CD Net Battery Energy	DC Wh/km	164	173	168	243
CD AC Electrical Energy Cons.	Wh/km	188	199	193	279
CD Range	km	34.7	32.8	33.8	23.4

4.1.4.2.3 Utility Factor Weighting

To analyze vehicle energy consumption for a vehicle using two energy sources, it is necessary to take into account how often the vehicle is operating in each mode. The Society of Automotive Engineers J2841 definition of utility factor (UF) and the SAE J1711 test method are the standard way to analyze these operations [22,23].

J2841 establishes a value for weighting fuel and electric energy consumption for PHEVs on the basis of National Household Travel Survey (NHTS) data from 2005. In essence, PHEV Charge Depleting energy consumption is weighted against the percentage of the fleet of vehicles that will use the CD range in a given day; the UF represents that percentage. The remaining percentage (1 – UF) is then used to weight the Charge Sustaining energy consumption to represent the remaining drivers on that same day.

J1711 establishes a method for testing a vehicle to determine the point at which a CD PHEV transitions to its CS mode, so that the vehicle UF can be calculated. In the process, the CD and CS energy consumption values are quantified. Once the vehicle CD range and CS fuel consumption are measured, the UF can be assigned, and a value for the UF-weighted energy consumption can then be determined. The UF method is a fleet-average, combined city and highway factor. Equation 51 shows the method for calculating the utility factor based on Charge Depleting range, x. D_{norm}, C_1, C_2, etc. are known constants. Figure 4-4 shows the trend for how the CD range affects utility factor.

$$UF = 1 - e^{-\left[C_1*\left(\frac{x}{D_{norm}}\right)+ C_2*\left(\frac{x}{D_{norm}}\right)^2 + \ \ldots\right]} \qquad \textbf{Equation 51}$$

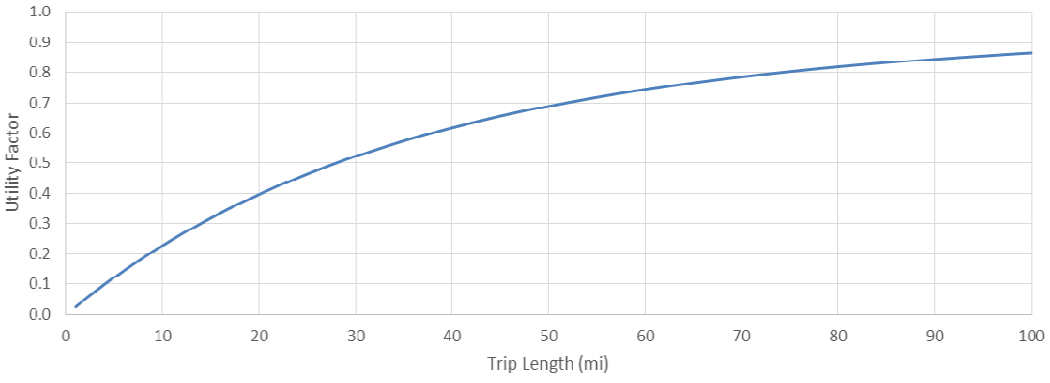

Figure 4-4: Utility factor vs. trip length

Using this equation and the CD combined range from Table 4-12, the utility factor for the improved case Series HEV is 0.41. Other utility factor values are included in the J1711 plot shown in Figure 4-5.

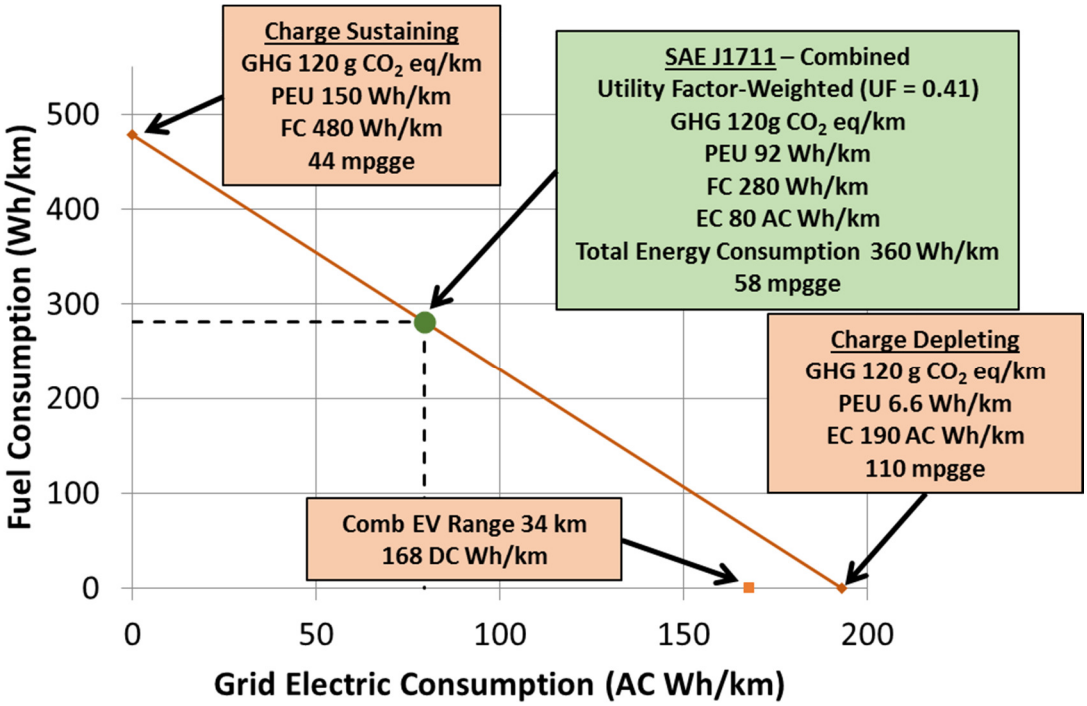

Figure 4-5: Improved SHEV J1711 plot

These results show that this Series HEV is able to just barely meet the total energy consumption goal and the WTW GHG goal. As discussed earlier, this design is a large benefit over the BEV since range is achieved while maintaining a reasonable mass. Cost is also an important consideration. This vehicle will be more expensive than a conventional vehicle with the addition of the battery back and two electric machines, however the increased efficiency along with consumer acceptability balances that tradeoff with the added CD mode and efficient CS mode. Unfortunately, the motors in a Series HEV cannot be scaled down to reduce cost since the power is required to meet acceleration and gradeability goals, but again, tradeoffs must be made to meet targets. Overall, this design is able to meet all of the modeling targets and therefore exhibits a successful sizing study.

4.2 Power Split Fraction Study

This study is presented to explore the implications caused by fluctuations in Power Split Fraction when it comes to overall system efficiency. Since PSF is related to engine operation and battery losses, both of these parameters are of interest for this study and since these are two of the main areas of loss within a Series hybrid are thought to directly relate to the overall system efficiency. In the below sections, PSF is defined, calculations for the parameter are illustrated, the vehicle used within this study is outlined, and finally results on the trends discovered are discussed.

4.2.1 Definition

When studying conventional vehicles, only one fuel source and one torque producing component is present; the fuel tank and engine. To propel a vehicle through a chosen drive trace, the engine has to convert fuel to mechanical energy to produced torque to be used by

the drivetrain. Additionally, losses for components are fairly well understood and control strategy does not come into play too much when it comes to operating efficiency. Overall, reducing losses within the engine greatly improves the overall powertrain efficiency which in turn improves fuel economy.

Although this is true for conventional vehicles, hybrid vehicles introduce much more complexity to a vehicle powertrain since multiple fuel and torque sources are present; HV battery and fuel tank, as well as a drive motor, generator, and engine. With these additional components, controls for the vehicle also grow more complex since torque can come from either the HV powertrain or the engine. As described in the sections above for Series hybrids, propelling the vehicle can be done by the drive motor obtaining power from either the ESS or the combination of the engine and generator. Since again most losses are understood and proportional to how much torque is being produced, overall powertrain efficiency is greatly reliant on the efficiency of the engine and battery. Minimizing losses in both of these components improves overall fuel economy and thus both are targets for improvements. This is where Power Split Fraction comes into play.

PSF is defined as the amount of energy produced by the genset which goes directly to propelling the vehicle. More specifically, since the generator is simply a converter between mechanical and electrical energy, PSF focuses on engine operation. This parameter, as mentioned previously, ranges from 0 to 1. A value of 0 means that all of the energy produced by the engine is stored in the battery before being used to power the vehicle. This would be illustrated by the vehicle operating in a CD mode throughout an entire drive cycle after which the vehicle idle charges to replenish all of the energy taken out of the battery. A PSF value of 1 implies that 100% of energy produced by the engine goes directly to propelling the vehicle. This means that no energy goes in or out of the battery for the propel case, and thus the vehicle operates as if there is no ESS. The engine is operated at the exact demand of the vehicle thus there is no excess energy or buffering from the battery.

Within both of these cases, the main parameters of interest which control overall system efficiency are battery losses which are related to R_{int}, and engine efficiency. This study of PSF seeks to find the best balance between operating the engine efficiently to meet demand and using the HV battery to buffer energy while minimizing losses due to charging/discharging. To accomplish this, the 1 Hz model will be used to establish a vehicle and then manipulate the minimum operating power of the engine and battery energy capacity which in turn relates to internal resistance for losses. The result is finding how PSF affects the overall system efficiency so intelligent control strategies can be developed for SHEV operation.

4.2.2 Vehicle Characteristics and Assumptions

For the purpose of this PSF study, the improved Series vehicle found during the powertrain sizing study in Section 4.1.4.2 is used. This vehicle has components already sized to meet the demands of the various drive cycles including the targets associated with acceleration, top speed, range, and gradeability. Table 4-13 clarifies exact vehicle parameters from the section above. It is important to note that two types of batteries are shown. These are the large and small batteries used for this study. The large battery is used to demonstrate a vehicle with low battery losses since the internal resistance is much smaller compared to

the 3.1 kWh battery. In contrast, this small battery has higher loss which will affect powertrain efficiency.

After establishing the vehicle glider and powertrain characteristics, it is important to discuss the assumptions applied to this study. Due to the interest in engine and battery performance, many of the vehicle parameters remain fixed while several others are varied. The vehicle characteristics which remain constant include vehicle mass, engine size, motor and generator sizes, as well as all other glider characteristics. The parameters varied for this particular study are the minimum operating power for the engine and also battery size. The minimum engine power increases from 1.8 kW to its optimum point of 37.5 kW through several increments. Results are also found for running a Thermostatic control strategy versus a Load-following strategy, as well as for at the PSF limits of 0 and 1. These iterations occur for both the large and small batteries to see the different trends for each. It is important to note that although the battery sizes and thus battery masses change, the vehicle mass is held constant. This is to simplify the study to only two independent variables and thus control the experiment. Although in the physical world the vehicle mass would change, this detail is neglected here. Mass considerations do represent a good study for future work.

Table 4-13: SHEV characteristics for PSF study

Test Mass	1692 kg	
C_{rr0}	.009	
C_{rr1}	0 $(m/s)^{-1}$	
C_DA	.75 m^2	
Wheel Radius	.32 m	
Top Speed	135 kph (85 mph)	
0-60 mph Acceleration	8.9 s	
Highway Gradeability @ 60 mph @ Test Mass	> 5%	
Powertrain Configuration	Series PHEV, E85 Fuel	
Powertrain Sizing:		
Engine Peak Power	84 kW	
Engine Peak Efficiency	38.5%	
Generator Power (Peak/Continuous)	75/41 kW	
Motor Peak Power	100 kW @ 3000 rpm	
Motor Peak Torque	320 Nm	
Single Speed Transmission Gearing	7.05:1 (N/V = 94 rpm/mph)	
Battery Energy Capacity	7.1 kWh	3.1 kWh
Battery Peak Power	114 kW	50 kW
Battery Internal Resistance	.169 Ω	.387 Ω
Battery Mass/ESS Mass	95/109 kg	42/50 kg
Battery Usable Energy	5.7 kWh	1.2 kWh
Regenerative Brake Fraction	85 %	
Accessory Load	600 W	

4.2.3 Calculations

To actually calculate PSF, several parameters are derived from known powertrain outputs. Since PSF is by definition the amount of energy produced by the genset which directly

goes to propelling the vehicle, the genset output is divided into two cases; propel and storage. A propel flag is set up in the model so it can be easily seen where the genset is outputting power when the vehicle is being propelled. This propel power can then be compared to the total output power of the genset for the propel case using the instantaneous PSF which is found through comparing how much of the propel power output by the genset meets the current vehicle demand. Once instantaneous powers are found, these values can be integrated over the entire drive cycle to then find energy terms and the drive cycle average PSF. This drive cycle average PSF calculation is demonstrated in Equation 52.

$$PSF = \frac{(E_{gen,use})^+}{(E_{gen,elec})^+} \qquad \textbf{Equation 52}$$

Where $(E_{gen,use})^+$ is the total genset energy used for propulsion and $(E_{gen,elec})^+$ is the total output energy of the genset over the entire drive cycle. As mentioned previously, this parameter will be calculated across several different operating strategies to find PSF points ranging from 0 to 1. With these results gathered, the effects of PSF can then be seen where engine efficiency, battery losses, and overall powertrain efficiency are concerned.

4.2.4 Results

4.2.4.1 7.1 kWh Battery

The first case explored for this Power Split Fraction study is a powertrain with a large battery and low internal resistance. As mentioned previously, this vehicle is run through UDDS, HwFET, and US06 drive cycles to give a comprehensive look at various operating conditions and reactions to aggressive versus mild driving habits. Figure 4-6 shows the correlation between PSF and the minimum operating power set for the engine. As shown, this lower limit is increased from 1.8 kW to 37.5 kW. The lower bound is used since this is the lowest mechanical engine power that can still overcome all losses involved with the generator, drive motor, and accessory load without requiring the battery to discharge. The 37.5 kW limit is chosen since this is "optimum" operating point where the engine runs at its highest efficiency. As demonstrated in the figure, PSF decreases with increasing $P_{eng,min}$. This trend is consistent for all three drive cycles, although PSF does not decrease as significantly for the high power demand US06 case. This suggests that the more aggressive drive schedule requires engine power to consistently be used for propulsion and doesn't allow as much opportunity for storage.

Control strategies are also compared in Figure 4-6. As shown here, the Thermostatic (T'stat) operation reacts much like the final case for the Load-following strategy. This makes sense considering the operating point set during the Thermostatic case is 37.5 kW just like for the final case of the Load-following. The only differences between these two cases are that the Thermostatic strategy still operates as a "bang-bang" strategy while the Load-following shuts the engine off at power demands less than 37.5 kW. Additionally, this Load-following case allows fluctuations in engine operation higher than 37.5 up to the maximum limit of approximately 56 kW, providing a slight range of power outputs as opposed to a single point.

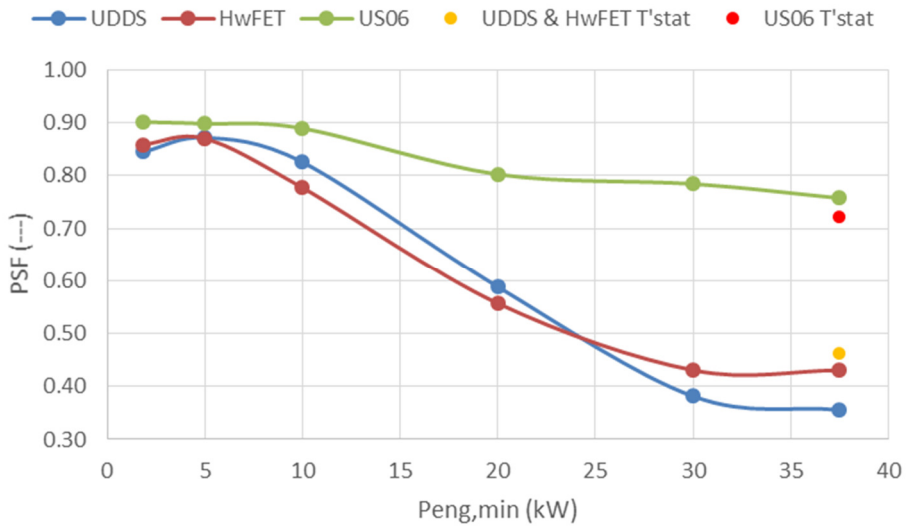

Figure 4-6: PSF vs. $P_{eng,min}$ for 7.1 kWh battery

After examining the effects of $P_{eng,min}$ on PSF, it is important to look at several other variables which will affect overall powertrain efficiency. One of these factors is average engine efficiency over each drive cycle. Figure 4-7 and Figure 4-8 show how this parameter is affected by higher engine operating limits and in turn, lower PSFs. For each cycle, engine efficiency starts out lower before ramping up to the overall maximum efficiency possible for this particular engine at 38.6%. It can be seen that for the very mild UDDS cycle, the starting efficiency is low compared to other cycles since the engine is not heavily loaded and thus is in a lower efficiency range. Contrastingly, the aggressive US06 cycle loads the engine heavily more consistently, thus it starts out at a higher efficiency right away before ramping up to the maximum value. As expected, the T'stat case remains at the optimum point for all three cycles since this is part of the control strategy.

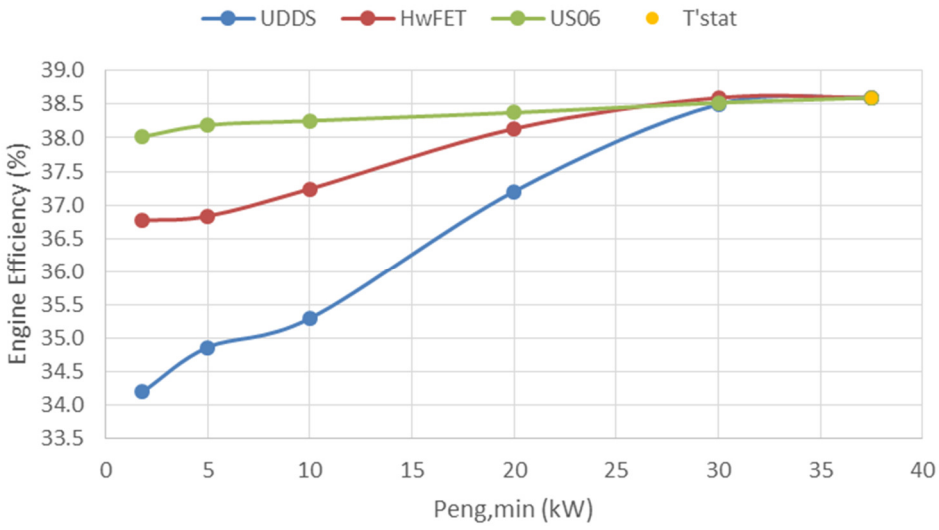

Figure 4-7: Engine efficiency vs. $P_{eng,min}$ for 7.1 kWh battery

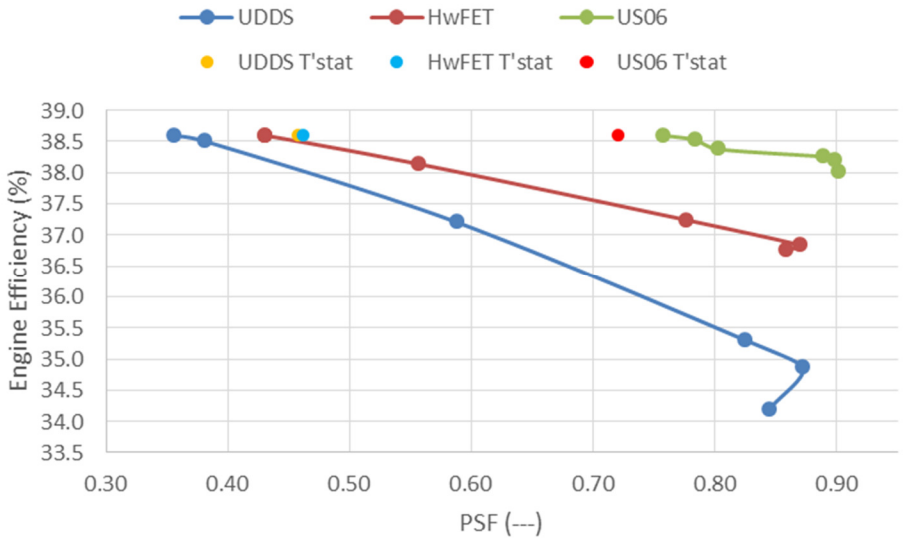

Figure 4-8: Engine efficiency vs. PSF for 7.1 kWh battery

Figure 4-9 demonstrates the overall fuel consumption compared to the minimum operating limit of the engine. As expected for the UDDS case, fuel consumption goes down as engine efficiency increases. Fuel is thus managed in a more ideal manner, minimizing how much is required to complete the cycle. For the US06 and HwFET cycles, overall consumption remains relatively constant with only slight changes. Both of these cases already have fairly high efficiencies, thus there is not much change in operation. It should also be noted that the Thermostatic case is again very close to the final case of the Load-following strategy.

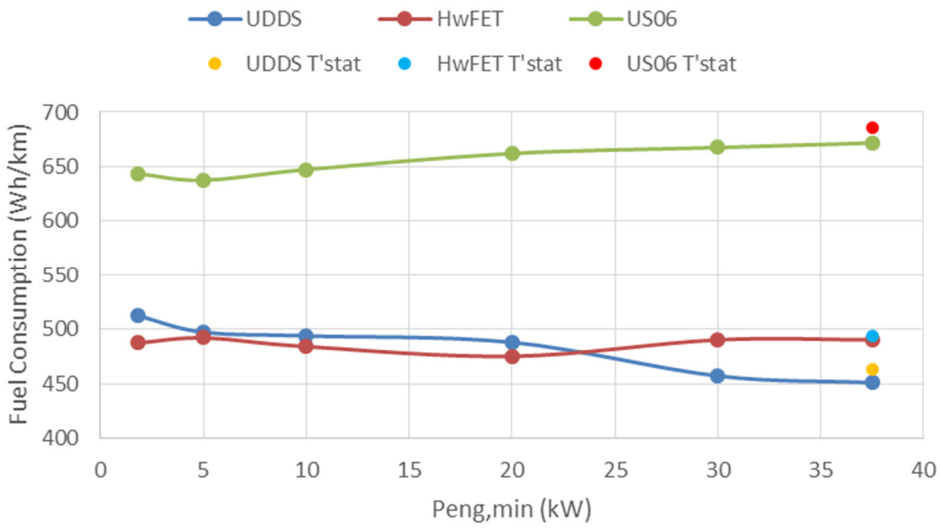

Figure 4-9: Fuel consumption vs. $P_{eng,min}$ for 7.1 kWh battery

Much like for the engine efficiency, average drive cycle battery losses increase with increasing $P_{eng,min}$. When the powertrain has a high PSF, the engine is supplying most of the propulsion power, thus the battery is not being charged/discharged very often to

compensate for lack of engine power. On the other hand, when PSF is decreased, the engine is providing less power to propel the vehicle, thus the EV powertrain must provide the extra power to meet the demand. This trend is shown in Figure 4-10. It is important to note that regenerative braking is still present thus there are at least a small amount of battery losses at any operating point, however these are very low when the engine has a wider range of operation and can meet lower demands. One other note is that here, the Thermostatic case for the US06 drive cycle has much higher losses than for the Load-following strategy. This is because the battery is constantly being charged/discharged at high rates due to the aggressive nature of the velocity trace, thus more losses are incurred.

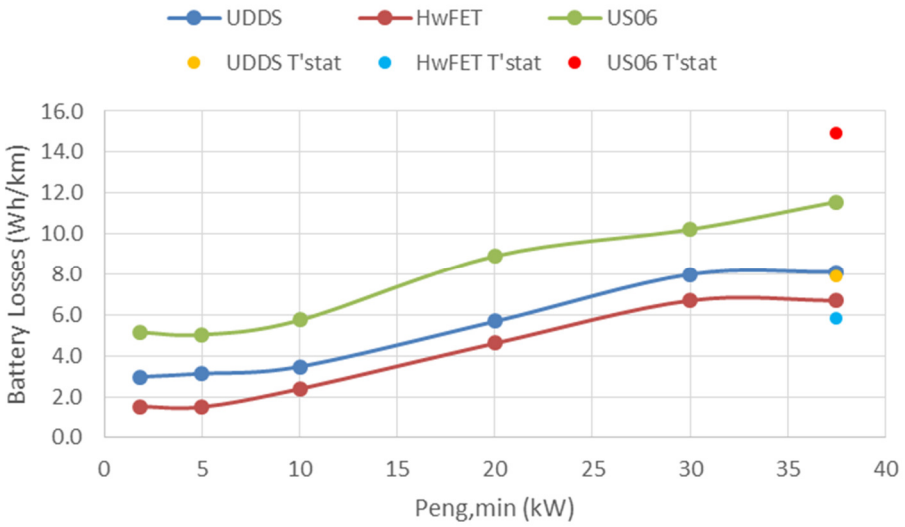

Figure 4-10: Battery losses vs. $P_{eng,min}$ for 7.1 kWh battery

After observing the variations in engine efficiency and battery losses, it is important for the overall study to observe the effects of PSF on overall powertrain efficiency. For decreasing PSF and minimum engine operating power, the engine efficiency rises while battery losses also increase. Because of these factors, overall efficiency is very slightly affected. Figure 4-11 shows the reactions of net powertrain efficiency to increasing $P_{eng,min}$. For the UDDS case, net powertrain efficiency rises. This occurs since engine efficiency increases quite significantly (almost 4.5%) while battery losses also increase by about 5 Wh/km. When balancing these two parameters, engine efficiency obviously has the greater effect since in spite of the increased battery losses, improving the engine efficiency causes an overall increase in powertrain efficiency. This trend is not true for the US06 case. As seen in the figures above, engine efficiency only increases slightly when increasing $P_{eng,min}$.(about .6%). On the other hand, battery losses for this cycle increase by about 6 Wh/km. This increase in battery losses is able to overcome the benefits of a slight increase in engine efficiency to cause the overall net powertrain efficiency to decrease slightly. To further support these cases, the HwFET represents the median case, since it has moderate engine efficiency and battery loss increases and the overall powertrain efficiency remains relatively constant. Again please note that the Thermostatic case is fairly consistent with the final Load-following power limit.

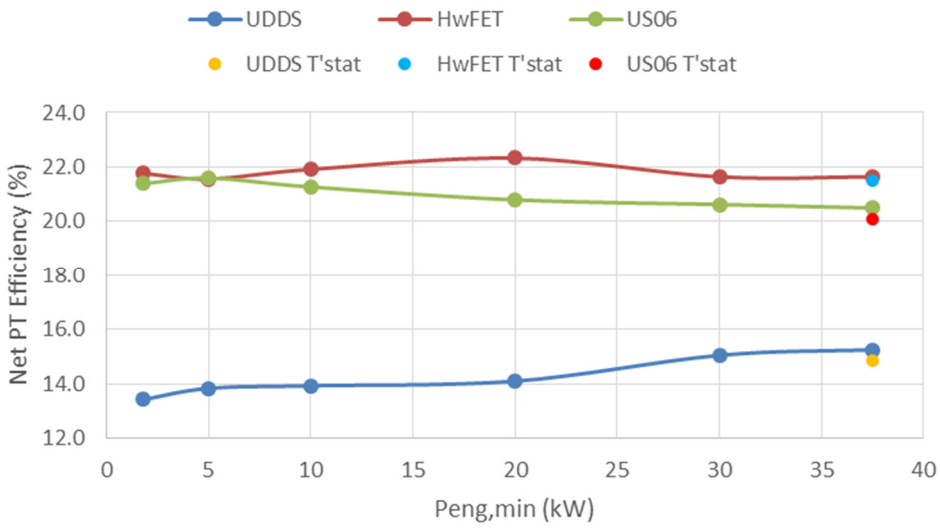

Figure 4-11: Net powertrain efficiency vs. $P_{eng,min}$ for 7.1 kWh battery

Although not shown above, it is important to note the limiting cases for PSF. For the operating points described above, obvious trends can be seen in each of the figures. For the limiting cases of PSF = 0 and 1, these trends hold true. Figure 4-12 demonstrates the engine efficiency for the UDDS drive cycle. Seen in yellow is the PSF = 0 case, while PSF = 1 is shown in red. As demonstrated previously, the lower the PSF, the higher the engine efficiency. The lowest case of 0 is not able to go any higher since the engine is limited to the maximum efficiency. When PSF = 1 however, the efficiency takes an even further dive towards low values. Since the engine is always on for this case, the engine operates even when no demand is required, causing it to idle in an area of extremely low efficiency. This brings the overall average cycle efficiency down.

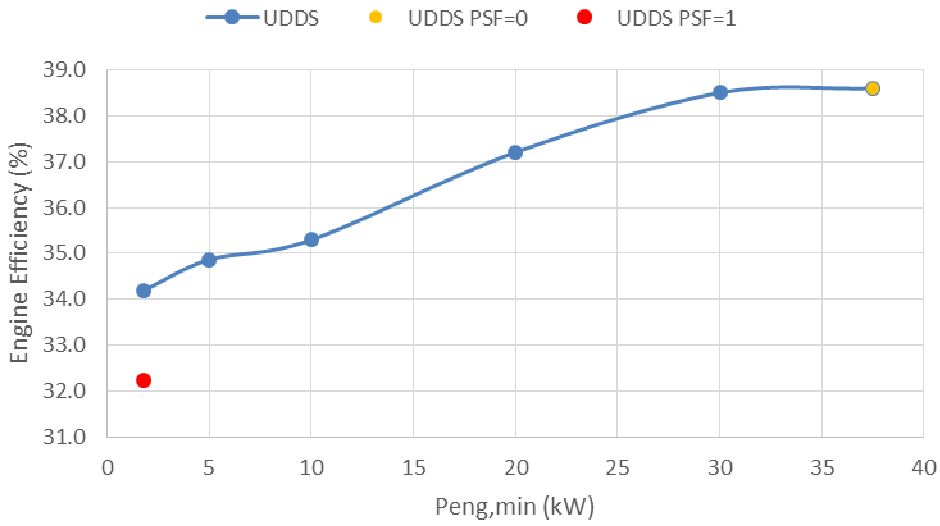

Figure 4-12: PSF limits for engine efficiency vs $P_{eng,min}$ for 7.1 kWh battery

As with the engine efficiency, the battery losses for the limiting PSF cases hold the trends previously shown by Figure 4-10. The PSF = 0 case requires the vehicle to essentially

operate as a CD hybrid during each drive cycle after which it idle charges the battery back to its original SOC. As a result, the battery losses must be summed for the power leaving and entering the battery during the actual drive schedule and entering the battery during the idle charging period afterwards. For PSF = 1, however, the engine operates all the time essentially eliminating any charging/discharging from the battery. This case is shown in Figure 4-13 by the value of zero for PSF = 1. PSF = 0, on the other hand, requires a significant increase in battery losses due to the CD followed by idle charging. These trends are common among all the cycles, thus only the UDDS case has been shown here for reference.

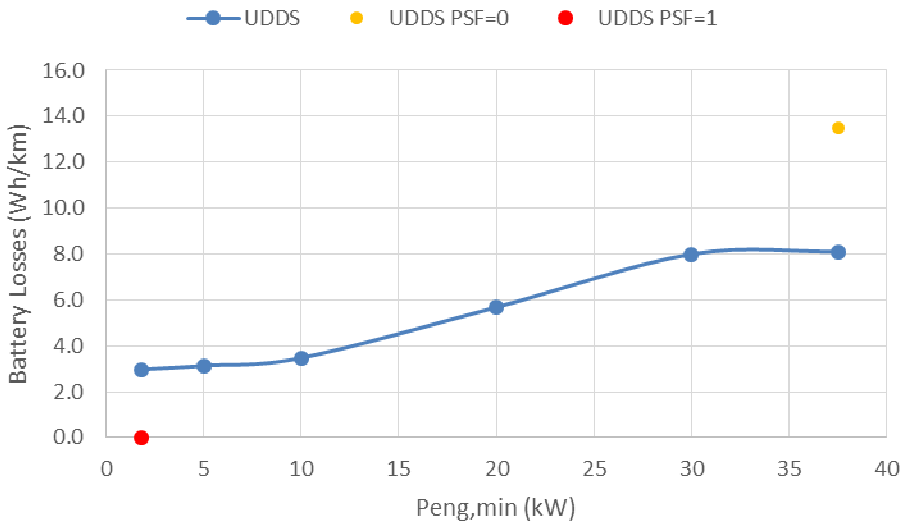

Figure 4-13: PSF limits for battery losses vs $P_{eng,min}$ for 7.1 kWh battery

For further detail, Table 4-14 shows all values for parameters of the 7.1 kWh battery found. It can be seen that overall, the net powertrain efficiency is lower for PSF = 1. This is again, since the engine is constantly on even at low efficiency areas. The PSF = 0 case remains fairly close to the endpoint of the trendline for the UDDS cycle, however does decrease for the US06 case. This is again due to the battery losses having a much more significant impact with this aggressive cycle, considering these losses spike to about 30 Wh/km. For additional data on all cases, see Appendix B for full results.

Table 4-14: Results for PSF limiting cases for 7.1 kWh battery

		PSF = 0			PSF = 1		
Metric	**Units**	**UDDS**	**HwFET**	**US06**	**UDDS**	**HwFET**	**US06**
Engine Efficiency	[%]	38.6	38.6	38.6	32.2	35.8	37.1
Fuel energy	[Wh/km]	446	472	661	700	535	782
Battery Losses	[Wh/km]	13.5	14.1	30.6	0.0	0.0	0.0
Net Powertrain Efficiency	[%]	15.5	22.5	20.8	9.8	19.8	17.6

4.2.4.2 3.1 kWh Battery

After studying the effects of a large battery with low internal resistance, a small battery with much higher internal resistance is observed. For the most part, the trends explored here greatly mimic those found for the 7.1 kWh battery pack. The main difference is the

effect battery losses play on overall powertrain efficiency. It should also be noted that this battery is not able to take on complete Charge Depleting operation due to power limits on the battery. Because of this, the engine is required to be on during certain instances within the US06 drive cycle, thus initial SOC was manipulated to ensure this engine on state while maintaining charge balancing. It is also important to note that for this case an SOC target of 60% was used with an SOC window of ±20%.

Figure 4-14 demonstrates the changes incurred on PSF with increasing $P_{eng,min}$. As mentioned, this closely matches the decreasing trend observed in the large battery case. Once again the US06 PSF does not decrease as significantly as the UDDS or HwFET cycles, and the Thermostatic cases almost exactly match the 37.5 kW Load-following cases.

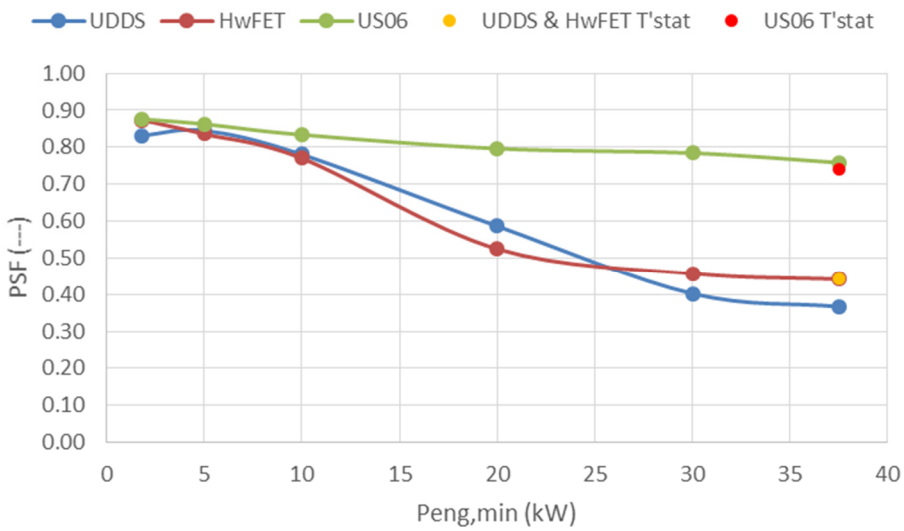

Figure 4-14: PSF vs. $P_{eng,min}$ for 3.1 kWh battery

The engine efficiency and fuel consumption for the 3.1 kWh battery case is also consistent with the trends seen for the larger battery. Figure 4-15 and Figure 4-16 show the increasing engine efficiency with increasing minimum engine operating power and decreasing PSF. Figure 4-17, in turn, shows similar fuel consumption values for both the Load-following and Thermostatic results. Obviously the fact that loading the engine more during its operating time and reducing the areas of low efficiency in which it operates does in fact increase engine efficiency. Additionally, for the UDDS case, fuel consumption again is reduced due to this increase in engine efficiency.

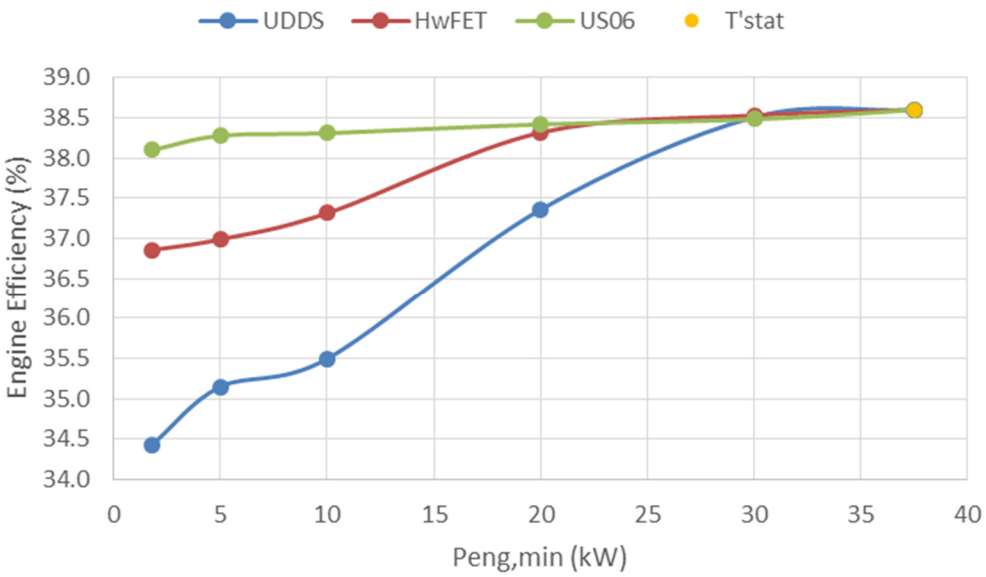

Figure 4-15: Engine efficiency vs. $P_{eng,min}$ for 3.1 kWh battery

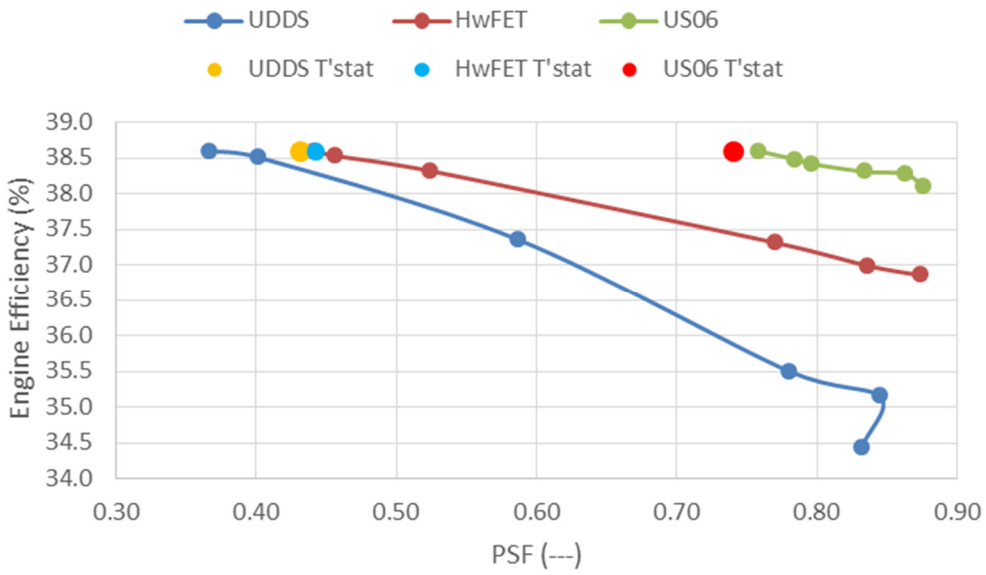

Figure 4-16: Engine efficiency vs. PSF for 3.1 kWh battery

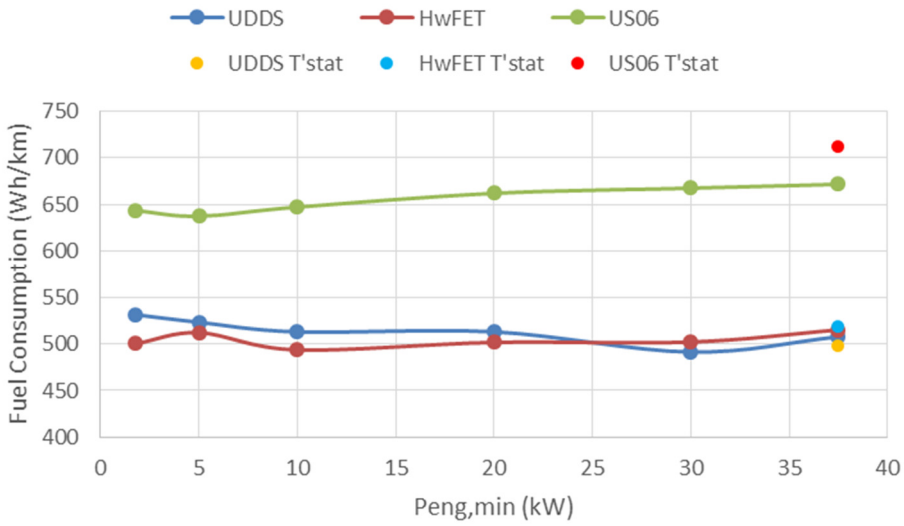

Figure 4-17: Fuel consumption vs. $P_{eng,min}$ for 3.1 kWh battery

As mentioned, battery losses is the main area of variation between the large and small battery cases. Figure 4-18 shows the losses for the 3.1 kWh battery as $P_{eng,min}$ increases. The overall trend for these values is very similar when compared to the 7.1 kWh battery, however, the scale is much larger here. Instead of ranging from approximately 3 - 8 Wh/km for the UDDS drive cycle, the smaller battery causes losses beginning at around 7.5 Wh/km and increasing all the way up to about 20 Wh/km. This is due to the major increase in battery internal resistance causing the penalty for charging/discharging the battery to become more harsh.

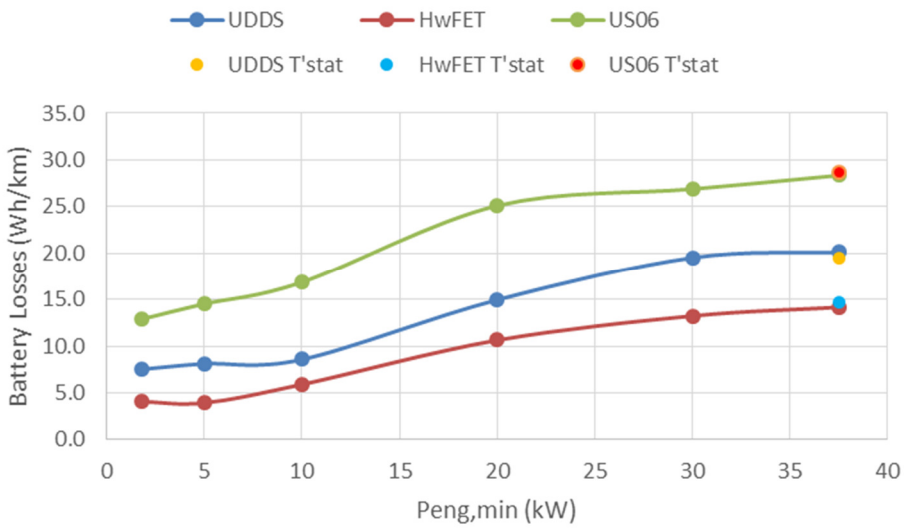

Figure 4-18: Battery losses vs. $P_{eng,min}$ for 3.1 kWh battery

With the increased scale of battery losses, overall powertrain efficiency will obviously be affected. Figure 4-19 shows the trends for all three drive cycle cases. As previously, the US06 and HwFET net powertrain efficiencies are not greatly influenced by the increasing losses due to decreasing PSF. Additionally, the UDDS efficiency does exhibit an overall

increase through decreasing PSF. In both of these cases however, efficiencies are for the most part slightly lower than for the larger battery. This is where the effects of increased battery losses can actually be seen. In addition to all values being slightly less, the UDDS also experiences less of an increase in powertrain efficiency from $P_{eng,min}$ = 1.8 kW to 37.5 kW when compared to the larger battery. This illustrates how the increased engine efficiency is not able to counteract the increased battery losses as drastically. Overall, this net powertrain efficiency is still ultimately affected by engine efficiency, however, the effects of battery losses are noticeable and should be considered when designing a SHEV powertrain.

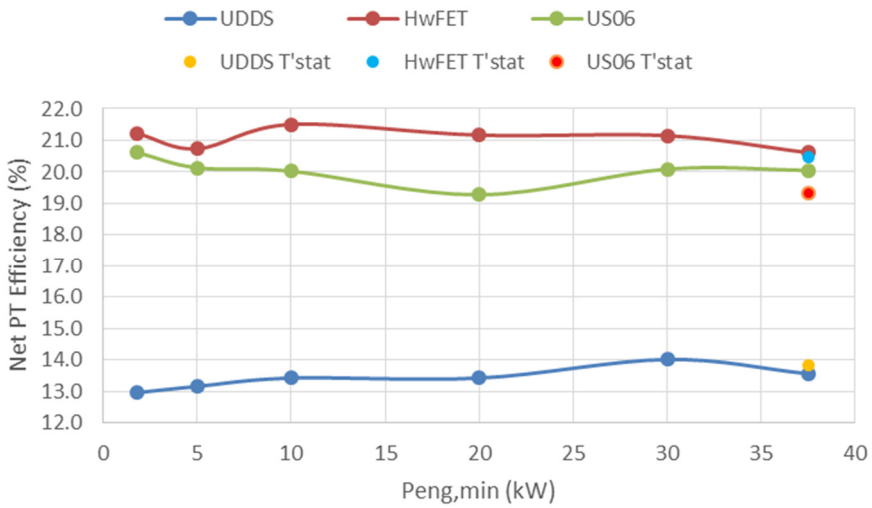

Figure 4-19: Net powertrain efficiency vs. $P_{eng,min}$ for 3.1 kWh battery

Finally, the limiting cases for PSF exhibit the same trends as for the large 7.1 kWh battery. Once again, engine efficiency is very low at PSF=1, and is limited to the maximum value of 38.6% at PSF=0. Additionally, battery losses are zero for PSF=1 considering the SOC window for the battery is so low that the vehicle operates as if there is no battery present. For PSF=0, battery losses are quite significant since a double penalty is incurred with discharging the entire battery and then charging up the entire battery. These factors illustrate how the performance of various batteries is similar when it comes to overall trends, however, battery energy capacity greatly affects how large of an impact is made on net powertrain efficiency due to battery losses. Figure 4-20 and Figure 4-21 graphically show the results discussed here.

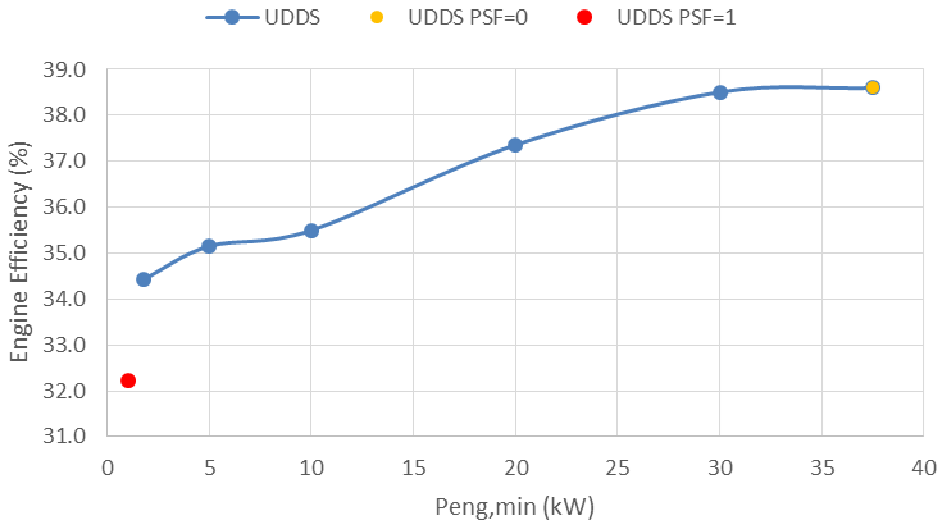

Figure 4-20: PSF limits for engine efficiency vs $P_{eng,min}$ for 3.1 kWh battery

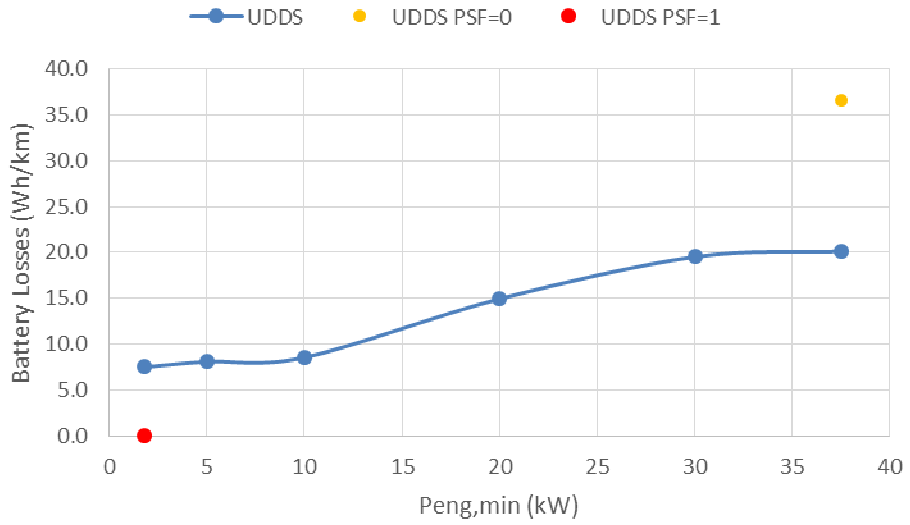

Figure 4-21: PSF limits for battery losses vs $P_{eng,min}$ for 3.1 kWh battery

For further detail, Table 4-15 shows all values for parameters of the 3.1 kWh battery found. It can be seen once again that overall, the net powertrain efficiency is lower for PSF = 1 and higher for the PSF = 0 case. The main variation here is when observing PSF=0 for the US06 cycle, several moments of extremely high power cause the battery to not physically be able to supply enough power to the drive motor due to the size of the battery. Because of this, 5 trace misses occur, meaning the battery power is not able to meet the vehicle demand. Even so, the overall trend for the limiting cases has been found and it is an acceptable compromise to allow these trace misses while gathering these results. For additional data on all cases, see Appendix B for full results.

Table 4-15: Results for PSF limiting cases for 3.1 kWh battery

		PSF = 0			PSF = 1		
Metric	**Units**	**UDDS**	**HwFET**	**US06**	**UDDS**	**HwFET**	**US06**
Engine Efficiency	[%]	38.6	38.6	38.6	32.2	35.8	37.1
Fuel energy	[Wh/km]	464	490	755	700	535	782
Battery Losses	[Wh/km]	36.6	38.1	94.6	0.0	0.0	0.0
Net Powertrain Efficiency	[%]	14.9	21.7	18.2	9.8	19.8	17.6

Overall, this PSF study demonstrates that when designing a CS SHEV powertrain, engine efficiency and battery losses should both be considered. Large batteries with a lower internal resistance and thus lower losses do allow for slightly higher powertrain efficiencies, however, compared to the small battery, this increase in efficiency is only a rise in at most 1%. On the other hand, increased engine efficiency has a much more significant effect on powertrain efficiency. When observing the results for the 7.1 kWh battery, the drive cycle average powertrain efficiency increases almost a full 2 % demonstrating the effects of increasing engine efficiency with decreasing PSF. This trend is true for the small battery as well, however it is not near as drastic, only showing an increase of 1%. With these results in mind, it is shown that there does not seem to be an "optimum" PSF. Although values of approximately .4 for UDDS and HwFET drive cycles, and .79 for US06 display several of the highest engine and powertrain efficiencies, these benefits are quite slight and do not seem to be significant. As a whole, a SHEV with larger battery and thus lower battery losses, and with an engine having a very high efficiency will produce the most ideal powertrain efficiency. Again, battery size does not seem to have a major effect on overall efficiency compared to engine efficiency, so engine size and type should obviously be the component of highest interest when designing a Series hybrid. This engine performance then directly relates to overall efficiency.

5 Conclusions

As shown throughout this work, the overall objectives of this thesis have been completely accomplished. Firstly, a tool has been developed to help understand the in-depth functional details of several advanced vehicle powertrains and to aid in the designing of hybrid powertrains. Hybrid vehicles are very complex and difficult to understand machines. Many details are involved with energy management and numerous components have to work together to operate the vehicle in a successful manner. Although the modeling tool described here does not explore all of the minute details of these technologies, it does provide simple energy flow insight to aid in education and a "first look" behind the operation of a hybrid vehicle. Using a backwards energy flow approach, the demand at the wheels of a vehicle is determined after properly defining the entire vehicle with inputs. The required energy to meet this demand can then be traced back to the energy source to find total energy consumption values for various drive cycles. Using a 1 Hz model allows users to understand what is happening at any second within the model in addition to showing overall drive cycle results. Through producing detailed results and allowing for component specific inputs, this model is also successful in aiding in the design of hybrid powertrains, as demonstrated in Section 4.1. Components can be easily manipulated and the results due to changes quickly available for support in the development process. Overall, the model developed and introduced here is geared towards education and is successful in being accomplishing its design goals.

Aside from the model as a whole, the model within this thesis is also quite successful in exploring several different hybrid energy management strategies. This model first illustrates Battery Electric Vehicles, the simplest of strong hybrid powertrains. The next vehicle architecture explained within this work is a Series Hybrid Electric Vehicle. Focusing on SHEV operation, two different control strategies are developed; Thermostatic and Load-following. Both of these strategies have advantages, however the Load-following strategy has the freedom to operate over a wider range of genset operating points and introduces the Power Split Fraction parameter. Overall, these two SHEV energy management strategies are defined and developed in a clear manner so a user can easily see the effects of the different strategies when it comes to drive cycle results. To ensure accurate results are output from this model, validation is completed through simple energy balances through the powertrains, comparison to Simulink models, and most importantly actual test data gathered as part of the EcoCAR 2 competition.

Finally, this thesis uses the validated model to provide insight on the effects of Power Split Fraction on overall powertrain efficiency. Throughout the study performed, two battery sizes were used and the minimum engine operating power was increased over a range of values up to the optimum operating point. Demonstrated by the results, PSF decreases with increasing $P_{eng,min}$, while engine efficiency and battery losses increase. Although these trends are quite evident for both battery sizes, overall powertrain efficiency is not greatly affected, since the increased engine efficiency compensates for the additional battery losses. In spite of this, the efficiency is increased slightly for the UDDS case, while it remains relatively constant for the HwFET and US06 cases. Overall PSF is found to not be an incredibly useful parameter. When designing and choosing components for a SHEV, attention should be focused on engine sizing/efficiency since this component directly relates to how efficient an overall powertrain is. The control strategy should then attempt

to keep the engine running at a high efficiency to then push the powertrain efficiency to its highest level. The results of this study are useful for further understanding the most impactful components within Series powertrains and can be used for future controls development.

Although this model accomplishes all of the goals outlined at the beginning of this thesis, there are numerous areas of possible future work. One possible area is to expand this model to include a Parallel vehicle powertrain. This addition would greatly benefit this model considering it is a common design for hybrids today. Completing a hybrid powertrain would require additional components, namely a transmission, as well as an energy management strategy to properly control the torque sources of the vehicle. Aside from this large addition, other area of future work would be to introduce a diesel engine model. This would allow for more design freedom in evaluating hybrid powertrains and aid in the selection process considering diesel fuel would affect emissions and energy consumption. Decel fuel cutoff would also affect emissions and energy consumption and would thus be a valuable addition to this model. Finally, this model would benefit from a lumped thermal model. Although this 1 Hz model can track energy flow, thermal effects are not considered. Since components can be scaled and operated under various conditions, it would be quite valuable to at least gain an estimate for what coolant system would be required to reject the amount of heat generated by the system. This would greatly benefit the design process and thus would be a great addition to this model.

As shown here, this thesis has completed each objective laid out at the beginning of this thesis. A modeling tool has been developed to be applied in hybrid vehicle design and analysis, energy management strategies have been defined and implemented, and PSF has been studied to demonstrate its effects on overall powertrain efficiency. Additionally, applicable future work has been laid out to further refine this modeling tool for higher fidelity results while maintaining the goal of simplicity. Overall, this work seeks to provide an educational tool and aid in the development of the automotive engineers of tomorrow.

References

1. “U.S. Product Supplied for Crude Oil and Petroleum Products.” U.S. Energy Information Administration, 03 March 2014. Web. 18 March 2014. <http://www.eia.gov/dnav/pet/pet_cons_psup_dc_nus_mbbl_a.htm>.
2. U.S. Environmental Protection Agency Office of Transportation and Air Quality, (2013), “Fast Fact: U.S. Transportation Sector Greenhouse Gas Emissions 1990-2011”, EPA-420-F-13-033a.
3. “The eGallon: How Much Cheaper Is It to Drive on Electricity?” U.S. Department of Energy, 10 June 2013. Web. 26 March 2014. http://energy.gov/articles/egallon-how-much-cheaper-it-drive-electricity
4. EcoCAR 2: Plugging In to the Future, http://www.ecocar2.org/, accessed on 2013-04-16
5. EcoCAR 2 Non Year Specific Rules, Rev N 01/13/2014, Available from Argonne National Labs (not public)
6. P. Christopher Manning, Eli White, R. Jesse Alley, Jonathan King, Douglas J. Nelson (2012), "Vehicle System Design Process for a Series-Parallel Plug-in Hybrid Electric Vehicle", SAE Technical Paper 2012-01-1774, *SAE 2012 International Powertrains, Fuels & Lubricants Meeting*, September 18, 2012, Saluhallsgangen, Sweden, presented at SAE Congress 2013.
7. Manning, P.C., White, E., Caroncino, K., Ashworth, T., Kelly, B., Shoults, L., and Nelson, D. (2013), “Vehicle Design and Implementation of a Series-Parallel Plug-in Hybrid Electric Vehicle”, SAE Technical Paper 2013-01-2492, 2013, doi:10.4271/2013-01-2492.
8. Ord, D., White, E., Manning, P., Khare, A., Shoults, L., and Nelson D., (2014), "Powertrain Design to Meet Performance and Energy Consumption Goals for EcoCAR 3," SAE Technical Paper 2014-01-1915, 2014, doi:10.4271/2014-01-1915.
9. Alley, R., King, J., White, E., and Nelson D., (2012), "Hybrid Architecture Selection and Component Sizing to Reduce Emissions and Petroleum Energy Consumption", SAE Technical Paper 2012-01-1195, *SAE 2012 International World Congress*, April 24-26, Detroit, Mi.
10. "Autonomie." Argonne National Laboratory, Mar. 2012. <http://www.autonomie.net/>.
11. Sovran, G., Blaser, D., (2003), “A Contribution to Understanding Automotive Fuel Economy and Its Limits,” SAE Technical Paper 2003-01-2070, *SAE Transactions*, Washington, D.C., doi:10.4271/2003-01-2070
12. Alley, Robert Jesse (2012), “VTool: A Method for Predicting and Understanding the Energy Flow and Losses in Advanced Vehicle Powertrains”, MS Thesis in Mechanical Engineering, VPI&SU, Blacksburg, VA.
13. Ord, David, (2014), “Advanced Powertrain Design Using Model Based Design”, MS Thesis in Mechanical Engineering, VPI&SU, Blacksburg, VA.
14. Wang, Q., Liang, W., Kuang, M., and McGee, R., (2011), "Vehicle System Controls for a Series Hybrid Powertrain," SAE Technical Paper 2011-01-0860, 2011, doi:10.4271/2011-01-0860.

15. Jalil, N., Kheir, N.A., Salman, M., (1997), "A Rule-Based Energy Management Strategy for a Series Hybrid Vehicle," *American Control Conference*, Vol.1, pp.689-693 June 1997, doi: 10.1109/ACC.1997.611889
16. Rask, E., Santini, D., and Lohse-Busch, H., (2013), "Analysis of Input Power, Energy Availability, and Efficiency during Deceleration for X-EV Vehicles," *SAE Int. J. Alt. Power.* 2(2):350-361, 2013, doi:10.4271/2013-01-1473.
17. Sovran, G. and Blaser, D., (2006), "Quantifying the Potential Impacts of Regenerative Braking on a Vehicle's Tractive- Fuel Consumption for the U.S., European, and Japanese Driving Schedules," SAE Technical Paper 2006-01-0664, 2006, doi:10.4271/2006-01-0664.
18. Sovran, G., (2011), "The Impact of Regenerative Braking on the Powertrain-Delivered Energy Required for Vehicle Propulsion.," SAE Technical Paper 2011-01-0891, 2011, doi:10.4271/2011-01-0891.
19. Greenhouse Gasses, Regulated Emissions and Energy Use in Transportation Model (GREET), <http://greet.es.anl.gov/>
20. Brinkman, T. Weber, Wang, M., Darlington, T., (2005), "Well-to-Wheels Analysis of Advanced Fuel/Vehicle Systems - A North American Study of Energy Use, Greenhouse Gas Emissions, and Criteria Pollutant Emissions", Argonne Nation Labs. www.transportation.anl.gov/pdfs/TA/339.pdf
21. Burke, Andrew F. (2007), "Batteries and Ultracapacitors for Electric, Hybrid, and Fuel Cell Vehicles", *IEEE Proceedings - Special Issue on Electric, Hybrid & Fuel Cell Vehicles*, Vol 95, No.4, April 2007, pp. 806-820.
22. SAE J2841 (2010), Utility Factor Definitions for Plug-In Hybrid Electric Vehicles Using Travel Survey Data.
23. SAE J1711 (2010), Recommended Practice for Measuring the Exhaust Emissions and Fuel Economy of Hybrid-Electric Vehicles, Including Plug-in Hybrid Vehicles.

Appendix A: 1 Hz Model "How To" Guide

A-1 Getting Started – Inputs

This section is quite important for any user of this 1 Hz model. Here, the inputs sheet is discussed in detail to explain how parameters are manipulated and the effects of changing certain items. Overall, pay close attention to cells which are highlighted in yellow. These cells represent the "user inputs" and are the values which should be changed to correctly define the vehicle and all of its components. The cells which are not highlighted are, for the most part, results calculated from the highlighted cells. There are several exceptions to this rule which will be discussed further below. It is also important to note that comments are attached to certain cells for further clarification. Comments are denoted by a red triangle in the upper right hand corner of a cell, and can be viewed by simply hovering the cursor over the cell. These comments give abbreviation definitions, as well as illustrate how certain parameters are calculated to help users input appropriate values.

The first section to be changed when using this model is to completely define the vehicle glider characteristics. These parameters, control the aspects of the physical vehicle and define the tractive effort required to propel the vehicle through the various drive cycles. Values such as coefficients of rolling resistance (C_{rr0} and C_{rr1}), aerodynamic drag (C_d), frontal area (A), mass (m), and even the accessory load acting constantly on the vehicle (P_{acc}). These parameters, along with several others, should be updated when changing vehicle types, or when studying changes in vehicle mass to illustrate the effects of heavier vehicles due to factors like varying component sizes. An important item to keep in mind is the unit present with each parameter. Users must be sure to use correct units when inputting values for accurate results.

Aside from defining the vehicle, characteristics for regenerative braking are also input by the user. Again, the highlighted parameters can be manipulated by the user to represent the desired system. Comments should be viewed in this section for further background on how the power and torque limits for regen braking are derived. It is also important to note here that the "Regen Fraction" parameter is a target value. This input is used in calculations for how much regen braking occurs in the vehicle, however, the actual, calculated value for regen braking is displayed in the results tab.

Most other component definition tables are quite intuitive with only several parameters highlighted for manipulation. Please note that motor and generator coefficients should only be changed if in depth knowledge about a desired electric machine is known. Otherwise, simply use the scaling torque parameter for good approximations of permanent magnet motors. Also note that several engine parameters reference other sheets in the model. When selecting a fuel, the drop-down menu allows one of three fuels to be selected. This menu references the "Fuel Properties and WTW" sheet. These fuel values are derived from the GREET model and are good approximations for each parameter [19]. It should be understood that unless engine parameters for B20 diesel engines are added to the "Engine Sizing" sheet, selecting B20 as a fuel will not produce accurate results. The engine will operate like a gasoline engine and only the fuel properties will come into play. One area of future work is to add diesel engine parameters for further development freedom. Finally, the Thermostatic and Load-following parameters included within the engine characteristics should be manipulated for each respective control strategy. These values

directly control the engine speed and torque as well as change the operating window of the vehicle during the Load-following strategy.

Overall, pay close attention to the parameters entered onto this sheet since this directly controls all outputs within this model. Any mistake on this sheet will cause results to be inaccurate and non-representative of the desired vehicle.

A-2 Drive Cycle Sheets

Drive cycle sheets are very easy to understand. While the amount of data present can be overwhelming to a new user, most information on these sheets is simply calculations being completed. Columns B – DH are all responsible for modeling a vehicle operating along the various drive traces and are completely self-reliant, not needing user input within these sheets. The area of greatest importance is the last four rows in each drive cycle sheet. These rows represent the sum, maximum, minimum, and average for each column respectively. This data can be useful when looking for total drive cycle loss or total component energy consumption. It is important to note that the cells highlighted in green within the "average" row calculate results only dependent on propel or regen. This means that only values where the vehicle is being propelled are considered, which is applicable for parameters such as positive tractive power [$(P_{tr})^+$] where the regen case is not included and otherwise many zeros would cause the calculation to be inaccurate. Aside from this, the header row displays which component is being analyzed by certain columns and where each case is propelling, regening, or is looking at net values. Also please note that comments are included in the title cell for each column. This is to clarify parameter definitions and illustrate any decision making taking place within the model.

A-3 Results Summary Sheet

Much like for the drive cycle sheets, the results tab within this model does not rely on user interaction. The main function is to display data referenced directly from the drive cycle sheets or to post-process for calculating certain data. The flow of this sheet also works very similar to the drive cycle specific sheets. Power and energy requirements at the wheels are first displayed, followed by the BEV, Thermostatic SHEV, and finally the Load-following SHEV results. Each of these results include a table with Wh/km values and also a table right below which displays Wh/mi results. This is to allow easy comparison with other models that may contain only one set of these units.

The area where user interaction is required is for the SHEV cases. Since Charge Sustaining results are of most interest when values are charge-balanced, there are macros available to automatically charge balance the system for each drive cycle. One button for each drive cycle is present in the sheet and will charge balance that particular drive cycle by iterating the initial SOC and keeping track of several values to ensure that the total battery energy used over the drive cycle does not exceed 1% of total fuel energy used. It is VERY important for the user to keep track of which drive cycles have been charge balanced when observing results since each column is filled in and thus appears to have results. It is recommended to highlight cells as iterations are completed to clarify which drive cycles have been charge balanced and which have not. This eliminates the possibility of confusion for the user. Aside from this, it is important for users to understand that without applying the charge balancing macro, no new results will appear since the macro is what actually

references the drive cycle sheets and no direct results will be gathered without activating the button. Again, users should pay close attention to comments for help in trouble shooting macro performance as using certain inputs can affect how long each macro will run to attempt to charge balance. If a macro runs for more than 5 – 10 minutes, the sheet should be closed, re-opened, and inputs checked since the charge balancing most likely is not able to be completed. This could be due to component sizes not being able to meet average power demand or a large amount of CD operation during the first iteration causing the program to run numerous iterations in order to charge balance. If these areas are considered and thought through when operating, these macros will produce accurate, useful output values.

If it is desired to record additional data within the macro, or additional rows or columns are added and macros require changes, it is possible for the user to edit the Visual Basic code behind each macro. Using the "Developer" tab found within the main menu ribbon at the top of the screen, select the "Macros" option. Choose which macro should be edited and select the "edit" command. This brings up a separate screen for macro development. Here, follow the comments for instructions on what each part of the macro does in order to maintain functionality when changes are made. Users MUST pay close attention to cell references since these are the parameters which fetch values from each sheet and thus must be completely accurate for useful results to be produced. It is recommended that unless macros must absolutely be revised, users should allow these items to operate as intended so errors do not occur.

A-4 User Defined Sheet

The user defined tab within this model allows a user the freedom to input a desired drive cycle of any kind and acquire similar results as for the hard coded schedules. The appearance of this sheet is slightly different when compared to the other drive cycle sheets, due to the results for this separate drive cycle being displayed directly on the sheet. This helps reduce clutter and confusion on the results tab since this user defined drive trace may not always be utilized. When it is in use, a velocity and grade vs. time trace can be input into the appropriate columns. The user then needs to simply highlight the second row of the drive trace (time = 1) and autofill the entire row to the end of the drive trace. This automatically completes the calculations for this drive cycle and displays the results within the sum, minimum, maximum, and average cells above the title cells. These values then allow the results table at the top of the sheet to be filled. Again, both SHEV cases have macro buttons which must be clicked to produce results for the charge balanced case. It is important to note that for the use of this sheet, drive cycles should be kept at less than 2000 seconds in length. If this length is exceeded, the sum rows should be edited to account for the additional range. Overall this sheet is quite useful since it allows design freedom. For additional clarification, there is a guide located on the sheet itself for immediate aid without referencing this document directly.

A-5 Other Important Notes

Overall, this 1 Hz model is designed to be intuitive and user friendly. Most user interaction is only required on the inputs and results tabs unless a unique drive trace is inputted into the "User Defined" tab. In spite of its simplicity, several general rules should be kept in

mind when operating this model. Firstly, since macros are utilized, the excel workbook must have macros enabled to complete some post-processing such as charge balancing. This is done when opening excel and going to the "Developer" menu. Here, users should select "Macro Security" and "Enable all macros". Macros will now be able to run and complete results can be acquired.

One of the most important items vital for the performance of this model has to do with adding rows or columns. **DO NOT ADD ROWS OR COLUMNS!** Macros work through very specific cell references which are not updated when rows or columns are added between existing ones (unlike normal cell formulas). If additional calculations are desired, they should be added after the last existing row or column which will maintain these cell references. If a user does decide to add rows or columns between existing ones, macro cell references **MUST** be changed to maintain accurate results for Series cases. Aside from these items, operation of the spreadsheet should be smooth, easy to understand, and robust to aid in the hybrid powertrain development process.

Appendix B: Results for Power Split Fraction Study

Large Battery Results

Battery = 7.1 kWh, $P_{eng,min}$ = 1.8 kW, Load-following				
Metric	**Units**	**UDDS**	**HwFET**	**US06**
Fuel energy	[Wh/km]	512.70	487.65	643.64
Fuel Economy	[mpgge]	40.85	42.95	32.54
Battery internal energy	[DC Wh/km]	3.12	3.82	3.81
AC grid energy	[AC Wh/km]	3.58	4.39	4.37
Powertrain Eff (Propel based)	[%]	25.77	24.60	31.18
Powertrain Eff (Net based)	[%]	13.44	21.77	21.40
Actual Regen Brake Fraction	[---]	0.83	0.85	0.83
Power Split Fraction	[---]	0.84	0.86	0.90
Battery Losses	[Wh/km]	2.97	1.52	5.15
Engine Eff	[%]	34.20	36.77	38.02
Engine Starts (per distance)	[1/km]	1.67	0.48	1.09
Engine On Time (per distance)	[s/km]	63.22	33.20	28.90
Engine Starts (per cycle)	[---]	20.0	8.0	14.0
Engine On Time (per cycle time)	[%]	55.2	71.6	62.5
SOC Initial	[%]	24	24	24
SOC End	[%]	22	21	23
Number of Cycles for Charge Balance	[---]	3	3	2

Battery = 7.1 kWh, $P_{eng,min}$ = 5 kW, Load-following				
Metric	**Units**	**UDDS**	**HwFET**	**US06**
Fuel energy	[Wh/km]	497.47	492.31	637.65
Fuel Economy	[mpgge]	42.10	42.54	32.85
Battery internal energy	[DC Wh/km]	3.86	1.82	4.40
AC grid energy	[AC Wh/km]	4.44	2.10	5.05
Powertrain Eff (Propel based)	[%]	26.56	24.36	31.47
Powertrain Eff (Net based)	[%]	13.85	21.56	21.60
Actual Regen Brake Fraction	[---]	0.83	0.85	0.83
Power Split Fraction	[---]	0.87	0.87	0.90
Battery Losses	[Wh/km]	3.13	1.50	5.03
Engine Eff	[%]	34.87	36.84	38.19
Engine Starts (per distance)	[1/km]	1.67	0.36	1.01
Engine On Time (per distance)	[s/km]	56.63	33.02	26.69
Engine Starts (per cycle)	[---]	20.0	6.0	13.0
Engine On Time (per cycle time)	[%]	49.5	71.2	57.7
SOC Initial	[%]	24	24	24
SOC End	[%]	23	21	23
Number of Cycles for Charge Balance	[---]	1	2	1

Battery = 7.1 kWh, $P_{eng,min}$ = 10 kW, Load-following				
Metric	**Units**	**UDDS**	**HwFET**	**US06**
Fuel energy	[Wh/km]	494.11	484.36	647.43
Fuel Economy	[mpgge]	42.39	43.24	32.35
Battery internal energy	[DC Wh/km]	2.12	3.31	1.17
AC grid energy	[AC Wh/km]	2.43	3.80	1.34
Powertrain Eff (Propel based)	[%]	26.74	24.76	31.00
Powertrain Eff (Net based)	[%]	13.94	21.92	21.27
Actual Regen Brake Fraction	[---]	0.83	0.85	0.83
Power Split Fraction	[---]	0.83	0.78	0.89
Battery Losses	[Wh/km]	3.47	2.38	5.74
Engine Eff	[%]	35.30	37.24	38.25
Engine Starts (per distance)	[1/km]	1.58	0.48	1.09
Engine On Time (per distance)	[s/km]	48.29	28.93	26.07
Engine Starts (per cycle)	[---]	19.0	8.0	14.0
Engine On Time (per cycle time)	[%]	42.2	62.4	56.4
SOC Initial	[%]	24	24	24
SOC End	[%]	22	21	24
Number of Cycles for Charge Balance	[---]	2	2	1

Battery = 7.1 kWh, $P_{eng,min}$ = 20 kW, Load-following				
Metric	**Units**	**UDDS**	**HwFET**	**US06**
Fuel energy	[Wh/km]	488.23	475.45	662.19
Fuel Economy	[mpgge]	42.90	44.05	31.63
Battery internal energy	[DC Wh/km]	-4.39	4.09	-2.30
AC grid energy	[AC Wh/km]	-5.04	4.70	-2.64
Powertrain Eff (Propel based)	[%]	27.06	25.23	30.31
Powertrain Eff (Net based)	[%]	14.11	22.33	20.80
Actual Regen Brake Fraction	[---]	0.83	0.85	0.83
Power Split Fraction	[---]	0.59	0.56	0.80
Battery Losses	[Wh/km]	5.68	4.61	8.90
Engine Eff	[%]	37.20	38.14	38.38
Engine Starts (per distance)	[1/km]	0.94	0.70	0.54
Engine On Time (per distance)	[s/km]	28.73	21.02	25.84
Engine Starts (per cycle)	[---]	11.3	11.5	7.0
Engine On Time (per cycle time)	[%]	25.1	45.4	55.9
SOC Initial	[%]	24	24	24
SOC End	[%]	28	20	24
Number of Cycles for Charge Balance	[---]	4	2	1

Battery = 7.1 kWh, $P_{eng,min}$ = 30 kW, Load-following				
Metric	**Units**	**UDDS**	**HwFET**	**US06**
Fuel energy	[Wh/km]	457.48	490.52	667.68
Fuel Economy	[mpgge]	45.78	42.70	31.37
Battery internal energy	[DC Wh/km]	2.51	-1.47	-3.96
AC grid energy	[AC Wh/km]	2.89	-1.69	-4.56
Powertrain Eff (Propel based)	[%]	28.88	24.45	30.06
Powertrain Eff (Net based)	[%]	15.06	21.64	20.63
Actual Regen Brake Fraction	[---]	0.83	0.85	0.83
Power Split Fraction	[---]	0.38	0.43	0.78
Battery Losses	[Wh/km]	7.99	6.70	10.21
Engine Eff	[%]	38.50	38.60	38.52
Engine Starts (per distance)	[1/km]	0.58	0.61	0.54
Engine On Time (per distance)	[s/km]	17.56	18.18	24.52
Engine Starts (per cycle)	[---]	7.0	10.0	7.0
Engine On Time (per cycle time)	[%]	15.3	39.2	53.0
SOC Initial	[%]	24	24	24
SOC End	[%]	23	24	25
Number of Cycles for Charge Balance	[---]	2	1	1

Battery = 7.1 kWh, $P_{eng,min}$ = 37.5 kW, Load-following				
Metric	**Units**	**UDDS**	**HwFET**	**US06**
Fuel energy	[Wh/km]	451.30	490.52	671.81
Fuel Economy	[mpgge]	46.41	42.70	31.18
Battery internal energy	[DC Wh/km]	4.43	-1.47	-4.59
AC grid energy	[AC Wh/km]	5.10	-1.69	-5.27
Powertrain Eff (Propel based)	[%]	29.27	24.45	29.87
Powertrain Eff (Net based)	[%]	15.27	21.64	20.50
Actual Regen Brake Fraction	[---]	0.83	0.85	0.83
Power Split Fraction	[---]	0.36	0.43	0.76
Battery Losses	[Wh/km]	8.11	6.70	11.57
Engine Eff	[%]	38.60	38.60	38.60
Engine Starts (per distance)	[1/km]	0.56	0.61	0.54
Engine On Time (per distance)	[s/km]	16.68	18.18	23.98
Engine Starts (per cycle)	[---]	6.7	10.0	7.0
Engine On Time (per cycle time)	[%]	14.6	39.2	51.8
SOC Initial	[%]	24	24	24
SOC End	[%]	22	24	25
Number of Cycles for Charge Balance	[---]	3	1	1

Battery = 7.1 kWh, $P_{eng,min}$ = 37.5 kW, Thermostatic				
Metric	**Units**	**UDDS**	**HwFET**	**US06**
Fuel energy	[Wh/km]	463.67	493.79	685.55
Fuel Economy	[mpgge]	45.17	42.42	30.55
Battery internal energy	[DC Wh/km]	-0.26	-3.51	-6.68
AC grid energy	[AC Wh/km]	-0.30	-4.04	-7.68
Powertrain Eff (Propel based)	[%]	28.49	24.29	29.27
Powertrain Eff (Net based)	[%]	14.86	21.50	20.09
Actual Regen Brake Fraction	[---]	0.83	0.85	0.83
Power Split Fraction	[---]	0.46	0.46	0.72
Battery Losses	[Wh/km]	7.89	5.84	14.94
Engine Eff	[%]	38.60	38.60	38.60
Engine Starts (per distance)	[1/km]	0.08	0.08	0.08
Engine On Time (per distance)	[s/km]	17.18	18.30	25.40
Engine Starts (per cycle)	[---]	1.0	1.3	1.0
Engine On Time (per cycle time)	[%]	15.0	39.5	54.9
SOC Initial	[%]	24	24	24
SOC End	[%]	24	31	38
Number of Cycles for Charge Balance	[---]	1	4	17

Battery = 7.1 kWh, PSF = 0				
Metric	**Units**	**UDDS**	**HwFET**	**US06**
Fuel energy	[Wh/km]	445.51	471.86	661.39
Fuel Economy	[mpgge]	47.01	44.39	31.67
Battery internal energy	[DC Wh/km]	0.00	0.00	0.00
AC grid energy	[AC Wh/km]	0.00	0.00	0.00
Powertrain Eff (Propel based)	[%]	29.65	25.42	30.34
Powertrain Eff (Net based)	[%]	15.46	22.50	20.82
Actual Regen Brake Fraction	[---]	0.83	0.85	0.83
Power Split Fraction	[---]	0.00	0.00	0.00
Battery Losses	[Wh/km]	13.51	14.06	30.59
Engine Eff	[%]	38.60	38.60	38.60
Engine Starts (per distance)	[1/km]	0.08	0.06	0.08
Engine On Time (per distance)	[s/km]	16.51	17.49	24.51
Engine Starts (per cycle)	[---]	1.0	1.0	1.0
Engine On Time (per cycle time)	[%]	14.4	37.7	53.0
SOC Initial	[%]	98.5	98.5	98.5
SOC End	[%]	71	58	54
Number of Cycles for Charge Balance	[---]	1	1	1

Battery = 7.1 kWh, PSF = 1				
Metric	**Units**	**UDDS**	**HwFET**	**US06**
Fuel energy	[Wh/km]	700.27	534.89	782.18
Fuel Economy	[mpgge]	29.91	39.16	26.78
Battery internal energy	[DC Wh/km]	2.09	1.43	6.15
AC grid energy	[AC Wh/km]	2.40	1.64	7.07
Powertrain Eff (Propel based)	[%]	18.87	22.42	25.66
Powertrain Eff (Net based)	[%]	9.84	19.85	17.61
Actual Regen Brake Fraction	[---]	0.00	0.00	0.00
Power Split Fraction	[---]	0.99	1.00	0.98
Battery Losses	[Wh/km]	0.00	0.00	0.09
Engine Eff	[%]	32.23	35.79	37.14
Engine Starts (per distance)	[1/km]	3.42	0.79	1.09
Engine On Time (per distance)	[s/km]	114.42	46.35	46.25
Engine Starts (per cycle)	[---]	41.0	13.0	14.0
Engine On Time (per cycle time)	[%]	100.0	100.0	100.0
SOC Initial	[%]	30	30	30
SOC End	[%]	30	30	29
Number of Cycles for Charge Balance	[---]	1	1	1

Small Battery Results

Battery = 3.1 kWh, $P_{eng,min}$ = 1.8 kW, Load-following				
Metric	**Units**	**UDDS**	**HwFET**	**US06**
Fuel energy	[Wh/km]	531.19	500.23	668.05
Fuel Economy	[mpgge]	39.43	41.87	31.35
Battery internal energy	[DC Wh/km]	0.52	1.57	2.29
AC grid energy	[AC Wh/km]	0.60	1.81	2.64
Powertrain Eff (Propel based)	[%]	24.87	23.98	30.04
Powertrain Eff (Net based)	[%]	12.97	21.22	20.62
Actual Regen Brake Fraction	[---]	0.83	0.85	0.83
Power Split Fraction	[---]	0.83	0.87	0.88
Battery Losses	[Wh/km]	7.52	4.07	12.89
Engine Eff	[%]	34.43	36.86	38.10
Engine Starts (per distance)	[1/km]	1.67	0.48	1.09
Engine On Time (per distance)	[s/km]	63.22	33.26	29.25
Engine Starts (per cycle)	[---]	20.0	8.0	14.0
Engine On Time (per cycle time)	[%]	55.2	71.8	63.3
SOC Initial	[%]	44	44	46
SOC End	[%]	44	43	45
Number of Cycles for Charge Balance	[---]	1	1	1

Battery = 3.1 kWh, $P_{eng,min}$ = 5 kW, Load-following				
Metric	**Units**	**UDDS**	**HwFET**	**US06**
Fuel energy	[Wh/km]	523.19	512.00	684.05
Fuel Economy	[mpgge]	40.03	40.91	30.62
Battery internal energy	[DC Wh/km]	-1.04	-3.33	-3.31
AC grid energy	[AC Wh/km]	-1.19	-3.82	-3.81
Powertrain Eff (Propel based)	[%]	25.25	23.43	29.34
Powertrain Eff (Net based)	[%]	13.17	20.73	20.13
Actual Regen Brake Fraction	[---]	0.83	0.85	0.83
Power Split Fraction	[---]	0.85	0.84	0.86
Battery Losses	[Wh/km]	8.11	3.93	14.51
Engine Eff	[%]	35.15	36.99	38.28
Engine Starts (per distance)	[1/km]	1.67	0.36	0.93
Engine On Time (per distance)	[s/km]	56.54	32.96	27.86
Engine Starts (per cycle)	[---]	20.0	6.0	12.0
Engine On Time (per cycle time)	[%]	49.4	71.1	60.2
SOC Initial	[%]	44	44	46
SOC End	[%]	48	46	47
Number of Cycles for Charge Balance	[---]	2	1	1

Battery = 3.1 kWh, $P_{eng,min}$ = 10 kW, Load-following				
Metric	**Units**	**UDDS**	**HwFET**	**US06**
Fuel energy	[Wh/km]	512.90	493.57	687.83
Fuel Economy	[mpgge]	40.84	42.43	30.45
Battery internal energy	[DC Wh/km]	0.00	3.25	-2.73
AC grid energy	[AC Wh/km]	0.00	3.73	-3.14
Powertrain Eff (Propel based)	[%]	25.76	24.30	29.18
Powertrain Eff (Net based)	[%]	13.43	21.51	20.02
Actual Regen Brake Fraction	[---]	0.83	0.85	0.83
Power Split Fraction	[---]	0.78	0.77	0.83
Battery Losses	[Wh/km]	8.56	5.90	16.84
Engine Eff	[%]	35.50	37.31	38.31
Engine Starts (per distance)	[1/km]	1.58	0.48	0.54
Engine On Time (per distance)	[s/km]	48.29	28.84	27.70
Engine Starts (per cycle)	[---]	19.0	8.0	7.0
Engine On Time (per cycle time)	[%]	42.2	62.2	59.9
SOC Initial	[%]	44	44	46
SOC End	[%]	44	42	47
Number of Cycles for Charge Balance	[---]	1	1	1

Battery = 3.1 kWh, $P_{eng,min}$ = 20 kW, Load-following				
Metric	**Units**	**UDDS**	**HwFET**	**US06**
Fuel energy	[Wh/km]	512.87	501.55	714.40
Fuel Economy	[mpgge]	40.84	41.76	29.32
Battery internal energy	[DC Wh/km]	-4.47	-0.10	-5.16
AC grid energy	[AC Wh/km]	-5.14	-0.12	-5.93
Powertrain Eff (Propel based)	[%]	25.76	23.91	28.09
Powertrain Eff (Net based)	[%]	13.43	21.17	19.28
Actual Regen Brake Fraction	[---]	0.83	0.85	0.83
Power Split Fraction	[---]	0.59	0.52	0.80
Battery Losses	[Wh/km]	14.94	10.63	25.11
Engine Eff	[%]	37.36	38.32	38.42
Engine Starts (per distance)	[1/km]	0.95	0.67	0.54
Engine On Time (per distance)	[s/km]	28.94	20.75	27.62
Engine Starts (per cycle)	[---]	11.3	11.0	7.0
Engine On Time (per cycle time)	[%]	25.3	44.8	59.7
SOC Initial	[%]	44	44	46
SOC End	[%]	54	41	48
Number of Cycles for Charge Balance	[---]	6	2	1

Battery = 3.1 kWh, $P_{eng,min}$ = 30 kW, Load-following				
Metric	**Units**	**UDDS**	**HwFET**	**US06**
Fuel energy	[Wh/km]	491.24	501.96	685.47
Fuel Economy	[mpgge]	42.64	41.73	30.56
Battery internal energy	[DC Wh/km]	1.85	1.25	6.57
AC grid energy	[AC Wh/km]	2.13	1.44	7.55
Powertrain Eff (Propel based)	[%]	26.89	23.90	29.28
Powertrain Eff (Net based)	[%]	14.02	21.15	20.09
Actual Regen Brake Fraction	[---]	0.83	0.85	0.83
Power Split Fraction	[---]	0.40	0.46	0.78
Battery Losses	[Wh/km]	19.52	13.22	26.89
Engine Eff	[%]	38.51	38.53	38.48
Engine Starts (per distance)	[1/km]	0.63	0.64	0.55
Engine On Time (per distance)	[s/km]	18.81	19.08	25.61
Engine Starts (per cycle)	[---]	7.5	10.5	7.1
Engine On Time (per cycle time)	[%]	16.4	41.2	55.4
SOC Initial	[%]	44	44	75
SOC End	[%]	47	48	50
Number of Cycles for Charge Balance	[---]	2	2	11

Battery = 3.1 kWh, $P_{eng,min}$ = 37.5 kW, Load-following				
Metric	**Units**	**UDDS**	**HwFET**	**US06**
Fuel energy	[Wh/km]	507.64	515.05	686.85
Fuel Economy	[mpgge]	41.26	40.67	30.49
Battery internal energy	[DC Wh/km]	-3.88	-2.87	6.76
AC grid energy	[AC Wh/km]	-4.46	-3.30	7.77
Powertrain Eff (Propel based)	[%]	26.03	23.29	29.22
Powertrain Eff (Net based)	[%]	13.57	20.61	20.05
Actual Regen Brake Fraction	[---]	0.83	0.85	0.83
Power Split Fraction	[---]	0.37	0.44	0.76
Battery Losses	[Wh/km]	20.12	14.15	28.35
Engine Eff	[%]	38.60	38.60	38.60
Engine Starts (per distance)	[1/km]	0.63	0.64	0.55
Engine On Time (per distance)	[s/km]	18.76	19.08	24.54
Engine Starts (per cycle)	[---]	7.5	10.5	7.1
Engine On Time (per cycle time)	[%]	16.4	41.2	53.1
SOC Initial	[%]	44	44	75
SOC End	[%]	41	50	50
Number of Cycles for Charge Balance	[---]	2	2	8

Battery = 3.1 kWh, $P_{eng,min}$ = 37.5 kW, Thermostatic				
Metric	**Units**	**UDDS**	**HwFET**	**US06**
Fuel energy	[Wh/km]	497.43	518.59	712.03
Fuel Economy	[mpgge]	42.11	40.39	29.42
Battery internal energy	[DC Wh/km]	-0.85	-3.63	-2.46
AC grid energy	[AC Wh/km]	-0.97	-4.18	-2.83
Powertrain Eff (Propel based)	[%]	26.56	23.13	28.18
Powertrain Eff (Net based)	[%]	13.85	20.47	19.34
Actual Regen Brake Fraction	[---]	0.83	0.85	0.83
Power Split Fraction	[---]	0.43	0.44	0.74
Battery Losses	[Wh/km]	19.49	14.67	28.72
Engine Eff	[%]	38.60	38.60	38.60
Engine Starts (per distance)	[1/km]	0.13	0.10	0.39
Engine On Time (per distance)	[s/km]	18.43	19.22	26.38
Engine Starts (per cycle)	[---]	1.5	1.7	5.0
Engine On Time (per cycle time)	[%]	16.1	41.5	57.0
SOC Initial	[%]	44	44	63
SOC End	[%]	59	61	64
Number of Cycles for Charge Balance	[---]	2	6	1

Battery = 3.1 kWh, PSF = 0				
Metric	**Units**	**UDDS**	**HwFET**	**US06**
Fuel energy	[Wh/km]	463.62	490.05	755.45
Fuel Economy	[mpgge]	45.18	42.74	27.72
Battery internal energy	[DC Wh/km]	0.00	0.00	0.00
AC grid energy	[AC Wh/km]	0.00	0.00	0.00
Powertrain Eff (Propel based)	[%]	28.50	24.48	26.56
Powertrain Eff (Net based)	[%]	14.86	21.66	18.23
Actual Regen Brake Fraction	[---]	0.83	0.85	0.83
Power Split Fraction	[---]	0.00	0.00	0.00
Battery Losses	[Wh/km]	36.56	38.05	94.56
Engine Eff	[%]	38.60	38.60	38.60
Engine Starts (per distance)	[1/km]	0.08	0.06	0.08
Engine On Time (per distance)	[s/km]	17.2	18.2	28.0
Engine Starts (per cycle)	[---]	1.0	1.0	1.0
Engine On Time (per cycle time)	[%]	15.0	39.2	60.5
SOC Initial	[%]	98.5	98.5	98.5
SOC End	[%]	33	0.03	-0.17
Number of Cycles for Charge Balance	[---]	1	1	1

Battery = 3.1 kWh, PSF = 1				
Metric	**Units**	**UDDS**	**HwFET**	**US06**
Fuel energy	[Wh/km]	700.27	534.89	782.18
Fuel Economy	[mpgge]	29.91	39.16	26.78
Battery internal energy	[DC Wh/km]	2.09	1.43	6.27
AC grid energy	[AC Wh/km]	2.40	1.65	7.21
Powertrain Eff (Propel based)	[%]	18.87	22.42	25.66
Powertrain Eff (Net based)	[%]	9.84	19.85	17.61
Actual Regen Brake Fraction	[---]	0.00	0.00	0.00
Power Split Fraction	[---]	0.99	1.00	0.98
Battery Losses	[Wh/km]	0.01	0.01	0.21
Engine Eff	[%]	32.23	35.79	37.14
Engine Starts (per distance)	[1/km]	3.42	0.79	0.62
Engine On Time (per distance)	[s/km]	114.42	46.35	46.25
Engine Starts (per cycle)	[---]	41.0	13.0	8.0
Engine On Time (per cycle time)	[%]	100.0	100.0	100.0
SOC Initial	[%]	60	60	60
SOC End	[%]	59	59	57
Number of Cycles for Charge Balance	[---]	1	1	1

Medium Battery Results (For Reference Only)

Battery = 5 kWh, $P_{eng,min}$ = 1.8 kW, Load-following				
Metric	**Units**	**UDDS**	**HwFET**	**US06**
Fuel energy	[Wh/km]	514.63	492.13	655.05
Fuel Economy	[mpgge]	40.70	42.56	31.97
Battery internal energy	[DC Wh/km]	3.77	2.66	3.78
AC grid energy	[AC Wh/km]	4.33	3.06	4.34
Powertrain Eff (Propel based)	[%]	25.67	24.37	30.64
Powertrain Eff (Net based)	[%]	13.39	21.57	21.03
Actual Regen Brake Fraction	[---]	0.83	0.85	0.83
Power Split Fraction	[---]	0.88	0.85	0.83
Battery Losses	[Wh/km]	4.41	2.12	9.82
Engine Eff	[%]	34.23	36.82	38.08
Engine Starts (per distance)	[1/km]	1.67	0.48	0.62
Engine On Time (per distance)	[s/km]	63.22	33.20	29.33
Engine Starts (per cycle)	[---]	20.0	8.0	8.0
Engine On Time (per cycle time)	[%]	55.2	71.6	63.4
SOC Initial	[%]	30	30	30
SOC End	[%]	27	29	28
Number of Cycles for Charge Balance	[---]	2	1	2

Battery = 5 kWh, $P_{eng,min}$ = 5 kW, Load-following				
Metric	**Units**	**UDDS**	**HwFET**	**US06**
Fuel energy	[Wh/km]	509.84	496.84	676.29
Fuel Economy	[mpgge]	41.08	42.16	30.97
Battery internal energy	[DC Wh/km]	0.75	0.85	5.42
AC grid energy	[AC Wh/km]	0.86	0.98	6.23
Powertrain Eff (Propel based)	[%]	25.91	24.14	29.67
Powertrain Eff (Net based)	[%]	13.51	21.37	20.36
Actual Regen Brake Fraction	[---]	0.83	0.85	0.83
Power Split Fraction	[---]	0.87	0.87	0.77
Battery Losses	[Wh/km]	4.81	2.24	22.04
Engine Eff	[%]	35.02	36.86	38.41
Engine Starts (per distance)	[1/km]	1.67	0.36	0.54
Engine On Time (per distance)	[s/km]	56.54	33.02	26.96
Engine Starts (per cycle)	[---]	20.0	6.0	7.0
Engine On Time (per cycle time)	[%]	49.4	71.2	58.3
SOC Initial	[%]	30	30	30
SOC End	[%]	26	30	27
Number of Cycles for Charge Balance	[---]	3	1	2

Battery = 5 kWh, $P_{eng,min}$ = 10 kW, Load-following				
Metric	**Units**	**UDDS**	**HwFET**	**US06**
Fuel energy	[Wh/km]	498.63	484.36	661.77
Fuel Economy	[mpgge]	42.00	43.24	31.65
Battery internal energy	[DC Wh/km]	2.35	4.29	0.01
AC grid energy	[AC Wh/km]	2.70	4.94	0.01
Powertrain Eff (Propel based)	[%]	26.50	24.76	30.33
Powertrain Eff (Net based)	[%]	13.82	21.92	20.81
Actual Regen Brake Fraction	[---]	0.83	0.85	0.83
Power Split Fraction	[---]	0.87	0.78	0.85
Battery Losses	[Wh/km]	5.41	3.37	9.70
Engine Eff	[%]	35.34	37.24	38.23
Engine Starts (per distance)	[1/km]	1.58	0.48	0.54
Engine On Time (per distance)	[s/km]	48.29	28.93	27.39
Engine Starts (per cycle)	[---]	19.0	8.0	7.0
Engine On Time (per cycle time)	[%]	42.2	62.4	59.2
SOC Initial	[%]	30	30	30
SOC End	[%]	31	26	30
Number of Cycles for Charge Balance	[---]	2	2	1

Battery = 5 kWh, $P_{eng,min}$ = 20 kW, Load-following				
Metric	**Units**	**UDDS**	**HwFET**	**US06**
Fuel energy	[Wh/km]	492.70	480.55	687.87
Fuel Economy	[mpgge]	42.51	43.58	30.45
Battery internal energy	[DC Wh/km]	-3.37	3.63	-1.79
AC grid energy	[AC Wh/km]	-3.87	4.17	-2.06
Powertrain Eff (Propel based)	[%]	26.81	24.96	29.18
Powertrain Eff (Net based)	[%]	13.98	22.09	20.02
Actual Regen Brake Fraction	[---]	0.83	0.85	0.83
Power Split Fraction	[---]	0.60	0.55	0.79
Battery Losses	[Wh/km]	8.82	6.25	19.28
Engine Eff	[%]	37.32	38.20	38.45
Engine Starts (per distance)	[1/km]	0.92	0.67	0.58
Engine On Time (per distance)	[s/km]	28.11	20.80	26.42
Engine Starts (per cycle)	[---]	11.0	11.0	7.5
Engine On Time (per cycle time)	[%]	24.6	44.9	57.1
SOC Initial	[%]	30	30	30
SOC End	[%]	34	26	27
Number of Cycles for Charge Balance	[---]	4	3	2

Battery = 5 kWh, $P_{eng,min}$ = 30 kW, Load-following				
Metric	**Units**	**UDDS**	**HwFET**	**US06**
Fuel energy	[Wh/km]	459.73	490.52	679.01
Fuel Economy	[mpgge]	45.56	42.70	30.85
Battery internal energy	[DC Wh/km]	3.73	0.18	-2.93
AC grid energy	[AC Wh/km]	4.29	0.21	-3.37
Powertrain Eff (Propel based)	[%]	28.74	24.45	29.56
Powertrain Eff (Net based)	[%]	14.99	21.64	20.28
Actual Regen Brake Fraction	[---]	0.83	0.85	0.83
Power Split Fraction	[---]	0.38	0.44	0.78
Battery Losses	[Wh/km]	10.02	8.35	15.21
Engine Eff	[%]	38.50	38.60	38.51
Engine Starts (per distance)	[1/km]	0.58	0.61	0.54
Engine On Time (per distance)	[s/km]	17.64	18.18	25.10
Engine Starts (per cycle)	[---]	7.0	10.0	7.0
Engine On Time (per cycle time)	[%]	15.4	39.2	54.3
SOC Initial	[%]	30	30	30
SOC End	[%]	29	30	32
Number of Cycles for Charge Balance	[---]	2	1	2

Battery = 5 kWh, $P_{eng,min}$ = 37.5 kW, Load-following				
Metric	**Units**	**UDDS**	**HwFET**	**US06**
Fuel energy	[Wh/km]	472.67	490.52	678.74
Fuel Economy	[mpgge]	44.31	42.70	30.86
Battery internal energy	[DC Wh/km]	1.23	0.18	-2.21
AC grid energy	[AC Wh/km]	1.41	0.21	-2.54
Powertrain Eff (Propel based)	[%]	27.95	24.45	29.57
Powertrain Eff (Net based)	[%]	14.58	21.64	20.29
Actual Regen Brake Fraction	[---]	0.83	0.85	0.83
Power Split Fraction	[---]	0.40	0.44	0.76
Battery Losses	[Wh/km]	12.62	8.35	16.44
Engine Eff	[%]	38.60	38.60	38.60
Engine Starts (per distance)	[1/km]	0.58	0.61	0.54
Engine On Time (per distance)	[s/km]	17.51	18.18	24.21
Engine Starts (per cycle)	[---]	7.0	10.0	7.0
Engine On Time (per cycle time)	[%]	15.3	39.2	52.3
SOC Initial	[%]	30	30	30
SOC End	[%]	30	30	33
Number of Cycles for Charge Balance	[---]	1	1	2